AN ABSTRACT OF THE DISSERTATION OF

Joseph Lapka for the degree of Doctor of Philosophy in Chemistry presented on December 4, 2013.

Title: Investigation of Mixed N,O-Donor Dipicolinamide Derivative Ligands for Use in Nuclear Fuel Separations

Abstract approved: _____

Alena Paulenova

In this work, three isomeric forms of N, N'-diethyl, N, N'-ditolyldipicolinamide (EtTDPA) were synthesized. The elements thorium through americium, which make up a significant portion of the actinides in used nuclear fuel (with the exception of curium), and two fission products, molybdenum and technetium, were tested for their ability to be extracted by EtTDPA into a polar fluorinated diluent from nitric acid solutions at varying concentrations of both nitric acid and organic ligand. These ligands were then further analyzed for their stability when subject to the harsh conditions inflicted during used fuel reprocessing. Degradation products were determined and the effect of their presence on the extraction and separation of the actinide and lanthanide elements was investigated. Finally, thermodynamics of the complexation between EtTDPA and neodymium were investigated by spectroscopic, calorimetric, and solvent extraction methods. The data presented here will hopefully be used in the future ligand design and implementation in solvent extraction systems for the reprocessing of used nuclear fuel.

Investigation of Mixed N,O-Donor Dipicolinamide Derivative Ligands for Use in
Nuclear Fuel Separations

by
Joseph Lapka

A DISSERTATION

submitted to

Oregon State University

in partial fulfillment of
the requirements for the
degree of

Doctor of Philosophy

Presented December 4, 2013
Commencement June 2014

Doctor of Philosophy dissertation of Joseph Lapka presented on December 4, 2013

APPROVED:

_____

Major Professor, representing Chemistry

_____

Chair of the Department of Chemistry

_____

Dean of the Graduate School

I understand that my dissertation will become part of the permanent collection of Oregon State University libraries. My signature below authorizes release of my dissertation to any reader upon request.

_____

Joseph Lapka, Author

ACKNOWLEDGEMENTS

TABLE OF CONTENTS

TABLE OF CONTENTS (Continued)

LIST OF FIGURES (Continued)

LIST OF FIGURES (Continued)

LIST OF FIGURES (Continued)

LIST OF TABLES

LIST OF COMMON ACRONYMS

An	Actinides
BTP	Bis-triazinylpyridine
BTBP	Bis-triazinylbipyridine
CCD	Chlorinated cobalt cicarbollide
CMPO	Carbamoylphosphine oxide
DPA	Dipicolinic acid
DTPA	Diethylenetriaminepentaacetic acid
EtTDPA	N, N'-diethyl, N, N'-ditolyldipicolinamide
FS-13	Trifluoromethylphenyl sulfone
HDEHP	Di-(2-ethylhexyl)phosphoric acid
Ln	Lanthanides
PEG	Polyethylene glycol
PUREX	Plutonium and Uranium Reduction Extraction
TBP	Tri-n-butyl phosphate
TODGA	N, N'-tetra-octyl-diglycolamide
TRUEX	Transuranic Extraction
UNEX	Universal Extraction

1. INTRODUCTION

Nuclear energy has been a long standing issue the world over with several economically and politically driven stances taken on the subject. Debates are often based on generally unfounded fears regarding the safety of power plant operations and misunderstandings about the health impact of radiation doses to the public at large. However, the question of how the nuclear industry should deal with its ever increasing supply of used nuclear fuel resulting from day to day operations, and its environmental and economic implications, is a valid one.

As of 2013, there are 100 operating reactors within the United States with two new reactor units currently under construction in both Georgia and South Carolina.[1] As of 2003 these light water-based power reactors produced used nuclear fuel at a rate of approximately 40,000 cubic feet every year.[2] Once its usable lifespan of 1.5-3 years in a reactor core has been exceeded, irradiated fuel is transferred to cooling ponds on site at each plant in order to allow the more radioactive elements to decay to more manageable levels from both a radiotoxicity and heat production perspective.[3] With no current official plan of used fuel treatment, these ponds continue to accumulate fuel at each power plant with a total of 45,000 metric tons at commercial reactors and an additional 2,000 metric tons from defense purposes built up as of 2001.[4]

One of the most well-known proposals for used nuclear fuel management is permanent storage of high level waste (HLW) in an underground geological repository. Several countries including the United States, France, Germany, Sweden, Finland, and Japan are investigating the feasibility of long term radioactive waste storage by this

method. In 1987 the United States originally selected the Yucca Mountain site located approximately 100 miles northwest of Las Vegas in the Nevada desert as a permanent disposal site for high level waste. The ill-fated project, though constructed, was plagued with problems from its inception. The project attracted large amounts of criticism from the public and scientists alike, with concerns about the long term ramifications from unforeseen changes in the environmental mobility of radioactive materials through possible earthquakes and other shifts in the hydrological properties of the surrounding area. As a result, funding for the Yucca Mountain repository was entirely terminated in 2011 by congressional order despite lawsuits from states such as Washington and Idaho which currently contain significant amounts of radioactive high level material stored at sites within their borders. Currently the Yucca Mountain project's license has been ordered for further review.

In the past, used nuclear fuel has been given the misnomers "spent nuclear fuel" or "nuclear waste" which has likely influenced public perception of nuclear energy and its byproducts. The fact is that the vast majority of irradiated fuel is neither spent nor waste. Roughly 96% of the initial fuel by mass is still useable for energy production in conventional light water reactors.[5] The fuel only becomes unusable from the buildup of neutron absorbers or "poisons" which limit the energy production while the fuel is within the reactor. It is possible to reprocess this fuel by separating out the useful fuel elements, mainly uranium and plutonium, which can then be recycled back into usable fuel. This considerably reduces the bulk volume of the waste. Further reprocessing can be done to separate the long-lived elements responsible for the long term heat contribution and

radiotoxicity and convert them to shorter lived isotopes through transmutation in fast reactors, while a portion of the shorter lived isotopes can be vitrified in glass matrices to immobilize them for short term disposal. Critics of recycling often cite the increased cost from construction of recycling plants and possible proliferation concerns from the separation of fissile isotopes into individual streams.[6,7] However, it should be noted that commercial recycling is practiced by countries such as France and thus recycling can be made economical on an industrial scale.

The purpose of the work presented in this dissertation is to help advance the knowledge of current recycling methods using new novel extractants, namely amide derivatized ligands based on dipicolinic acid. The mixed nitrogen and oxygen-donor character they possess allows them to simultaneously extract actinides and fission products from nitric acid solutions while providing an inherent preference for the extraction of the trivalent actinides over the trivalent lanthanides. This work contains material which has been adapted and rewritten from three previously published articles in peer reviewed journals, as well as several conference proceedings papers in order to incorporate new experimental work and form a more full-bodied piece of scientific literature.

Chapter 2 of this dissertation provides some background on the chemical composition of used nuclear fuel. This is followed by a review of the solution chemistries of the f-elements as well as their interactions with organic ligands along with chemical equilibria. A review of modern solvent extraction reprocessing techniques for used nuclear fuel leads to discussion of the ligands currently being studied.

Chapter 3 discusses the synthesis of the ligands and the methods used in the investigations throughout the work.

Chapter 4 presents the extraction behavior of actinides and selected fission products by these new ligands from nitric acid solutions as a function of varying nitric acid and ligand concentration as well as a discussion of their aqueous chemistries under acidic conditions. Work presented in this chapter has been published in the following peer reviewed journals and conference proceedings:

Lapka, J. L. *et al.* Extraction of uranium(VI) with diamides of dipicolinic acid from nitric acid solutions. *Radiochimica Acta* **97**, 291–296 (2009).

Lapka, J. L. *et al.* Extraction of molybdenum and technetium with diamides of dipicolinic acid from nitric acid solutions. *Journal of Radioanalytical and Nuclear Chemistry* **280**, 307–313 (2009).

Lapka, J. L. & Paulenova, A. The Extraction of Actinides from Nitric Acid Solutions with Diamides of Dipicolinic Acid. *IOP Conference Series: Materials Science and Engineering* **9**, (2010).

Chapter 5 discusses the stability of these ligands when subjecting them to the harsh conditions imposed during reprocessing of used nuclear fuel. The degradation products by hydrolysis and radiolysis are identified by gas chromatography mass spectrometry. The effect of these degradation products on the extraction and separation of americium and europium are determined. Work presented in this chapter has been published in:

Lapka, J. L., Paulenova, A., Herbst, R. S. & Law, J. D. The Radiolytic and Thermal Stability of Diamides of Dipicolinic Acid. *Separation Science and Technology* **45**, 1706–1710 (2010).

Chapter 6 presents the thermodynamics of complexation between these ligands and neodymium, including the stability constants, Gibb's free energies, enthalpies, and entropies obtained from spectroscopic, calorimetric, and solvent extraction methods. Work presented in this chapter has been published in:

> Lapka, J.L. & Paulenova, A. Complexation of Diamides of Dipicolinic Acid with Neodymium, GLOBAL 2013: International Nuclear Fuel Cycle Conference Proceedings, accepted

This is followed by the conclusion summarizing the work performed here as well as a listing of the references used in this dissertation.

2. BACKGROUND AND LITERATURE REVIEW

2.1. Composition of Used Nuclear Fuel
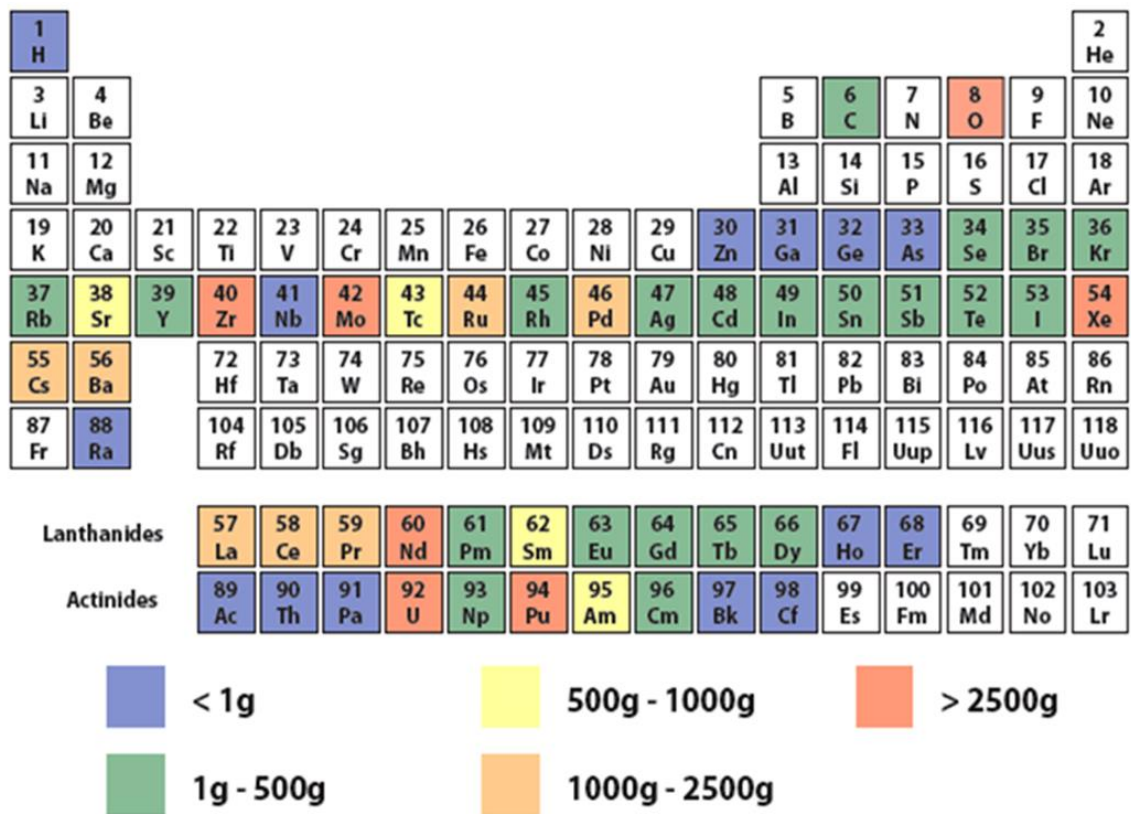
Figure 2.1: Masses of elements per initial heavy metal tons after 10 years cooling, PWR (adapted from Choppin, G. R.; Liljenzin, J.; Rydberg, J.; *Radiochemistry and Nuclear Chemistry, 3rd Ed.*)

Uranium-based fuels in light water reactors initially consist of uranium dioxide enriched to approximately 4% by weight uranium-235. Operation of the reactor causes a buildup of fission products, which absorb the neutrons required to sustain the fission reaction. Gradually the buildup of the fission products causes a drop in the neutron

economy and thus the fuel has a set lifespan which is dependent on the fuel burn-up rate. After a typical lifespan of 1.5-3 years in a reactor, approximately 95-96% of the fuel is still useable uranium which can no longer sustain a reasonable fission rate for energy production from the presence of these neutron "poisons". The remaining 4-5% of fuel consists of 3-4% fission products and ~1% transuranic elements produced during neutron capture events; the exact percentages are a function of the operation procedures at each individual reactor.

The primary source of the fuel's radioactivity lies in the 4-5% non-uranium elements, with an activity of approximately 10^{17}-10^{18} Bq per initial heavy metal ton (IHM) after one month of cooling time.[8,9] After ten years of cooling time, the fuel consists of a wide array of elements as shown in Figure 2.1. Allowing the fuel to cool for this length of time lowers the radioactivity by approximately four orders of magnitude to 10^{13}-10^{14} Bq per IHM and allows the fuel to be much more manageable.[9] The most abundant fission product elements at this time scale by both weight and mole fraction are xenon, molybdenum, neodymium, cesium, and ruthenium, accounting for almost 70% of the total fission product mass. Several of the fission products have cooled to the point of being completely stable as in the case of Ga, Ge, As, Br, In, Xe, La, Nd, Tb, Dy and Er, while other have been significantly reduced in their total radioactivity (Zn, Se, Rb, Mo, Pd, Ag, Sn, I, Gd, Ho, and Tm).

The actinide content is highly dependent to the plant operation specifics. Produced Pu-239 and Pu-241 also can fission in addition to the main U-235 fuel and leads to higher yields of heavier 4d-transition metals. Higher production of plutonium will lead to more

americium and curium isotopes being generated. For the same specifics in Figure 2.1, the majority by weight of the actinides are plutonium and americium. After the same 10 years of cooling the largest specific activity is from the plutonium, mainly from the Pu-241and Pu-238 isotopes. Second is Am-241 produced from the beta decay of Pu-241, followed closely by the curium isotopes Cm-242 and Cm-244.
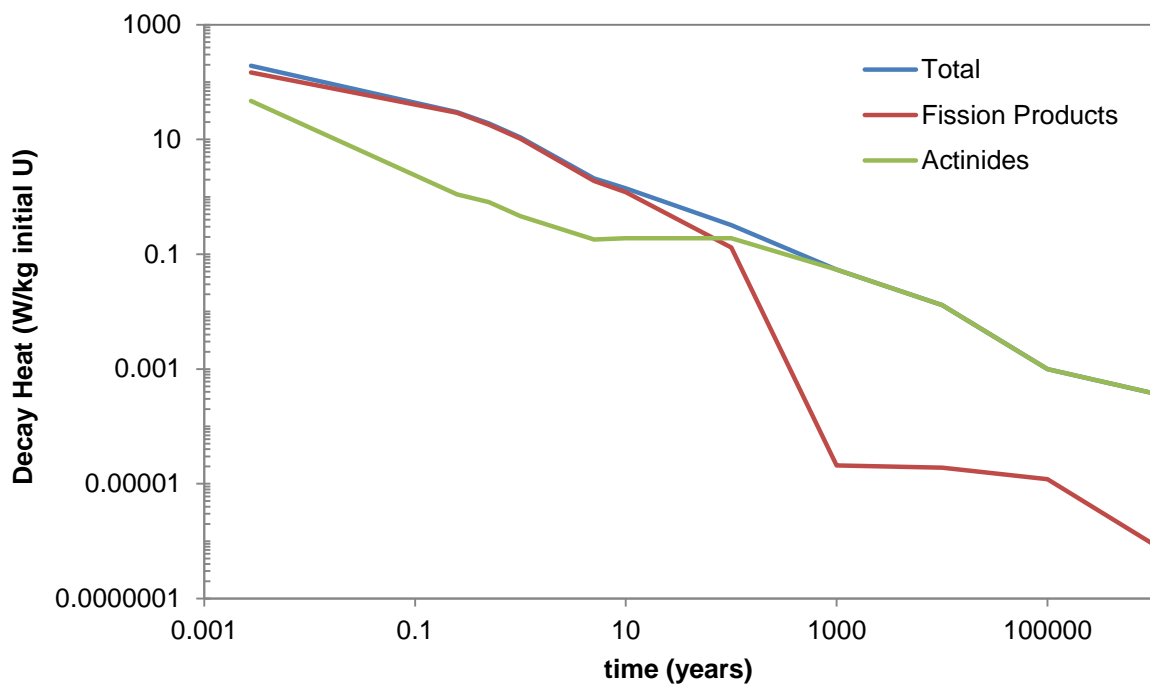
Figure 2.2: Heat output for LWR fuel (adapted from Choppin, G. R.; Liljenzin, J.; Rydberg, J.; *Radiochemistry and Nuclear Chemistry, 3rd Ed.)*

After ten years of cooling, the majority of the heat output comes from the decay of the fission products (Figure 2.2), mainly strontium-90, cesium-134, and cesium-137. Cesium-134 decays to non-problematic amounts within another ten years; however strontium-90 and cesium-137, with their half-lives of approximately 30 years and environmental mobility, continue to be radiotoxicity concerns. The shorter-lived high

energy alpha emitters also produce significant amounts of decay heat. However, the lanthanides dominate in the short term, and it is not until nearly 100 years do the actinides become the larger contributor to decay heat. Correlated to the decay heat, the bulk radioactivity is also dominated in the short term by the lanthanides.[10] Assuming transmutation of the minor actinides, removing the fission products from the still useful irradiated nuclear fuel significantly reduces the length of time any "waste" would need to be stored (approximately 300 years for the separated fission products) before reaching the radioactivity comparable to that of natural uranium. Even leaving the minor actinides with the fission products and only recycling the uranium and plutonium content requires only 9,000 years to decay to natural uranium levels. In comparison, simply storing used fuel in waste repositories without any fuel reprocessing requires over 300,000 years to decay to uranium levels. It is for these reasons that fuel reprocessing is of significant importance in maintaining a nuclear based energy program.

2.2. Hard-Soft Acid-Base Theory

The complexation behavior of metal ions in solution is rooted in the characteristics of their outer electron orbitals. Pearson theorized that the relative strength of a chemical reaction between two species could be predicted based on the rigidity of the electron clouds that participate in the bonding process.[11–14] The rigidity of the electron cloud is referred to as the polarizability of the ion or molecular group. Pearson's description is commonly utilized when describing the reactions between acids and bases, using the

Lewis definition of acids and bases as an electron acceptor and electron donor respectively. The electron pair in the highest occupied orbital of the Lewis base interacts with the lowest unoccupied orbital of the Lewis acid, forming an adduct whose molecular orbitals are lower in energy.

Lewis acids and bases can generally be categorized as either *hard* or *soft* (a group of "borderline" acids and bases also exists with behavior intermittent of these two categories). A *hard* Lewis acid or base is characterized by having a smaller electron cloud radii, as well as higher charge in the case of ions resulting in a higher charge density, and the electrons are held onto more tightly giving less covalent character and thus interactions are more ionic in nature. Molecular hard acids will have low energy for their highest occupied molecular orbital (HOMO) and hard bases higher lowest unoccupied molecular orbital (LUMO) energy resulting in little to no orbital overlap of the HOMO and LUMO and therefore lack of covalency. *Soft* acids and bases are the described by the opposite characteristics of having larger radii and lower charge states. The lower charge density of these groups means electrons are more easily shared between the two substituents giving more covalent character in formation of the bond. Molecular soft acids have high lying HOMOs and soft bases have low lying LUMOs which allows for more orbital overlap and more covalency.

Table 2.1: Common Hard/Soft Lewis Acids and Bases

Acids		Bases	
hard	*soft*	*hard*	*soft*
H^+, Li^+, Na^+, K^+	Hg^+, Au^+, Ag^+, Cu^+	H_2O, OH^-	H^-, R^-
Ca^{2+}, Ba^{2+}, Sr^{2+}	Pt^{2+}, Pd^{2+}, Cd^{2+}	RO^-	RS^-
Al^{3+}, An/Ln^{3+}, Sc^{3+}	Tl^{3+}	F^-, Cl^-	I^-
Zr^{4+}, An^{4+}, Ti^{4+}	Pt^{4+}, Te^{4+}	NH_3	PR_3
BF_3	BH_3	CH_3COO^-, CO_3^{2-}	SCN^-, CN^-, CO

However, these characteristics are not universal when determining the hard/soft character of a given substituent. Some common hard/soft characterized acids and bases are listed in Table 2.1. It can be seen that the potassium ion K^+ is listed in as a hard acid, while the copper(I) ion Cu^+ is considered soft despite the same electronic charge and the smaller radius of the cuprous ion. The difference in their behavior lies in the fact that copper has d-electrons which are less tightly held and thus more available for covalent bonding. Thus the rules of size and charge are only followed down groups of the periodic table, i.e. F^- is a harder Lewis base than Cl^- and so on within the halides.

A more rigorous definition of the chemical hardness η is needed to explain why an ion such as Te^{4+} is considered to be a soft acid, while Zr^{4+}, which belongs to the same period, is considered a hard acid. Pearson and Parrs proposed that the chemical hardness could be related to change in electronic energy of the chemical environment ∂E relative to the change in the number of electrons within a fixed environment ∂N:

$$\eta = \frac{1}{2}\left(\frac{\partial^2 E}{\partial N^2}\right) = \frac{I - A}{2} \qquad (2.1)$$

11

where I is the ionization energy and A the electron affinity for a given species.[12] A molecule or complex which minimizes the difference in the values of I and A between both the acid and base constituents minimizes the chemical hardness, resulting in more sharing of electrons, while hard acids and bases resist transfer of electrons in both direction giving larger values of η and more ionic character.

2.3. f-Element Chemistry

2.3.1. Lanthanides

The lanthanide elements are present in used nuclear fuel as a result of actinide fission. Fission of the three most common fuels (U-233 from the thorium fuel cycle, U-235 and Pu-239 bred in from the standard uranium light water reactor) by thermal neutrons results in a distribution of mass fragments.[15] Because the most probable mode of fission for these isotopes is asymmetric fission, two "humps" are seen in the mass distribution with one centered about A ~ 140 while the other is variable from A ~ 95-100 depending on the mass of the parent isotope that underwent fission.   The mass distribution about 140 is a result of the "magic number" corresponding to 82 neutrons.   Several of the light lanthanides have total mass numbers of approximately 140 and thus are some of the more primary constituents of irradiated fuel. The heavier lanthanides are much less abundant, or essentially non-existent, as in the case of thulium, ytterbium, and lutetium.[9]

Chemically all members of the lanthanide series behave in a very similar manner. The 4f-orbitals are buried beneath the further extending 6s and 5d orbitals.[16]   The

addition of another electron into the 4f-orbital therefore has little effect on the chemical interactions possible by each member of the lanthanides when the sizes of their ions do not restrict bonding behavior. Separations between individual members of the lanthanide series would be extremely difficult if not for their size difference; shrinking 17% from Ce^{3+} to Lu^{3+}.[17]   Since the f-orbitals are not spherically symmetrical the outer most electrons are not sufficiently shielded. Increasing the nuclear charge along the series therefore causes the outer most electrons to contract more than would otherwise be expected across the series (estimated from relativistic calculations to be approximately 20 pm), and as such this shrinking effect has been dubbed the "lanthanide contraction".[18] The lanthanide contraction is responsible for the nearly identical chemical behavior from the similar ionic radii of the 4d and 5d transition metals belonging to the same group of the periodic table.

The electronic configurations of the lanthanides all contain the [Xe] core for the inner shells. In metallic form both the 5d and 6s orbitals are initially populated until praseodymium is reached as seen in Table 2.2 With increasing nuclear charge the 4f orbital becomes more stable and from praseodymium onward electrons only populate the 4f and 6s orbitals with the exceptions of gadolinium and lutetium, where the addition of another electron disrupts either a half filled f-shell or where the shell is entirely populated.[19]

Table 2.2: Valance shell electronic configurations of the f-element metals

Element	Symbol	Electronic Configuration	Element	Symbol	Electronic Configuration
Lanthanum	La	$5d^1\,6s^2$	Actinium	Ac	$6d^1\,7s^2$
Cerium	Ce	$4f^1\,5d^1\,6s^2$	Thorium	Th	$6d^2\,7s^2$
Praseodymium	Pr	$4f^3\,6s^2$	Protactinium	Pa	$5f^2\,6d^1\,7s^2$
Neodymium	Nd	$4f^4\,6s^2$	Uranium	U	$5f^3\,6d^1\,7s^2$
Promethium	Pm	$4f^5\,6s^2$	Neptunium	Np	$5f^4\,6d^1\,7s^2$
Samarium	Sm	$4f^6\,6s^2$	Plutonium	Pu	$5f^6\,7s^2$
Europium	Eu	$4f^7\,6s^2$	Americium	Am	$5f^7\,7s^2$
Gadolinium	Gd	$4f^7\,5d^1\,6s^2$	Curium	Cm	$5f^7\,6d^1\,7s^2$
Terbium	Tb	$4f^9\,6s^2$	Berkelium	Bk	$5f^9\,7s^2$
Dysprosium	Dy	$4f^{10}\,6s^2$	Californium	Cf	$5f^{10}\,7s^2$
Holmium	Ho	$4f^{11}\,6s^2$	Einsteinium	Es	$5f^{11}\,7s^2$
Erbium	Er	$4f^{12}\,6s^2$	Fermium	Fm	$5f^{12}\,7s^2$
Thulium	Tm	$4f^{13}\,6s^2$	Mendelevium	Md	$5f^{13}\,7s^2$
Ytterbium	Yb	$4f^{14}\,6s^2$	Nobelium	No	$5f^{14}\,7s^2$
Lutetium	Lu	$4f^{14}\,5d^1\,6s^2$	Lawrencium	Lr	$5f^{14}\,6d^1\,7s^2$

In solution the lanthanides primarily adopt the 3+ oxidation state as their most stable form. The reasons for this can easily be seen by the filling of their electron orbitals in Table 2.2. Since the 5d and 6s shells extend much further from the nucleus than the 4f shell, electrons in these orbitals are more weakly bound and easily ionized, giving electron configurations of f^0-f^{14} for the trivalent lanthanide ions. Notable exceptions are cerium(IV), europium(II), and Yb(II) where removal or addition of another electron results in an empty, half-filled, or filled f-orbital respectively. The speciation of lanthanides in low pH non-complexing (i.e. perchlorate, triflate, etc.) aqueous media is the hydrated ion $Ln(H_2O)_x^{3+}$ where x = 8-9 molecules of water are coordinated in the inner sphere of the complex.[20] Lighter lanthanides have a coordination number of 9 due to their larger ionic radii and a decreasing trend in the hydration number is observed until

a break point at gadolinium, where a coordination number of 8 is the predominant form.[19] These coordination numbers tend to be adopted for non-aqueous media when the size or spacing between the inner sphere coordinating groups is not significantly different than that of water.[21]

2.3.2. Actinides

The most important actinide elements in fuel reprocessing are uranium, plutonium, neptunium, americium, and curium.[5] Berkelium and californium are also produced but in such yields that are of little consequence for a uranium light water reactor.[22] Actinides heavier than uranium are not found in nature (with exceptions such as natural Oklo reactor) due to their short half-lives compared to the age of the solar system, and are the result of successive neutron captures in uranium-238 and uranium-235. The elements lighter than uranium are the result of decay series from those heavy actinides.

The chemistry of the lighter actinides (other than actinium) is significantly different than any of the lanthanides. So different, in fact, that early conceptions of the actinide series placed these elements below the 5d block, mainly from the similar behavior of the strongly tetravalent thorium ion Th^{4+} to both Zr^{4+} and Hf^{4+} and uranium's ability to form multiple oxidation states akin to tungsten.[18,19] With the synthesis of new transactinide elements it was discovered that these elements had chemistry more similar to that of uranium than their assumed d-block analogues. The "actinide concept" was introduced by Glenn Seaborg in 1944 to explain this discrepancy, and instead placed the actinides directly below the lanthanides on the periodic table. This theory was proved to be correct

as it was shown these new elements had spectral lines unlike the d-block metals and with the synthesis of americium and curium they proved to have very similar elution behavior to their lanthanide analogues europium and gadolinium on chromatographic columns.[22]

It is easy to understand the initial belief of the actinides belonging to the d-block metals when looking at the electronic configuration of thorium (Table 2.2). Thorium was shown to have an electronic configuration of $7s^2 6d^2$, where its lanthanide equivalent cerium has one 5f-electron. After thorium the electronic configurations of the actinides become more like those of the lanthanides with one d-electron while filling the 5f-orbital and eventually mirroring the 4f-metals completely starting with plutonium.

While relativistic effects play a minor role in determining the chemistry of the lanthanides, the actinides are strongly influenced by the high velocities of the inner most electrons. The average radial velocity of a 1s electron can be calculated as a function of the nuclear charge Z:

$$v = Z\alpha c \ \approx \frac{Zc}{137} \tag{2.2}$$

where α is the fine structure constant and c is the speed of light.[23] For the actinides this equates to a 1s electron orbital velocity of roughly 2/3s the speed of light, while the other inner s and p orbital electrons experience a similar effect. The increased mass due to these relativistic electrons causes a contraction of the s and p-orbitals as a result of their greater probability density closer to the nucleus compared the d and f-orbitals. While the 7s and 7p orbitals are slightly contracted the 6d and 5f orbitals are expanded because of

16

the shielding provided by the 7s and 7p orbitals. The end result is that there is very little energy difference between the outer s, p, d, and f levels of the actinides and therefore the 6d and 5f shells play a much more important role in available chemical (occasionally even covalent) bonding relative to the lanthanides.

Table 2.3: Oxidation states of f-elements (underlined numbers are most common oxidation states in aqueous media, parentheses are only stable in solid state)[19]

Lanthanides	La	Ce	Pr	Nd	Pm	Sm	Eu	Gd	Tb	Dy	Ho	Er	Tm	Yb	Lu
				(II)		II	II			(II)			(II)	II	
	III	III	III	III	III	III	III	III	III	III	III	III	III	III	III
		IV	(IV)	(IV)					(IV)	(IV)					

Actinides	Ac	Th	Pa	U	Np	Pu	Am	Cm	Bk	Cf	Es	Fm	Md	No	Lr
		(II)					(II)			(II)		(II)	II	II	
	III	(III)	(III)	III	III	III	III	III	III	III	III	III	III	III	III
		IV	IV	IV	IV	IV	IV	IV	IV						
			V	V	V	V	V								
				VI	VI	VI	VI								
					VII	VII									

The small energy differences in the outer actinide orbitals allow for a wide range of available oxidation states in aqueous solution. Up until neptunium the primary aqueous stable ion corresponds to the f^0 configuration for that particular element, though other oxidation states are available for protactinium and uranium (Table 2.3). Beyond plutonium the most stable oxidation state is the 3+, resembling the lanthanides with the exception of nobelium which gains a more stable $5f^{14}$ configuration by remaining in the divalent 2+ state. Like the lanthanides the trivalent and tetravalent actinides are found in non-complexing media as the bare cation surrounded by an inner hydration sphere of

water molecules. Any bare pentavalent and hexavalent actinide ions are immediately hydrolyzed to form linear dioxocations of the forms AnO_2^+ and AnO_2^{2+} with the exception of protactinium, whose exact form is not agreed upon.[19,24] The heptavalent actinides are only stable in basic solutions when conditions are sufficiently oxidizing.

The actinide ions are also hydrated by water in their inner coordination sphere. The exact hydration numbers are of debate, with some reports stating a variation of 8-9 like the trivalent lanthanides while others report higher values of 10-12 due to the increased ionic radii of the actinides.[25–27] Reported values for the tetravalent ions range from 7-10 while the pentavalent and hexavalent actinides are generally agreed to have hydration numbers of 5 or 6 molecules of water. The strength of the complexes these ions form generally follows the effective cationic charge of the actinide ion which is related to the oxidation state:

$$An^{4+} > AnO_2^{2+} \sim An^{3+} > AnO_2^{2+}$$

(2.3)

with values of 3.3 and 2.2 for the effective cationic charges of AnO_2^{2+} and AnO_2^+ respectively, though geometric restrictions can cause an inversion of the complex strength between the trivalent and hexavalent states.[28]

2.3.3. *Separation of the Actinides and Lanthanides*

Actinides which have multiple oxidation states available can easily be separated using a variety of solvent extraction or chromatographic techniques by exploiting the differing

strength of complexation of the different oxidation states. However, it can be difficult to separate the trivalent actinides from the trivalent lanthanides, and this separation is one of the main focuses of modern fuel reprocessing methods.[29] Ligands that bind exclusively through hard donor oxygen atoms show little to no difference in complexation ability of the lanthanides and actinides.[30] However, it has been known that atoms with softer donor groups such as sulfur, or particularly nitrogen atoms, will selectively bind the actinides over the lanthanides.[31]

The differing chemical behaviors between the lanthanides and actinides of equal valence towards various electron donating groups can be attributed to the differences between the participation of the 4 and 5f-orbitals in chemical bonding. As stated previously the 4f electrons lie buried beneath the 5d and 6s orbitals and their inefficient shielding character causes the lanthanide ions to contract in size. A smaller sized ion with large charge density leads to a more rigid electron shell, thereby giving harder Lewis acid character. In contrast the 5f orbitals are much more available for chemical interactions due to their relativistic inner electrons. The extension of these orbitals combined with the generally larger size of the actinide ion compared to the lanthanide ion due to the addition of another energy level gives the actinides slightly more covalency and thus softer Lewis acid character. The increase in covalency is a result of the actinide's more available 5f-electrons (and some evidence of d-electrons) for participating in back-bonding into π^* orbitals ligands with aromatic nitrogens.[32] It should be noted that both the trivalent lanthanide and actinide ions are categorized as hard Lewis

acids, however, the difference in chemical hardness is sufficient enough to be exploited for separation purposes.[33]

2.4. Solvent Extraction

Solvent extraction, or liquid-liquid extraction, is an extremely powerful technique for the separation of chemically dissimilar compounds from a given solution and is used in both laboratory and industrial level applications.[34] Separation is performed by exploiting the differing affinities (polarity, hydrophobicity, etc.) of a given set of compounds for two immiscible phases. Generally these phases consist of water and a hydrophobic organic solvent, though ionic liquids can also be used in place of one of these phases and have recently generated much interest for the purposes of solvent extraction of metals from used nuclear fuel.[35–39] After sufficient mixing, solutes will partition into the particular phase which lowers the overall chemical potential of the system until equilibrium is reached.[40] This partitioning of solutes is often referred to as the distribution ratio or distribution coefficient D and defined as the ratio of the sums of all species of an analyte x in the organic phase to that of the aqueous:

$$D = \frac{\Sigma[x]_{org}}{\Sigma[x]_{aq}} \qquad (2.4)$$

Another important term is the separation factor, which gives the relative partitioning between two analytes of interest in solution. It is defined as the ratio of the distribution coefficients between two analytes *x* and *y*:

$$SF = \frac{D_y}{D_x}$$

(2.5)

In reprocessing of used nuclear fuel, metal ions are typically present in the form of dissolved nitrate salts resulting from the nitric acid dissolution process of the fuel. Inner sphere complexation by water molecules means that these salts are very hydrophilic and would be difficult to partition into an organic phase by simply contacting with a non-solvating diluent. In order to facilitate this process, organic soluble complexing agents are added to the system in order to increase the affinity of the metal ion of interest for the organic phase. The most widely used solvents for fuel reprocessing are aliphatic hydrocarbons; typically either n-dodecane or kerosene are the diluents of choice. Ligands utilized for separations will be designed containing functional groups which assist solvation into the organic phase. For example N, N'-tetraoctyldiglycolamide (TODGA, Figure 2.3) is designed to extract trivalent actinides and lanthanides from acidic solutions.[41] The octyl chains branching from the amide nitrogen increase the solubility of the ligand, and also the extracted metal-ligand complex, in the organic phase.
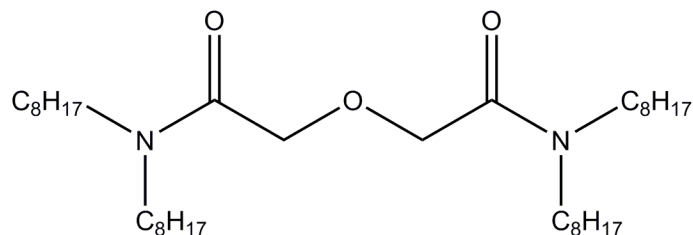
Figure 2.3: Structure of N, N'-tetraoctyldiglycolamide (TODGA)

2.4.1. *Neutral Solvate Ligands*

There are two main types of extraction mechanisms currently employed in the major fuel reprocessing schemes. The first solvent extraction methods used in reprocessing of used nuclear fuel were neutral solvate extraction mechanisms.[42] In this mechanism a ligand (L) which contains a basic electron donating group coordinates to a metal ion (M^z) with charge z forming either an inner or outer sphere coordination complex. During this process there is no change in electrostatic charge between the metal and metal:ligand complex. The previously mentioned TODGA molecule belongs to this class of ligands.

Traditionally reprocessing of fuel in this method has been done through the oxygen atoms of carbonyl or phosphoryl moieties, though other functional groups containing sulfur and more recently nitrogen donors have been investigated as well.[43–45] Once the metal ion has been coordinated, charge balance is required in order to promote phase transition of the metal:ligand complex. For fuel recycling this largely means compensation of the electric charge of a metal via the nitrate anions in solution from the dissolution of the chopped fuel by nitric acid:

$$M^{z+}_{(aq)} + zNO^-_{3\,(aq)} + nL_{(org)} \leftrightarrows [M(NO_3)_z \cdot L_n]_{(org)} \qquad (2.6)$$
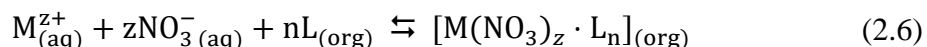
The extent of the distribution of the metal:ligand complex into the organic phase can then be affected by adjusting the concentration of the counter ion such as nitrate in Equation (2.6). Increasing the nitrate ion concentration would result in driving the equilibrium of the reaction to the right, resulting in more partitioning into the organic phase. Lowering the nitrate concentration would then allow the complex to dissociate with the metal and nitrate ion, and thereby back extracting into the aqueous phase. For the purposes of reprocessing, these ligands are for the extraction of metals from solutions of high acidity and salt content, usually ranging from 1-6 M acid but can be even higher than 10 M total anion concentrations depending on the ligand and solvent extraction system involved.[46]

2.4.2. Ion Exchange Ligands

Metals can also be extracted into the organic phase by ligands which can undergo ion exchange reactions. In these extractions a metal ion in the aqueous phase is exchanged for one or more ions in the organic phase. In fuel reprocessing the exchanged ion(s) is generally a hydrogen ion which has been deprotonated from a weak organic acid. For acidic extractants, as with neutral solvate ligands, the ion exchange extractants are often composed of carbonyl or phosphoryl functional groups.[47] However, now these moieties are combined with a hydroxyl group allowing for the release of a proton. As a result ion exchange extraction is highly dependent on the pH of the aqueous phase, with small changes in the acid concentration able to completely change the metal partitioning behavior. For a simple monoprotic acid HA, extraction takes place as:

$$M_{(aq)}^{z+} + zHA_{(org)} \leftrightarrows M(A)_{z(org)} + zH_{(aq)}^{+} \tag{2.7}$$
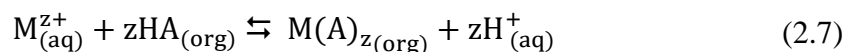
forming the metal:ligand complex which partitions to the organic phase and releasing a number of protons equal to the charge of the extracted ion.

Ion exchange can also be performed with a polyatomic metal anion using a Lewis acid; commonly a quaternary ammonium salt or other alkylammonium species.[40] Formation of a positively charged ion by protonation of a basic group such as a tertiary amine allows for extraction by the formation of an ion pair:

$$R_3N\text{:}_{(org)} + H_{(aq)}^{+} + X_{(aq)}^{-} \leftrightarrows R_3NH^+X_{(org)}^{-} \tag{2.8}$$
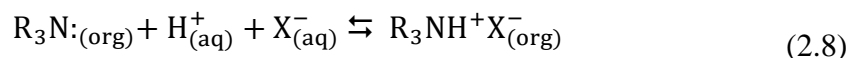
where X represents an anionic metal complex or polyatomic ion. For longer branching aliphatic chains the strength of the alkylammonium complex is an effect of the protonated amine substitution and proceeds as: quaternary$^+$ > tertiary$^+$ > secondary$^+$ > primary$^+$. Basic extractants can be used for separations in fuel reprocessing such as during the recovery of technetium by anionic exchange of TcO_4^-.[48] However, due to the nature of these extractants they are limited in their use to only metals capable of forming stable anionic complexes in solution.

Ion exchange reactions are often more complex than illustrated in Equation (2.7).[49] Since the hydrogen ion concentration will vary with the number of species being extracted when using acidic extractants, strict pH control is needed through the use of

buffers which often affect the extraction equilibria independently as well. Matters are also complicated due to the tendency of these acidic ligands to form dimeric species in non-polar organic solvents.[50,51] Despite these difficulties ion exchange ligands have been successively utilized as both organic phase extractants and aqueous phase soluble hold back reagents for the separations of actinides and lanthanides.

2.5. Reprocessing of Used Nuclear Fuel

Reprocessing of irradiated fuel has been performed since the development of nuclear weapons nearly seventy years ago during World War II. The end goal of the original process was the isolation of the weapons grade plutonium-239 produced in the plutonium production plants at the Hanford site in the state of Washington. Plutonium was initially separated by coprecipitation with bismuth phosphate, leaving uranium in solution as the sulfate complex.[42] After several more oxidation and precipitation steps a pure plutonium product was achieved. This method began to fall out of favor after the war as it produced lots of secondary solid wastes and did not recover the also useful uranium in solution. Consequently the bismuth phosphate process was phased out and replaced by solvent extraction methods in the late 1940s and early 1950s.[52]

2.5.1. PUREX

One of the first solvent extraction methods applied for the purpose of separating elements in irradiated nuclear fuel was the extraction of uranium and plutonium by

tributyl phosphate (TBP, Figure 2.4) developed at Oak Ridge National Laboratory in 1944.[53] Because of the secrecy surrounding the Manhattan Project the information about TBP's ability to extract nitrate salts of tetravalent and hexavalent actinides into aliphatic diluents from nitric acid was not published until 1949.[54] Because of its usefulness in the separation of uranium and plutonium TBP became the basis for the PUREX (**P**lutonium and **U**ranium **R**eduction **Ex**traction) process which is now the most prevalent form of used fuel reprocessing in the world and is considered to be one of the world's most well studied metal extractants.[55]
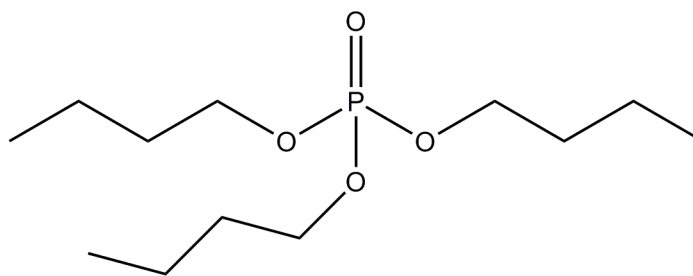
Figure 2.4: Tributyl phosphate (TBP)

TBP is a neutral solvate ligand which complexes metals through the electron donating oxygen of the phosphoryl group. In the PUREX process irradiated fuel dissolved in nitric acid is contacted with a 30% solution of TBP diluted in a heavy aliphatic hydrocarbon such as n-dodecane or kerosene. Because it is a neutral solvate extraction molecule, extraction with TBP is improved by increasing the nitrate ion concentration of the aqueous phase. Dissolved irradiated fuel has a typical nitric acid concentration in the range of 3-4 M and thus TBP extracts very efficiently under these conditions.[56] Tetravalent and hexavalent actinides are extracted into the organic phase, leaving

pentavalent and trivalent actinides as well as most fission products behind in the aqueous layer. 30% TBP is employed because as the percentage of TBP is increased the solution begins to extract other metals which are undesirable, such as americium, while also having other detrimental extraction characteristics, such as increased viscosity.[57]

After the extraction of the tetravalent plutonium and hexavalent uranium (as well as any neptunium in the tetravalent and hexavalent oxidation states), uranium is separated by the introduction of a reducing agent such as ferrous sulfamate.[58] Plutonium(IV) is reduced to plutonium(III) and stripped into the aqueous phase while the oxidation state of uranium(VI) is unaffected and is retained in the organic layer.

2.5.2. CCD/PEG

Cesium-137 and strontium-90 are two of the most important isotopes with regards to disposing of used nuclear fuel. Both of these isotopes have half-lives of approximately 30 years, produce significant amounts of heat from their radioactive decays, are environmentally mobile, and present significant radiotoxicity health hazards.[5] Neutral solvate extractants tend to extract these elements poorly due to their strongly ionic character. Some more common ion exchange extractants also have difficulty in the extraction and separation of cesium and strontium from other elements in solution.[59] As such a cation ion exchange separation process using chlorinated cobalt dicarbollide (CCD) polyethylene glycol (PEG, Figure 2.5) was developed by Idaho National Laboratory and the Khlopin Radium Institute.[60]
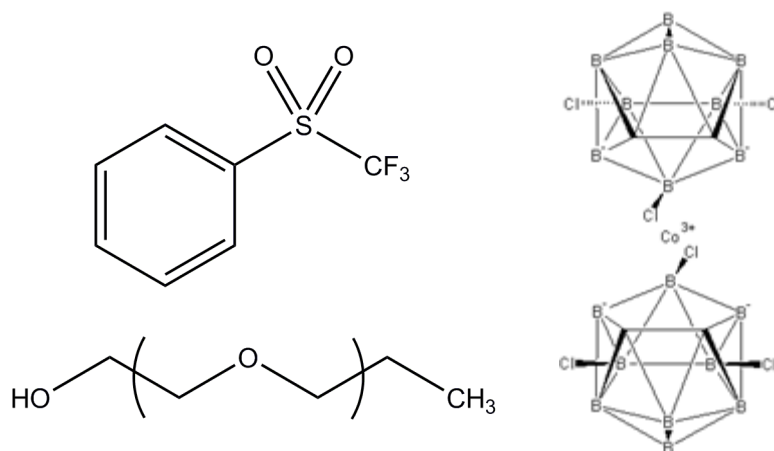
Figure 2.5: Trifluoromethylphenyl sulfone (FS-13, top left), polyethylene glycol (PEG, bottom left), and chlorinated cobalt dicarbollide (CCD, right)

Chlorinated cobalt dicarbollide is an extremely stable halogenated carborane-based anionic cage with an overall charge of -1. Despite its strong acid-like characteristics it has significant solvating power for metals in polar organic solvents.[61] Rather than a complexation reaction, metals partitioned to the organic phase are nearly completely dissociated from the CCD anion. CCD alone will extract cesium into the organic phase. Strontium requires the addition of polyethylene glycol (typically PEG-400) to assist in the dehydration and phase transfer of the Sr^{2+} ion. CCD is very hydrophobic and requires a polar organic solvent in order to allow for dissociation of the metal and CCD in the organic phase to carry out extractions.

Original experiments with CCD used various nitro-aliphatic and nitro-aromatic solvents such as nitrobenzene.[62] Though these solvents had reasonably good performance for this process, the health, environmental, and safety hazards associated with these solvents has led to the use of a less hazardous diluent. Currently the CCD/PEG process solvent of choice is phenyltrifluoromethyl sulfone or FS-13 (Figure

28

2.5), a polar solvent developed to support extractions with ionic salts of CCD. FS-13 was also chosen because of its good hydrolytic and radiolytic stability, high extraction yields, and lack of third phase formation.[63] Other developments in the separation of cesium and strontium include removal by crown ethers as well as calixarenes in the FPEX process.[30]

2.5.3. TRUEX
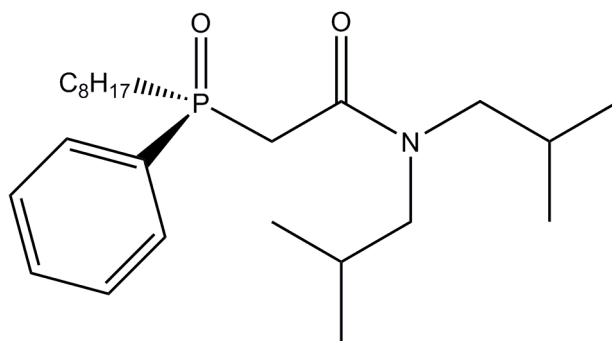
Figure 2.6: Carbamoylphosphine oxide (CMPO)

Octyl-phenyl-N,N-diisobutylcarbamoylmethylphosphine oxide (OΦDiBCMPO or CMPO, Figure 2.6) is a neutral ligand extractant developed at Argonne National Laboratory to be the most compatible with the solvent conditions used during PUREX.[64] Despite its seemingly bidentate nature the primary purpose of its structure is for the phosphoryl group donor to act as the main electron donor, with the carbonyl group acting as an intramolecular buffering agent, though it is possible for the carbonyl to act as a secondary donor group.[57] This intramolecular buffering suppresses the negative effect on the distributions of the metals due to the simultaneous extraction of nitric acid by the ligand at higher acidities.

When combined with the PUREX process's TBP in n-dodecane, CMPO is the basis

for the TRUEX (**TR**ans**U**ranium **EX**traction) process for the removal of trivalent f-elements from PUREX raffinates while providing good separation from the transition metals.[65,66] The concentration of TBP is the same which is used during PUREX and therefore does not effectively extract the trivalent actinides and lanthanides. Rather, TBP acts as a phase modifier which constrains the tendency of CMPO to form a second organic layer or "third phase" caused by nitric acid extraction when dissolved in n-dodecane alone and increasing the solubility of CMPO and its metal complexes in solution.[67] Furthermore the addition of TBP reduces competition between extractable metals and nitric acid, improving their dependencies on the acidity of the system. Distribution ratios remain relatively constant between 1-6 M nitric acid making TRUEX attractive from an engineering perspective, as on the engineering scale, exact acid concentrations can be difficult to maintain within a narrow range.[64] A Russian based variant of the TRUEX process has also been studied using a diphenyl rather than octyl-phenyl analogue of the CMPO used in the American TRUEX solvent.[30,68]

2.5.4. TALSPEAK

The extractant di-(2-ethylhexyl)phosphoric acid (HDEHP or DEHPA, Figure 2.7) has been known to be an efficient extractant for metal ions from mineral acid solutions since the late 1950s.[69] HDEHP is an ion exchange ligand that is soluble in non-polar organic diluents. Hydrogen bonding amongst the phosphoric acid groups between two HDEHP molecules leads to significant formation of dimers in solution.[50] These dimers are maintained in the extracted complex with the metal ion:

$$M_{(aq)}^{z+} + z(HDEHP)_{2\,(org)} \leftrightarrows M(HDEHP)_z(DEHP)_{z\,(org)} + zH_{(aq)}^+ \qquad (2.9)$$

releasing one proton per charge of the metal complex. For trivalent lanthanides and actinides this results in a third order dependence of the distribution ratio on the equilibrium proton concentration. This acid dependency requires the use of a buffer when stricter pH level control cannot be applied during engineering scale processes. The most common buffer used is lactic acid, though other simple carboxylic acids have been investigated such as malonic and citric acid.[70–72] When using HDEHP as an extractant there are nearly five orders of magnitude difference between the distribution ratios across the entire lanthanide series, however there is little to no separation between the trivalent actinides and lighter lanthanides which are of more importance from the perspective of waste management.[3,73]
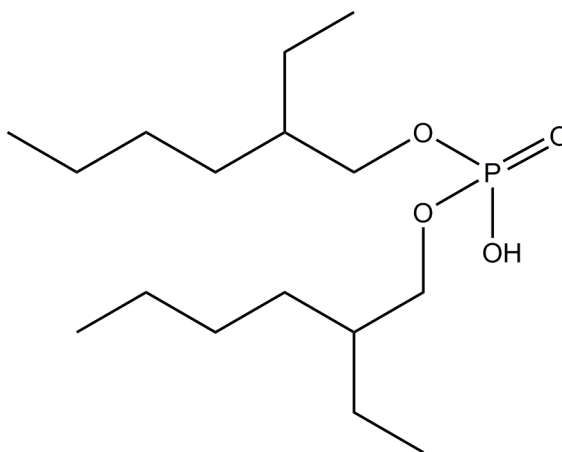
Figure 2.7: Di-(2-ethylhexyl)phosphoric acid (HDEHP)

Since the solution chemistries of the trivalent actinides and lanthanides are very similar, their separation from each other can be a challenging task. One of the simplest ways of separation is exploiting the slight prevalence in the complexation of the actinides compared to lanthanides of the same oxidation state by soft donor atoms, the nature of which is explained in section 2.3.3. The effects of altering the aqueous phase chemistry of the HDEHP in dilute acid solutions by the addition various carboxylic and aminopolycarboxylates such as diethylenetriaminepentaacetic acid (DTPA, Figure 2.8) were investigated by Weaver and Kappelmann in the 1960s.[74] The investigators found that when using a lactic acid buffer system, DTPA was able to effectively strip and separate trivalent f-elements with a separation factor $\alpha = 10$ between the distributions of the least separated lanthanide and actinide, these being neodymium and californium respectively. This reprocessing method has been dubbed TALSPEAK for "**T**rivalent **A**ctinide and **L**anthanide **S**eparations by **P**hosphorous-reagent **E**xtraction from **A**queous **K**omplexes". Attempts have been made to combine the TALSPEAK and TRUEX systems in a combined TRUSPEAK process. However, this combined neutral and acidic extractant process has had issues stemming from interaction of HDEHP and CMPO in the organic phase.[75,76]

Figure 2.8: Diethylenetriaminepentaacetic (DTPA)

2.5.5. UNEX

Each of the mentioned reprocessing strategies in the prior sections has been previously proposed to be performed stepwise as part of a greater partitioning and transmutation plan.[77] Figure 2.9 illustrates this expanded concept for the previously proposed UREX+ suite of reprocessing steps.[78] After chopping and dissolution of irradiated fuel in nitric acid, uranium, plutonium, and technetium are recovered by the PUREX process. Next the raffinate from the PUREX stream would be contacted with the CCD/PEG solvent for the removal of cesium and strontium. Actinides and lanthanides are then extracted using the mixed TBP/CMPO system of the TRUEX process. The transition elements remaining in the aqueous phase would then be sent for decay storage while the organic phase would then go on to the TALSPEAK partitioning of the lanthanides and actinides. Actinides would then undergo transmutation to shorter lived isotopes and the lanthanides placed into short term decay storage.

33
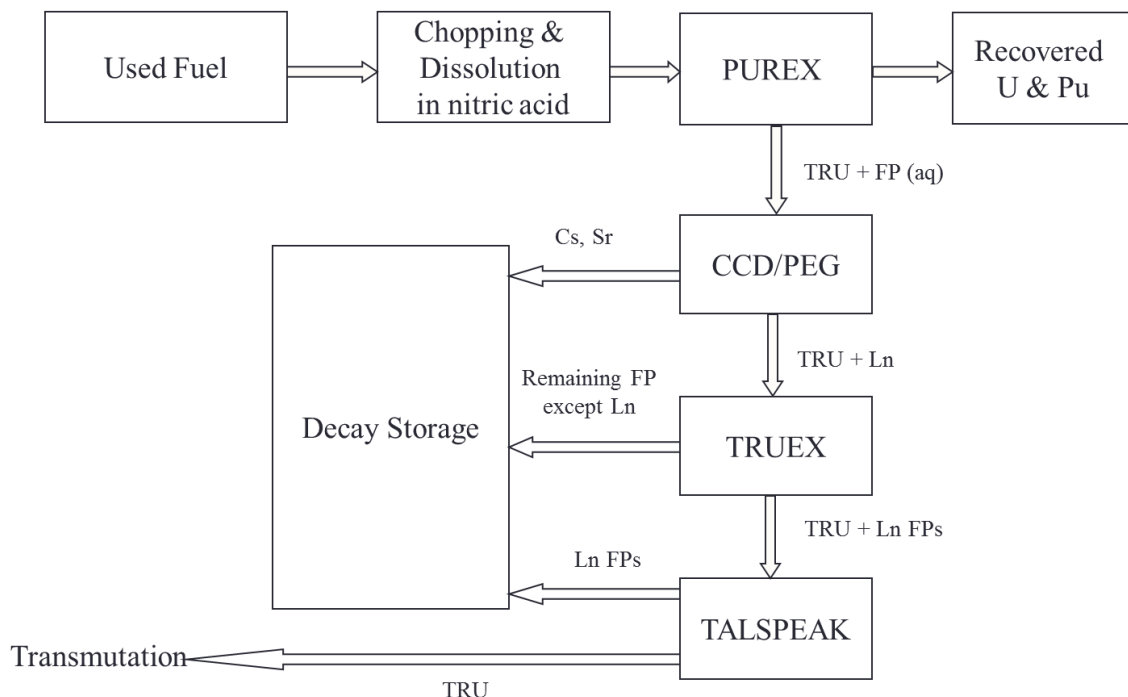
Figure 2.9: UREX+ multi-stage partitioning flowsheet of irradiated nuclear fuel

The UNEX (**Un**iversal Solvent **Ex**traction) process was developed by Idaho National Laboratory and the Khlopin Radium Institute as an alternative method of separating all important elements in used nuclear fuel. Rather than several individual steps, UNEX's goal is to simultaneously separate and recover all of the major radionuclides from legacy waste raffinates left after the removal of uranium during the PUREX process.[79] UNEX is essentially a combination of aspects from both the CCD/PEG and TRUEX processes. Conditions are made so that cesium and strontium are extracted in the same manner as described previously, but the addition of CMPO from the TRUEX process allows for the concurrent extraction of elements which are inextractable by the pure CCD/PEG process. The PUREX portion of the flowsheet remains unaffected and is performed as normal.

The reasoning behind this combination is rather than using a complex cascade of several different organic solvent extraction systems, a single consistent organic phase can be used. Separations of various elements would then be performed by the use of multiple aqueous phases of varying stripping agents and acidities to selectively partition the desired elements at each decontamination step as diagramed in Figure 2.10. This would have the effect of cutting down the amounts of hazardous waste generated by the use multiple organic phases and ultimately the monetary costs associated along with it.
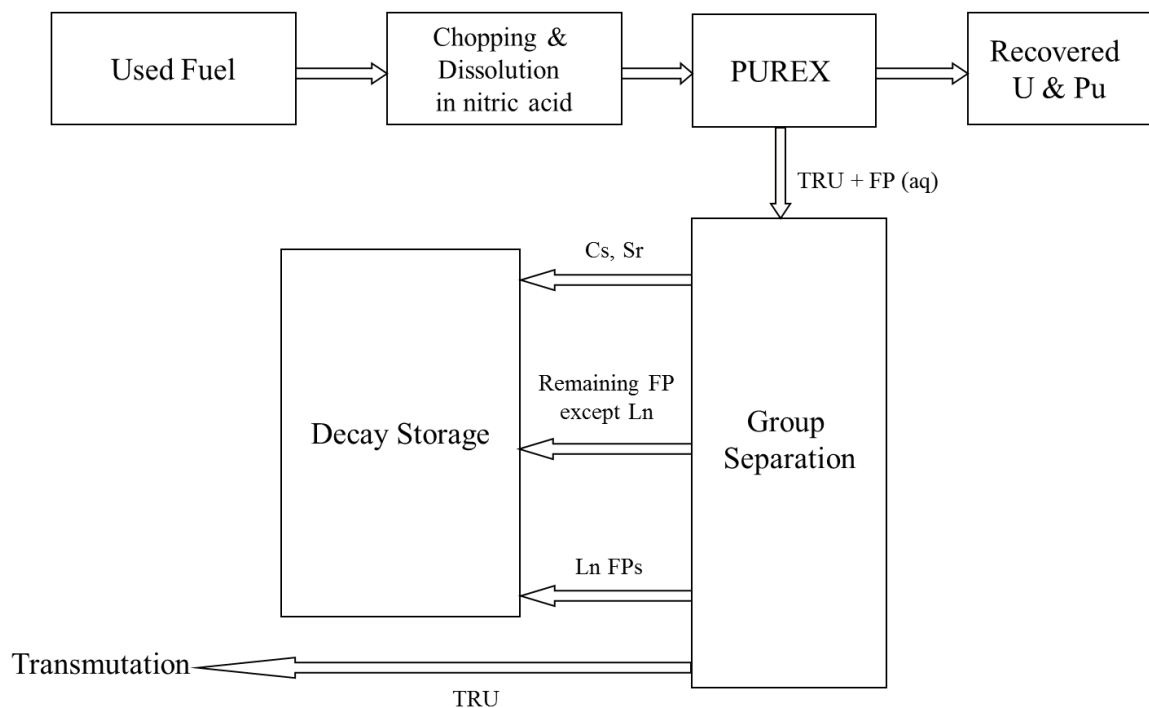
Figure 2.10: UNEX separation concept

The UNEX process is currently one of the only demonstrated methods for removal of all major radionuclides in a single process.[80] However, as of yet no tests have been conducted using actual PUREX raffinates. In its current inception the UNEX has

limitations with respect to its usage of the neutral extractant CMPO. The synthesis of CMPO is expensive and difficult compared to other neutral solvate ligands. CMPO and its metal:ligand complexes also both have limited solubility in polar diluents such as FS-13 compared to non-polar diluents, limiting CMPO's application in high level waste reprocessing. As a result, expanding the application of the UNEX process for potential applications in reprocessing used nuclear fuel requires finding a new suitable substitute for CMPO.

2.6. "CHON" Extractants

A rather common theme amongst extractants proposed for fuel reprocessing in the United States is the use of organophosphorous ligands, namely TBP, HDEHP, and CMPO. The use of organphosphorus ligands is often undesirable from the perspective of reprocessing management.[81] These ligands generate significant amounts of waste which is difficult to reduce in volume. Since the late 1980s there has been a drive to study new types of extractant molecules, particularly in Europe, where the extractant molecule only consists of carbon, hydrogen, nitrogen, and oxygen atoms.[82] The so-called "CHON principle" is centered around the fact that ligands which only contain CHON atoms can be completely incinerated to form gaseous products, while extractants containing phosphorous and sulfur atoms will form solid residues and contribute to acid rain if incinerated.[83]

2.6.1. Amides

One of the simplest types of CHON ligands are organic amides. Amides extract metals by coordination of the electron rich oxygen of the carbonyl group to the metal Lewis acid. The nitrogen, having sp^2 geometry, does not participate directly in extractions. The basicity of the carbonyl group and solubility of the ligand in the organic phase can easily be affected by changing the substituents from the nitrogen and carbon atoms. Initial studies using monoamide ligands led to the investigation of diamidic ligands, particularly derivatives of malonic acid, due to the increased solvating power provided by using a multidentate ligand.[84,85] Malonamides are the basis for the French DIAMEX (**DIA**mide **EX**traction) process and serve essentially the same purpose as the TRUEX process by simultaneously extracting trivalent actinides and lanthanides from PUREX raffinates.[86,87] Other amidic extractants of recent interest include derivatives of diglycolamide, mainly tetra-octyl-diglycolamide (TODGA) and tetra-ethyl-hexyl-diglycolamide (TEHDGA). These amides also serve the same purpose as CMPO and have undergone extensive research predominantly by German and Japanese scientists,[37,41,88–92] though interest has been generated in the US as possible replacements for CMPO in a modified TRUSPEAK design called ALSEP (**A**ctinide and **L**anthanide **SEP**aration).[93]

2.6.2. N-Donor Extractants
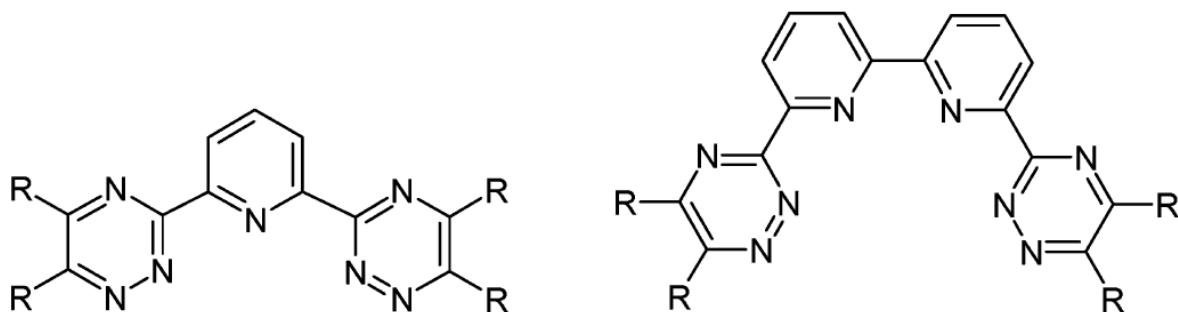
Figure 2.11: BTP (left) and BTBP (right) heterocyclic N-donor ligands

An issue generally associated with amides and other oxygen-based hard donor extractants is the negligible ability to differentiate and therefore preferentially complex the hard Lewis acid trivalent actinides over the lanthanides. In order to preferentially complex actinides several new N-donor ligands, which exploit the small difference in chemical hardness exhibited by the actinides, have been studied.[32,94,95] Though initial investigations showed poor extraction from acidic solutions due to the protonation of the nitrogen groups, interest in N-donor ligands experienced a resurgence with the discovery of the extraction properties of bis-triazinyl-pyridines (BTPs, Figure 2.11) by Kolarik *et. al.* in the late 1990s.[96] These BTP ligands showed excellent selectivity for trivalent actinides over the lanthanides, with separation factors of americium and europium greater than 100.[97] However, these ligands showed poor extraction kinetics and were especially unstable to degradation by hydrolysis and radiolysis.[98–100]

New research has been conducted using different substituents branching from the triazinyl rings as well as similar ligands based on the bistriazinylbipyridine (BTBPs, Figure 2.11) backbone.[43,101,102] These ligands have shown more resilience to degradation

by hydrolysis and radiolysis, although kinetics of extraction have continued to be a drawback and require the addition of a phase transfer reagent in order to achieve short equilibrium times.[103]

2.6.3. Mixed N, O-Donor Ligands

As mentioned previously the hard-donor oxygen ligands discussed in section 2.6.1 do not show selectivity for the extraction of trivalent actinides and lanthanides, while the soft nitrogen donor ligands in section 2.6.2 separate the trivalent f-elements but do not efficiently extract the lanthanides to an appreciable extent. In some reprocessing techniques such as UNEX, it is desirable to extract both actinides and lanthanides simultaneously while preferentially extracting the actinides. This can be achieved by using a ligand which contains both nitrogen and oxygen donor groups, which allows for a one stage extraction of both trivalent f-element groups followed by a secondary stripping stage where the actinides are retained in the organic phase by taking advantage of the more strongly complexing N-donor group.

Initial investigations of mixed N,O-donor ligands were performed using amide derivatives of 2-pyridine carboxylic acid also known as picolinic acid.[104] The bidentate configuration of these ligands does separate trivalent actinides and lanthanides with a reasonably high separation factor ($SF_{Am/Eu} \sim 8$), however the extraction of these metals into the organic phase is very poor and decreases with increasing aqueous phase acidity. The pKa of the pyridine nitrogen in picolinamides is approximately 1.9, and thus the ligand is highly protonated in acidic media. Protonation of the ligand competes with the

metal ions for complexation, requiring the addition of high concentrations of a salting out reagent such as $LiNO_3$ in order to get practical distribution ratios. Other amide ligands such as derivatives of phenanthroline exhibit high separation factors ($SF_{Am/Eu} \sim 20\text{-}50$), but also show a significant decrease in distribution ratios due to the ease of protonation.[105]
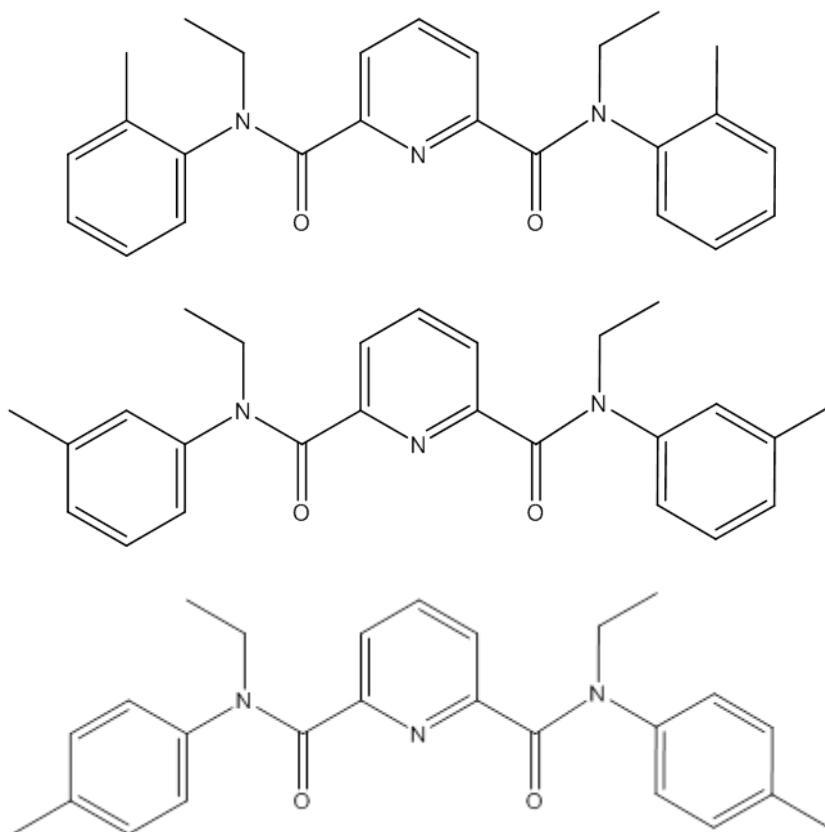
Figure 2.12: Isomers of EtTDPA ortho (top), meta (middle), para (bottom)

More recently diamides of dipicolinic acid have been studied for their extraction and separation of the trivalent f-elements in polar organic solvents.[106–109] Dipicolinamides are capable of acting as tridentate ligands with two oxygen donor groups and a central

pyridine nitrogen. The addition of this second carbonyl group severely inhibits protonation in highly acidic media with pK_as of approximately 0.14, though this second carbonyl group lowers the separation achieved to $SF_{Am/Eu} \sim$ 4-6.[110] It was reported that among other dipicolinamides, three isomers of *N,N'*-diethyl-*N,N'*-ditolyl-dipicolinamide (EtTDPA, Figure 2.12) showed the best extractability toward americium with a slight extraction preference over europium.[111] A synergistic effect was observed in the extraction of trivalent metals by different dipicolinamides (DPA) in the presence of CCD,[112] leading to diamides of dipicolinic acid being proposed as a replacement for CMPO in a modified UNEX solvent with the ultimate goal of the separation of trivalent actinides and lanthanides.[113]

Though the extraction of americium and the lanthanides were studied, little work was done on the chemistry and separation of the actinides from nitric acid solutions by EtTDPA. The purpose of the following work in this dissertation is to evaluate the actinide extraction chemistry as well as determine the stability of the ligand when subjected to hydrolysis and radiolysis and investigate the thermodynamics of metal complexation with EtTDPA.

2.7. Chemical Equilibria

2.7.1. *Equilibrium and Stability Constants*

Investigating chemical equilibria during solvent extraction allows for deeper insight into the nature of the extracted complexes as well as the prediction of the metal

partitioning under various conditions. For a general neutral solvate extraction in nitric acid, the reaction would proceed as:

$$y(M^{z+})_{(aq)} + n(L)_{(org)} + x(NO_3^-)_{(aq)} \leftrightarrows \left[L_n \cdot M_y(NO_3^-)_x\right]_{(org)} \qquad (2.10)$$
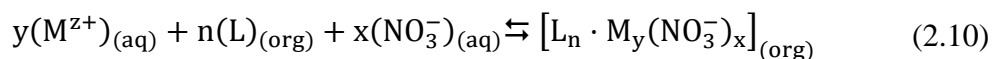
where z is the charge of the metal cation, and y, n, and x are the stoichiometries of the metal, ligand, and nitrate anion respectively. Using the definition of chemical activity $\{A\} = \gamma*[A]$ where the activity $\{A\}$ is equal to the product of the concentration of the species multiplied by the activity coefficient γ, the equilibrium constant K of Equation (2.10) can then be written in terms of the chemical activities of each species raised to their stoichiometric coefficient as the quotient of the products over reactants:

$$K = \frac{\{L_n \cdot M_y(NO_3)_x\}}{\{M^{z+}\}^y\{L\}^n\{NO_3^-\}^x} \qquad (2.11)$$

Species in the organic phase are often assumed to have activity coefficients of one, though this is not always a correct assumption depending on the nature of the solvent extraction system.[114,115] When such situations occur it is commonly corrected by using solutions of dilute concentrations based on the principle that the activity coefficient of an analyte approaches one at infinite dilution.[116] If there is only one primary species of metal extracted into the organic phase, Equation (2.11) can be rewritten using the definition of the distribution ratio from Equation (2.4) to produce Equation (2.12) and its logarithmic form Equation (2.13):

$$K = \frac{D}{\{M^{z+}\}^{y-1}\{L\}^n\{NO_3^-\}^x} \qquad (2.12)$$

$$\log D = \log K + n\log\{L\} + x\log\{NO_3^-\} + (y-1)\log\{M^{z+}\} \qquad (2.13)$$

Holding all other variables constant and taking the partial derivative of this equation with respect to a given variable gives the rate of change in the distribution ratio relative to the change in concentration of that reactant (L in this example):

$$\frac{\partial(\log D)}{\partial(\log L)} = n \qquad (2.14)$$

or in other words the stoichiometric dependence of that reactant on the extracted complex. This procedure can then be repeated to determine the stoichiometry of all the participants in the reaction assuming that there are no significant interfering reactions simultaneously occurring in solution.

The equilibrium constant K describes the extent that an overall reaction will proceed with respect to the concentrations of its constituents. However, it is often convenient to define a particular reaction using a stability or formation constant β rather than K. Whereas K can refer to a reaction with multiple products and reactants, the stability constant β refers only to the strength of formation of a complex between two species in

solution. To illustrate this concept, for the formation of a metal:ligand complex ML between a generic metal M (charges omitted) and a ligand L:

$$M + L \leftrightarrows ML \tag{2.15}$$

The equilibrium constant K for this expression as well as the stability constant β can be written as:

$$K = \beta = \frac{[ML]}{[M][L]} \tag{2.16}$$

For a species capable of forming a second metal:ligand complex the equilibrium constant K_2 for the second reaction would be written as:

$$K_2 = \frac{[ML_2]}{[ML][L]} \tag{2.17}$$

Since K is a step-wise constant, each stage of the reaction is incorporated into its own equilibrium constant describing how far that particular step proceeds. However, the stability constant β_n is the product of all the previous equilibrium constants from the first to the nth reaction $\beta = K_1 \cdot K_2 \ldots \cdot K_n$ or:

$$\beta_n = \prod_{i=1}^{n} K_i \tag{2.18}$$

giving an overall formation constant in terms of the equilibrium concentrations of the metal, ligand, and metal:ligand complex:

$$\beta_n = \frac{[ML_n]}{[M][L]^n} \qquad (2.19)$$

2.7.2. *Stability Constant Determination*

Determination of the metal:ligand stability constants is imperative for modeling the speciation of chemical systems in solvent extraction. Interactions between the metal ion and other chemical constituents in solution will affect the extraction of metals by a given ligand which will be governed by not only the strength of the metal:ligand complex, but also by the strength of the stability constant between the metal and other ions such as nitrate or chloride as well.[117–119] Various procedures have been applied for the determination of stability constants including potentiometric, spectrophotometric, and solvent extraction methods,[120,121] though any analytical technique capable of determining the concentrations of each species at equilibrium can be implemented.

Because the analytical response of an instrument to the metal:ligand complex is often unknown, a mass balance must be performed to obtain an equation in terms of the independently known measurable terms. Given a solution at equilibrium, the total concentration of a metal will be the sum of the individual concentrations of the free metal and all the metal complexes in solution:

$$[M]_{tot} = [M] + [ML] + [ML_2] + \ \ldots \qquad (2.20)$$

By substituting with Equation (2.16), the concentration can instead be expressed in terms of the stability constants and free metal and ligand concentrations:

$$[M]_{tot} = [M] + \beta_1[M][L] + \beta_2[M][L]^2 + \ ... \qquad (2.21)$$

For a system where only a 1:1 complex is formed and [M] and [L] are measurable, Equation (2.21) is a simple equation where β can be easily solved algebraically. Using spectrophotometry for instance, the stability constant would be related to the concentrations of [M] and [L], the extinction coefficient ϵ_λ at a given wavelength of the free metal and metal:ligand complex, and the total measured absorbance A:

$$A_\lambda = \epsilon_\lambda[M] + \epsilon_{1\lambda}\beta_1[M][L] \qquad (2.22)$$

Assuming the Lambert-Beer Law remains valid, the dependence of A on various equilibrium concentrations of [M] and [L] can be obtained and the values of ϵ and β can be determined. However this calculation can become significantly more difficult when determining the stability constants and extinction coefficients of multiple species in solution which exist simultaneously or when using a method where the equilibrium concentration is given by a more complex equation such as calorimetry. With calorimetry data, fitting the formation of even a 1:1 complex requires using a complicated quadratic equation.

46

When the concentrations of all species cannot be easily determined independently, such in the case of having multiple simultaneous equilibria, it is common to use data fitting software to deconvolute each component's contribution to the measured data. Programs such as SQUAD or Hyperquad are based on iterative non-linear least squares approaches to simultaneously solve multiple unknown values and output various coefficients such molar absorbances and enthalpies in addition to complex formation constants.[122–124] Computationally these programs are quite powerful and useful for data fitting, however there have been multiple instances of criticism due to the ease of obtaining stability constants where researchers will go to extraordinary lengths to add nonsensical species to their chemical model in order to fit experimental data.[124] To ensure that the correct model is being used it is common to validate initial investigations of stability constant values with a second complimentary technique.

3. METHODS

3.1. Synthesis of EtTDPA Isomers
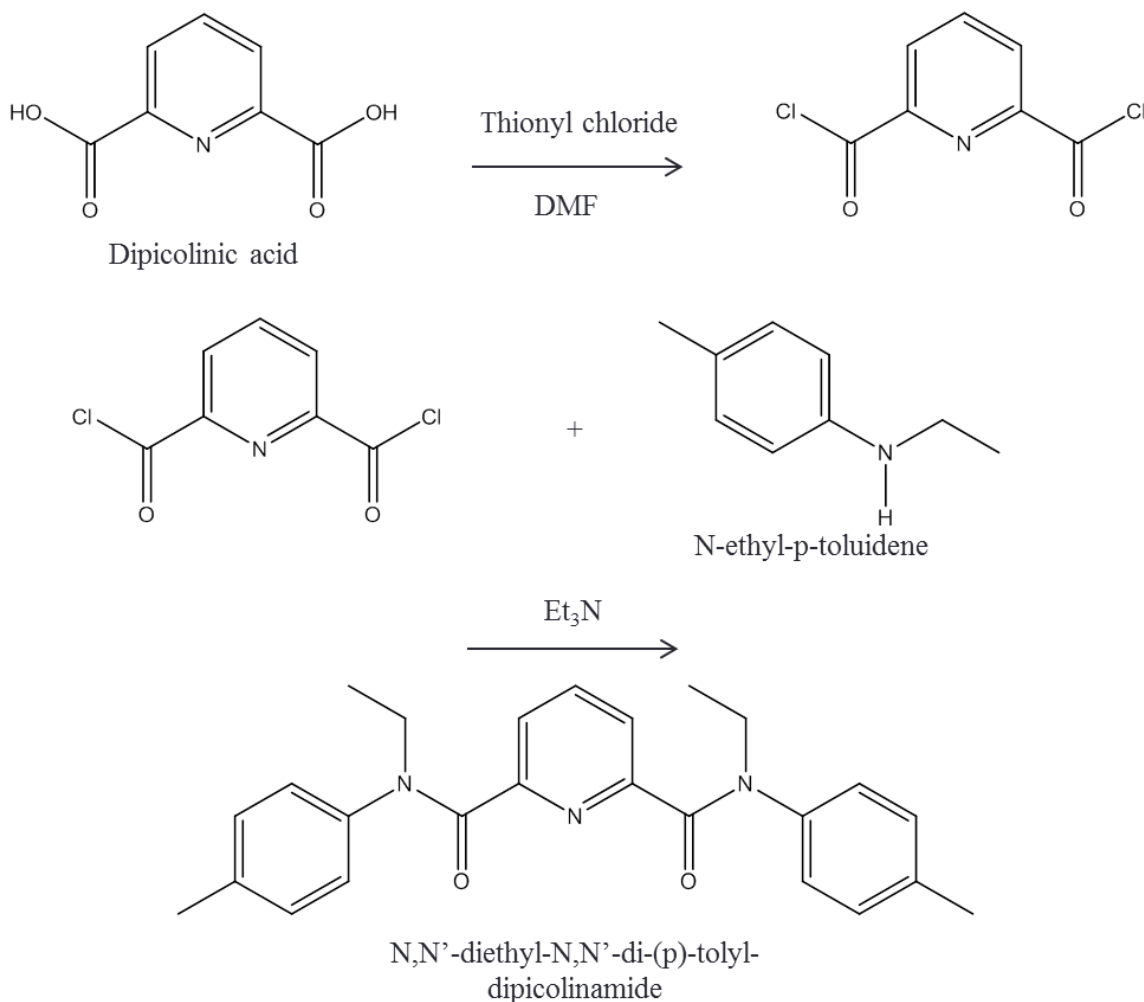
Figure 3.1: Synthesis of Et(p)TDPA

Chemicals used in the synthesis of EtTDPA obtained from TCI Co. LTD were of analytical grade and used without further purification. The synthesis of EtTDPA isomers was performed as previously published and shown in Figure 3.1.[125] Dipicolinic acid was boiled in the presence of stoichiometric excess thionyl chloride using a dimethylformamide (DMF) catalyst under a reflux apparatus until complete dissolution to

convert dipicolinic acid into its acid chloride analogue. The solution was then evaporated and allowed to crystalize before being dissolved in dichloromethane. This was followed by a contact with a 2% HCl solution and then by a saturated sodium carbonate solution to remove any unreacted or partially reacted dipicolinic acid. The acyl chloride solution was added drop wise to the desired isomer of N-ethyl toluidene and triethylamine diluted in dichloromethane, forming the triethylammonium precipitate in the process. 2% HCl was added to the flask to dissolve the precipitate and also to protonate excess triethylamine and N-ethyl-toluidene to make them soluble in the aqueous phase. The aqueous layer was removed and then contacted with a saturated sodium carbonate solution which was then separated and dried under vacuum. Crystals formed during this process were then dissolved in mixtures of hot petroleum and toluene. Recrystallized EtTDPA then went through successive recrystallization steps until the desired purity was achieved.

3.2. Solvent Extraction

3.2.1. *Chemicals*

FS-13 was obtained from Marshallton Research Laboratories Inc. (King, NC, USA). Fresh FS-13 was contacted with a solution of potassium permanganate in sulfuric acid to oxidize any sulfoxide remaining from incomplete oxidation of the sulfur atom during synthesis. The solution was then contacted with a sodium bicarbonate solution to neutralize and strip any acidic products into the aqueous layer.

The distribution ratios of europium, molybdenum, and technetium were determined using the radioactive tracers of Eu-152/154, Mo-99, and its decay product Tc-99m produced by neutron activation of stable europium and molybdenum by the OSU TRIGA reactor. An activated sample of molybdenum oxide was then dissolved in NaOH and diluted with 1 M nitric acid. Europium was irradiated as the oxide form and then dissolved in 1 M nitricacid.

A stock solution of hexavalent uranium with final concentration of 10 g/L of uranium was prepared by dissolution of uranyl nitrate hexahydrate (Mallinckrodt) in 3 M HNO_3. From this stock aqueous solutions with a constant concentration 0.5g/L UO_2^{2+} were prepared by combination of stock solutions of uranyl nitrate, HNO_3 and $LiNO_3$ in the desired ratio of their respective concentrations. Thorium solutions were prepared from the tetrahydrate nitrate $Th(NO_3)_4 \cdot 4H_2O$ in the same manner as described for uranium.

Neptunium-237 was obtained from Oak Ridge National Lab as the oxide form NpO_2. This sample was then dissolved in HCl and passed through a column containing a BioRad AG1 X-10 anion exchange resin to separate any actinide impurities. The column was rinsed with 8 M HNO_3, followed by 0.3 M hydrazine monohydrate, and 20 mM hydroquinone. Neptunium was then eluted from the column using 0.36 M nitric acid. The resulting solution was then heated in the presence of nitric acid and hydrogen peroxide to destroy any remaining organic impurities then evaporated to dryness and redissolved in 0.5 M nitric acid. The oxidation state of neptunium was adjusted to pentavalent by reduction of Np(VI) with dilute hydrogen peroxide followed by extraction of any remaining Np(IV) and Np(VI) with 30% tri-butyl phosphate solution in n-

dodecane. The purity of Np(V) was then verified using near-infrared spectroscopy on an OLIS RSM-1000 spectrophotometer by investigating the Np(V) peak at 980 nm. The purity of Np(V) was determined to be greater than 99%. After analysis of neptunium, protactinium-233 was allowed to grow back into the neptunium solution as the daughter product, in order to determine the distribution of Pa-233 by EtTDPA as well.

Pu-239 was obtained from Argonne National Laboratory as the chloride salt. The Am-241 impurity was removed by anion exchange chromatography using a Dowex 1X-4 column. Americium was washed from the column with 7M HNO_3 and Pu(IV) was eluted with 0.36M HCl. The Pu(IV) chloride solution was evaporated and dissolved in 4 M acid and adjusted to tetravalent oxidation state by hydrogen peroxide and sodium nitrite. Purity of the tetravalent oxidation state was confirmed by UV-vis spectrophotometry to be approximately 99% by the characteristic absorption peak at 475 nm.

3.2.2. *Analysis of Distribution Ratios*

The aqueous phases were contacted with an organic phase consisted of the desired concentration of EtTDPA in FS-13 at a 1:1 volume ratio. Prior to extraction, the organic phase was pre-equilibrated with an aqueous phase of the same composition as for the extraction experiment, except void of the metal of interest. Experiments were carried out in 2 mL plastic vials at room temperature ($21\pm1°C$). Organic and aqueous phases were vigorously agitated for 4 minutes at room temperature to ensure extraction equilibrium, split by centrifugation, and aliquots of each phase of the sample was taken for analysis. Metals with significant gamma ray emissions were analyzed using a Cobra gamma ray

spectrometer with a 3x3 NaI(Tl) well detector using their characteristic gamma ray energies. All distribution ratios are the result of averaging two or more experiments.
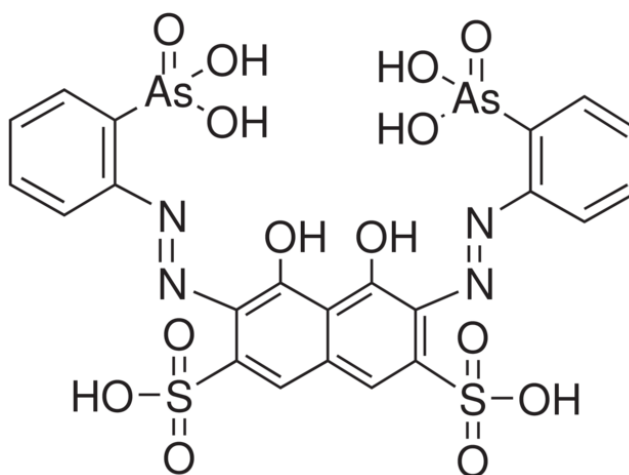
Figure 3.2: Arsenazo(III) complexant dye

Uranium and thorium do not produce significant gamma rays suitable for detection and required analysis by spectrophotometric methods. The procedure for uranium and thorium analysis was modified from a previously described method.[126] Arsenazo(III) [(2,7-bis(2,2'-arsonophenylazo)-1,8-dihydroxynaphthalene-3,6-disulfonic acid) Figure 3.2] was used as a spectrophotometric complexation agent. Calibration of the method was performed using twelve reference solutions with different concentrations of the hydrated salts of uranyl nitrate or thorium nitrate (4×10^{-4} – 1×10^{-2} g/L) and constant concentrations of Arsenazo(III). The response was found to be linear in this region. An aliquot of actinide nitrate stock solution was combined with 0.1 mL of 0.25% solution of Arsenazo(III), 0.95 mL of concentrated HNO_3, and the required volume of deionized water to keep the total volume of the reference solution at 2.5 mL and 6 M HNO_3. The

concentrated HNO_3 used to prepare these solutions was treated with urea to remove any traces of HNO_2 which could interfere with complex formation. The absorbance of the Arsenazo:metal complex was measured using an Ocean Optics QE65000 spectrophotometer at the wave length of 654 nm and 660 nm for uranium(VI) and thorium(IV) respectively in 1 cm quartz cuvettes against a 6M HNO_3 reference.

Activities of aqueous solutions were modeled using the Specific Ion Interaction Theory (SIT) equation:

$$\log \gamma_j = -z_j^2 \frac{0.51\sqrt{I}}{1 + 1.5\sqrt{I}} + \sum_k \epsilon_{jk} m_k \qquad (3.1)$$

where z is the charge of the ion, I is the standard calculation of ionic strength $I = \frac{1}{2}\Sigma cz^2$, m is the molality of the ion in solution, and the correction parameter of interaction between the ions ϵ using known literature values.[127]

3.3. Degradation of EtTDPA

3.3.1. Sample Preparation

For radiolytic degradation experiments the samples of organic solvent containing EtTDPA were pre-saturated with water or 3 M nitric acid and irradiated in sealed quartz vials to the desired gamma-ray doses. Samples were irradiated in the Oregon State University Co-60 irradiator (Gammacell), providing a center-line dose ranging from 0.30-

0.45 kGy/hr depending on the time frame of the experiment as calibrated by the manufacturer. A solution of EtTDPA in FS-13 was also contacted with 3 M nitric acid to account for degradation by hydrolysis over the duration of the irradiation times. Samples were then prepared for either gas chromatographic analysis or solvent extraction in the same procedure as described previously then spiked with tracer amounts of either Am-241 or Eu-152/154 to determine distribution ratios by gamma spectroscopy.

Hydrolysis of EtTDPA at elevated temperatures was performed by the addition of 3 M nitric acid to 0.2 M solutions of EtTDPA. Solutions were then vigorously mixed and placed in a water bath held at 50 °C for up to 96 hours without separation of the two phases. The solutions were periodically vortexed to ensure maximum phase contact throughout the investigation. Samples were then analyzed by the same procedure as mentioned previously for radiolysis.

3.3.2. Analysis of Samples

Gas chromatography mass spectroscopy was performed using an Agilent 5975E equipped with a non-polar 5-DB 30 m column. Samples were diluted to appropriate levels using dichloromethane and then injected in 1 μL amounts and flushed from the syringe with dichloromethane. Scans were performed from 35-550 m/z using a temperature profile of:

- 50 °C held for 5 min
- 1 °C/min for 60 min
- 2 °C/min for 60 min
- 300 °C held for 35 min

Samples requiring derivatization were performed by mixing a solution of the desired analyte with trimethylsulfonium hydroxide (TMSH, 0.1 M in methanol) at 40 ° C in screw cap vials with excess of TMSH account to for methylation of carboxylic and sulfonic acid groups. After dilution by dichlroromethane methylized samples were analyzed in the same manner described above.

Infrared analysis of organic phases were performed with a Nicolet 6700 Fourier transform infrared (FT-IR) spectrometer equipped with a 0.015 mm spacer and AgCl liquid cells. Samples of the organic phase were injected into the cell using a syringe. Data for each sample were obtained in the 400 - 4000 cm^{-1} region by collecting 32 scans each, with a resolution of 2 cm^{-1} and using the spectrum of the solvent FS-13 as a blank.

Thermogravimetric analyses of samples were performed using a Mettler-Toledo TGA 850. Experiments were run by placing samples of EtTDPA in pre-weighed aluminum pans and heated under air from 25-450 °C at a temperature rate of 5 °C/min.

3.4. Determination of Thermodynamic Constants

3.4.1. *Spectrophotometry*

Neodymium was obtained from Sigma-Aldrich as the oxide form Nd_2O_3 and as the trifluoromethylsulfonate salt $Nd(SO_3CF_3)_3$ and was of analytical grade. A working solution of $Nd(ClO_4)_3$ was prepared by dissolution of Nd_2O_3 with a slight stoichiometric excess of dilute perchloric acid and slowly evaporated under heat followed by secondary dissolution and evaporation steps until only trace amounts of acid remained. Metal

perchlorate or triflate crystals were then dissolved in HPLC grade acetonitrile. The exact concentration of Nd^{3+} was determined by titrations with ethylenediaminetetraacetic acid (EDTA) in acetate buffer solution with xylenol orange indicator.[128] EDTA was obtained from Sigma-Aldrich as a standardized solution.

Solutions of neodymium and EtTDPA dissolved in acetonitrile and held at constant 0.08M ionic strength with $Na(ClO_4)$ were examined by UV-Vis spectroscopy. Spectra were obtained using an OLIS[TM] RSM-1000 monochromator from 500-700 nm. The temperature was held constant at 25.0 ± 0.1 °C with a Julabo thermostat. The spectrophotometer was equipped with an automatic titration system that consisted of two separate syringes containing the metal and ligand solutions. Predetermined amounts of each solution were drawn into a mixing chamber and mixed before being injected into a 1 cm quartz cuvette for analysis. Enough titrant was added in order to obtain more than a 5:1 ligand metal ratio. Data were analyzed using HypSpec v. 1.1.33 to determine stability constants for each metal:ligand complex.

3.4.2. Calorimetry

Calorimetric titrations were performed using a TAM III Microcalorimeter (TA Instruments) in isothermal mode. Solutions of neodymium triflate dissolved in acetonitrile were placed in 1 mL titration ampoules as both a reference and reaction vessel. Injections of EtTDPA isomers were performed by a stepper motor syringe pump. The instrument temperature was held at a constant 25.0000 ± 0.0001 °C during experiments. Prior to performing titrations the instrument was electrically calibrated using an on-board power generator and then run in dynamic correction mode to account

for thermal inertia within the system. Heats of mixing and dilution were found to be non-significant sources of thermal energy and were neglected during thermodynamic calculations. Data were collected using TAM III Assistant software and analysed by HypDH v. 1.1.11 to determine thermodynamic complexation.

4. EXTRACTION OF ACTINIDES AND SELECTED FISSION PRODUCTS

4.1. Molybdenum(VI)

Molybdenum exhibits a very wide range of speciation due to its affinity for oxygen. Depending on solution conditions Mo can form mono, di-, or polynuclear complexes. At pH > 7 MoO_4^{2-} exists as the dominant ionic form with a tetrahedron geometry.[129] As pH decreases, the coordination number of Mo changes from 4 to 6 forming an octahedral complex. Depending on the concentration of molybdenum, a wide variety of polymeric species such as $Mo_3O_{11}^{4-}$ and $HMo_{24}O_{78}^{3-}$ can form under these conditions.[130]

With decreasing pH the formation of these polynuclear species is greatly inhibited. Thermodynamic analysis of increasing acidity reactions show increasing coordination number as the molybdate ion is continuously protonated.[131] The tetrahedral MoO_4^{2-} becomes protonated to $HMoO_4^-$ before formation of the octahedral diprotonated species $[MoO_2(OH)_2(H_2O)]$. Further protonation forms the dioxomolybdenum ion through the reaction:

$$[MoO_2(OH)_2(H_2O)_2] + H^+ \leftrightarrows [MoO_2(OH)(H_2O)_3]^+ \qquad (4.1)$$

Equilibrium data obtained in 2 M $HClO_4$ shows that at pH < 0 the $[MoO_2(OH)(H_2O)_3]^+$ cation will be the dominant species, with more than 90% of molybdenum in this configuration.[130]

It was reported previously that molybdenum is not extracted by TBP from nitric acid, but is well extracted from hydrochloric acid.[130] X-ray absorption near edge structure

(XANES) and extended X-ray absorption fine structure (EXAFS) spectroscopic techniques have confirmed that there is no coordination of the molybdyl cation by sulfuric, perchloric, or nitrate anions in their respective acidic solutions.[132]   In hydrochloric media the dioxomolybdenum ion undergoes formation of chloride complexes while maintaining the tetrahedral coordination:

$$[MoO_2(OH)(H_2O)_3]^+ + Cl^- \leftrightarrows [MoO_2(OH)Cl(H_2O)_2] \tag{4.2}$$

$$[MoO_2(OH)Cl(H_2O)_2] + Cl^- + H^+ \leftrightarrows [MoO_2Cl_2] + 3H_2O \tag{4.3}$$
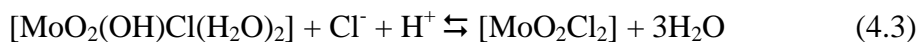
Vibrational spectroscopy data confirms that the $[MoO_2(OH)Cl_2(H_2O)_2]$ complex is the prevailing molybdenum species in solutions of hydrochloric acid at pH < 0.[133] Once the neutral MoO_2Cl_2 species is formed it can then be extracted by TBP or other complexants.

The results of extraction of molybdenum with isomers of 0.2 M EtTDPA at various nitric acid activities are plotted in Figure 4.1. Distribution ratios for all isomers of EtTDPA show no significant change with nitric acid concentrations greater than 2 M. Data obtained for 1 M HNO$_3$ shows slightly higher distribution ratios for Et(m)TDPA and Et(p)TDPA, possibly from formation of a cationic or anionic species other than the MoO_2^{2+} ion though this value is within the error of the other data sets. Extractions of molybdenum were then repeated using a 3 M nitric aqueous phase and varying the concentration of EtTDPA in the organic phase. As seen in Figure 4.2 no dependence on the EtTDPA concentration is observed from these conditions. Log-log analysis of these

data gives a solvation number of n=0 in both cases, indicating that the MoO_2^{2+} is a non-extractable molybdenum species in nitric acid.
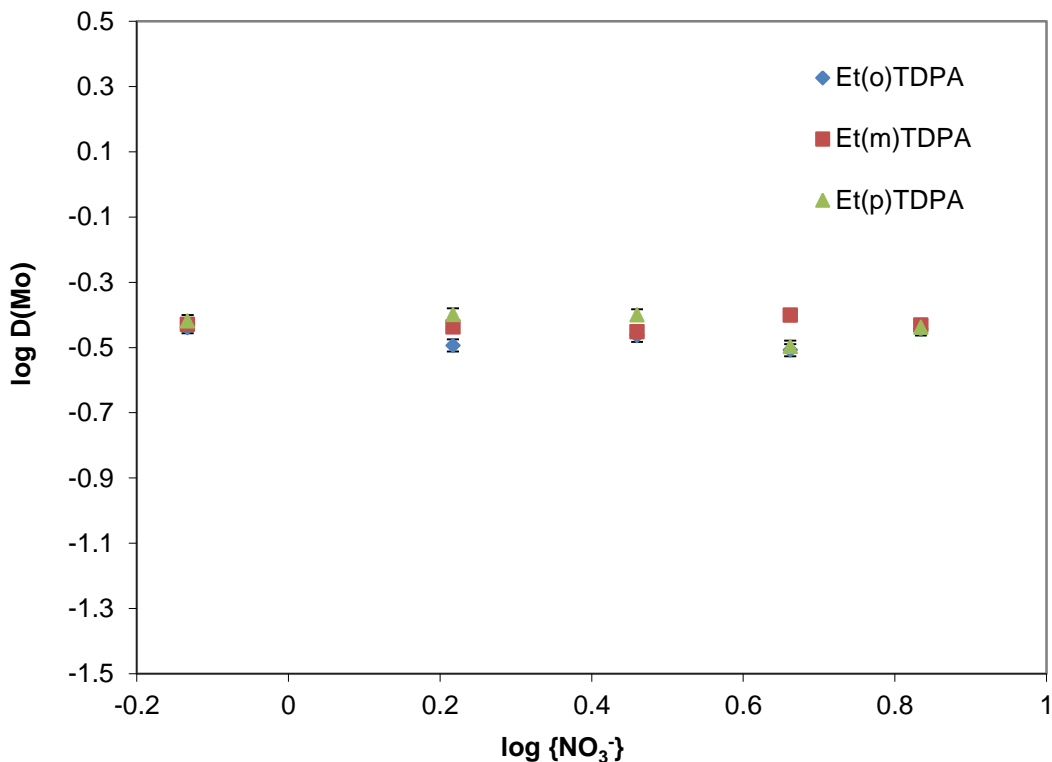
Figure 4.1: D(Mo) as a function of nitric acid activity with 0.2 M EtTDPA in FS-13

These extractions were then repeated using $LiNO_3$ to increase the nitrate concentration without increasing acidity. Each EtTDPA isomer showed little difference in extraction capability in nitric acid, so only extractions with the Et(p)TDPA isomer were performed. The obtained distribution ratios are plotted in Figure 4.3. Again, there was little to no effect of the total nitrate concentration at constant acid on the extractability of Mo. However, the distribution ratios do show a decrease compared to the same total nitrate concentration for acid with no added $LiNO_3$. This can be explained because EtTDPA extracts nitrate from the aqueous phase into the organic. The addition

of $LiNO_3$ acts as a salting out reagent for aqueous NO_3^- ions, increasing the organic nitrate concentration. The presence of these nitrates lowers the affinity of molybdenum for the organic phase even further, thereby decreasing the allowable concentration of molybdenum species in the organic phase.
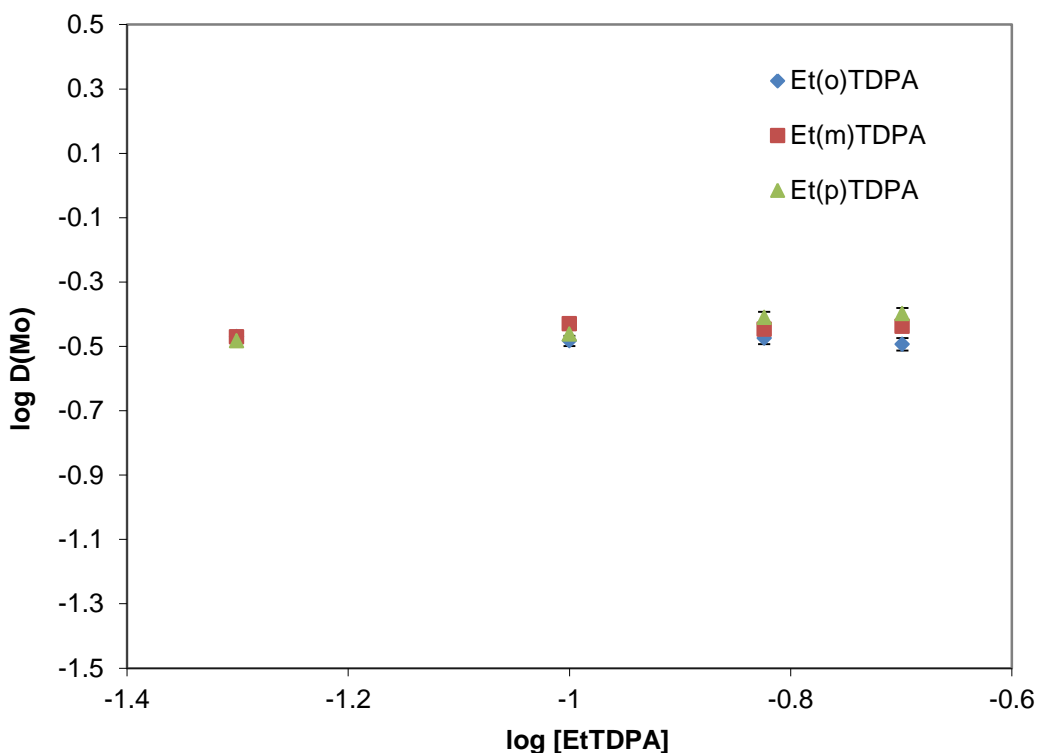
Figure 4.2: D(Mo) as a function of EtTDPA concentration at 3 M HNO_3 in FS-13

Typically oxalic acid is added to the aqueous phase in order to prevent Zr and Mo co-extraction. In comparison to recent TODGA results, much lower distribution ratios are observed for molybdenum by using EtTDPA as an extractant.[134] Without the presence of oxalic acid, TODGA distribution ratios are larger than EtTDPA by a factor of 10. Only by addition of oxalic acid are the extraction capabilities made similar. Therefore EtTDPA can be used to preferentially extract other metals with larger D values such as

americium without requiring oxalic acid to be added to PUREX raffinate to prevent Mo co-extraction.
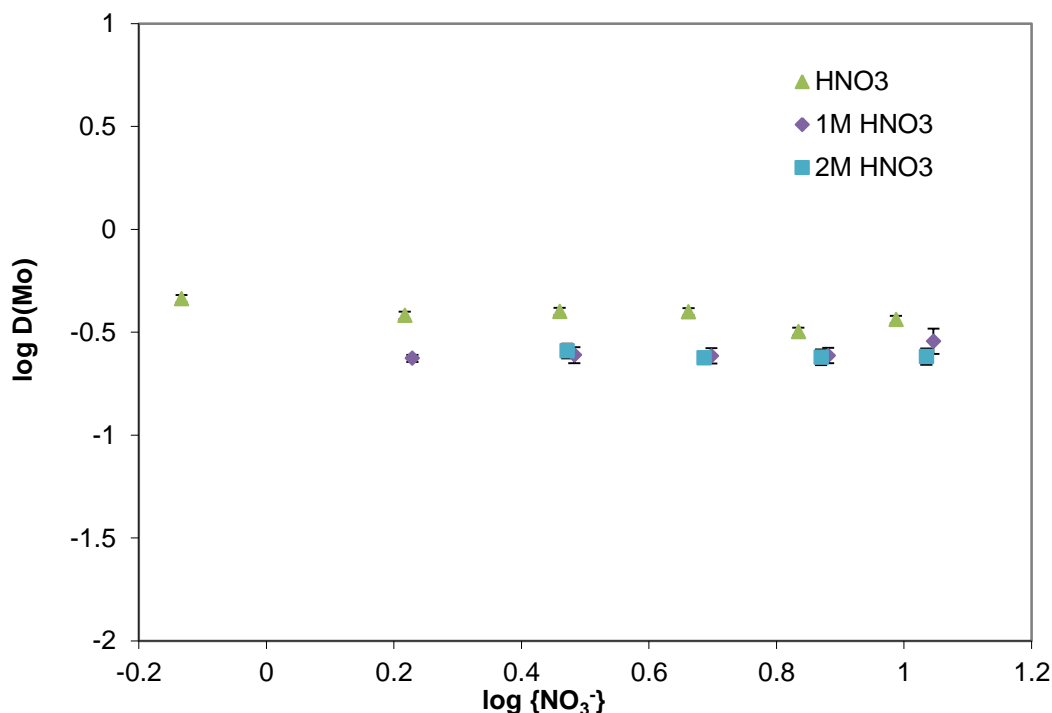
Figure 4.3: D(Mo) at constant HNO_3 and added $LiNO_3$ with 0.2 M Et(p)TDPA

Extraction data for Et(p)TDPA was also obtained in HCl aqueous media. As can been seen in Figure 4.4, increasing the HCl concentration has a profound effect on the distribution ratio of molybdenum compared to nitric acid. The large difference in trends can be explained by the Cl^- ion having a larger affinity for the MoO_2^{2+} cation at acid concentrations larger than 1 M compared to NO_3^-. These HCl and nitrate values for EtTDPA show similar extraction capabilities of Mo compared to TBP data as previously reported by Tkac *et. al.*[130] Molybdenum is not extracted in higher nitric acid concentrations for either EtTDPA or TBP. However, at hydrochloric acid concentrations greater than 1 M, molybdenum is well extracted by both EtTDPA and TBP. Slope

analysis of the distribution ratios gives a solvation number for Cl⁻ of approximately 2 at > 1 M HCl This indicates that the reaction goes as:

$$[MoO_2(OH)Cl(H_2O)_2] + H^+ + Cl^- + nEtTDPA \leftrightarrows [MoO_2Cl_2 \cdot EtTDPA_n] + 3H_2O \quad (4.4)$$

analogous to the results produced using tri-butyl phosphate as the extractant.
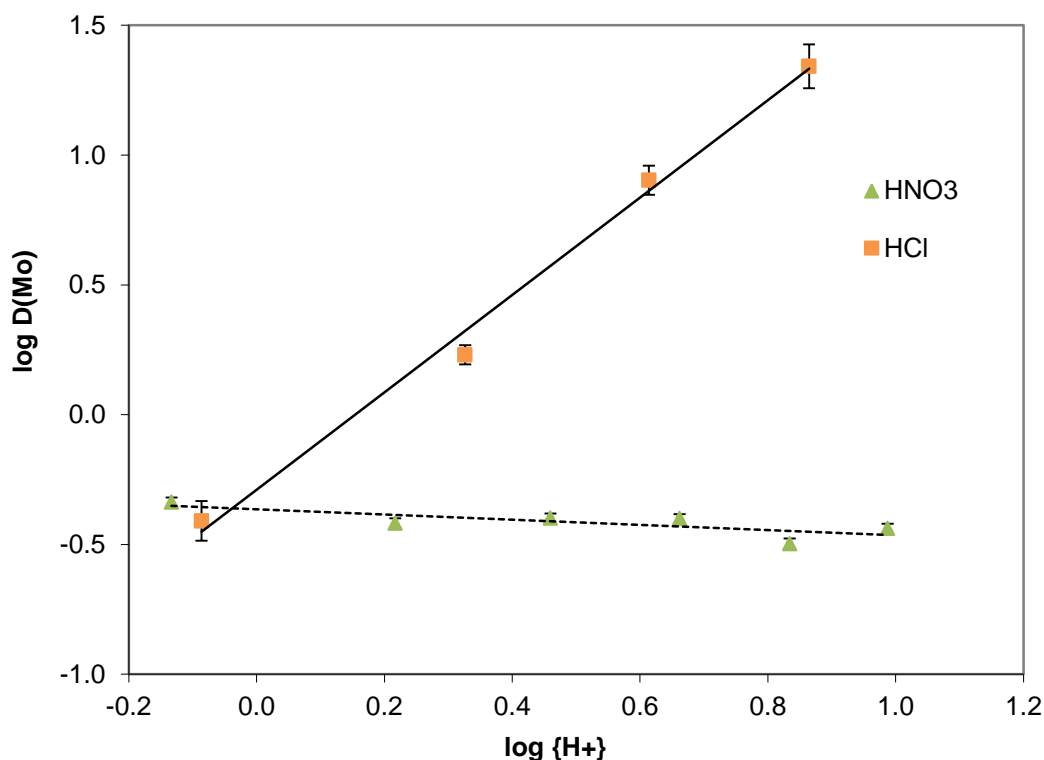
Figure 4.4: Comparison of D(Mo) by Et(p)TDPA between HCl and HNO₃ aqueous phases

4.2. Technetium(VII)

The pertechnetate (TcO₄⁻) anion competes with nitrate ions for complexation with neutral solvate ligands and is the basis of several new methods being developed for pertechnetate separation.[135] Data has been previously obtained for Tc extraction from

nitric acid with TBP in *n*-dodecane.[136] It was found that the extraction of technetium with TBP proceeds by the mechanism:

$$TcO_4^- + H^+ + 3TBP \leftrightarrows [HTcO_4 \cdot TBP_3] \qquad (4.5)$$
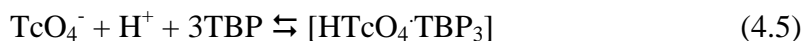
Regardless of TBP concentration, distribution ratios increased with increasing acidity until 0.6 M HNO_3 was obtained, followed by a steady decline at higher acidity. This effect is owed to the lower frequency of dissociation of the $HTcO_4$ molecule at these high acidities, allowing for extraction of the neutral molecule $[HTcO_4 \cdot TBP_3]$. At higher nitric acid concentrations pertechnetate competes with nitrate for H^+ ions, which would then proceed by ion exchange to extract nitric acid in the form:

$$[HTcO_4 \cdot TBP_3] + NO_3^- \leftrightarrows [HNO_3 \cdot TBP_3] + TcO_4^- \qquad (4.6)$$
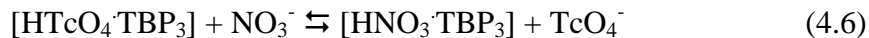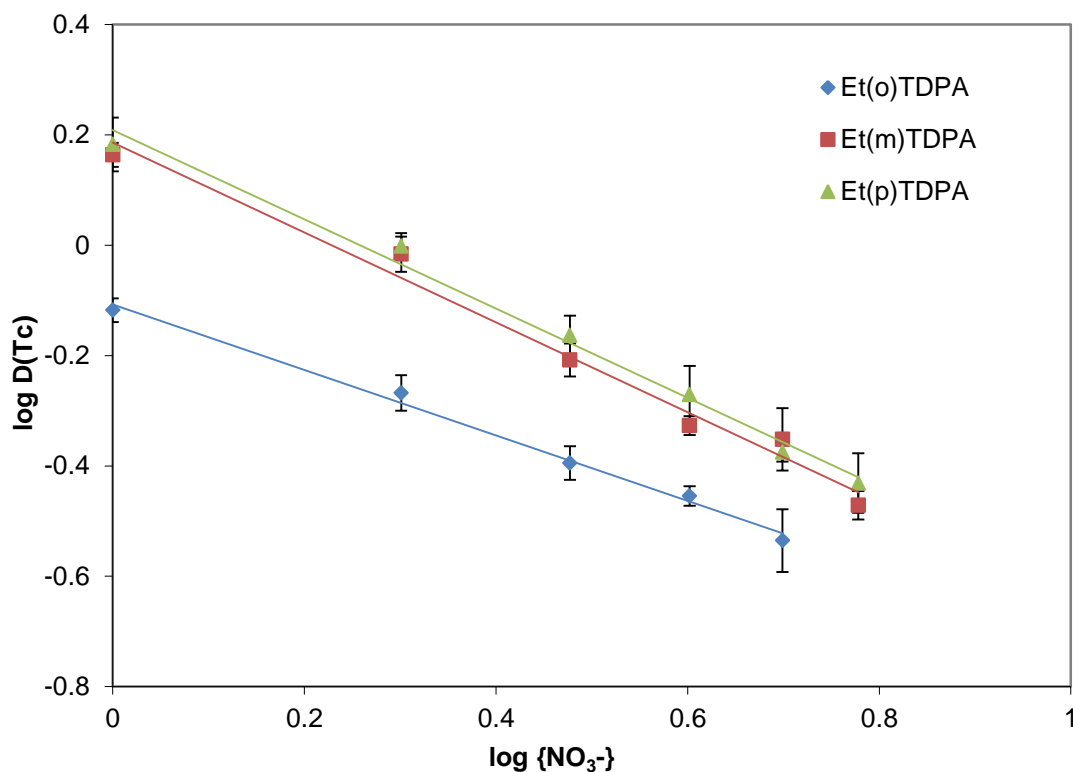
Figure 4.5: D(Tc) as a function of acid activity with 0.2 M EtTDPA in FS-13

Figure 4.5 shows the results of extraction of technetium with isomers of 0.2 M EtTDPA at increasing nitric acid concentrations. As can be seen in the figure there is a decrease in the distribution ratio of technetium with increasing acid concentration. This shows that there is indeed an ion exchange process occurring between the nitrate and pertechnetate ions similar to that observed using TBP as the extractant.

Since Et(p)TDPA showed higher relative extractability at most nitric acid concentrations it as once again used to examine the extraction behavior at constant acidity by addition of lithium nitrate and thus limiting competitive reactions between pertechnetic and nitric acid as described in Equations (4.5) and (4.6). Figure 4.6 shows a log scale plot of D(Tc) vs. total NO_3^- activity exhibiting a linear decrease with slopes of

approximately one. Initially the effect of additional nitrate causes a salting out effect of technetium from the aqueous phase resulting in larger distribution ratios. However, when the nitric acid concentration is increased further there is a significant drop in the extraction capability due to the more favored formation of the extractable nitric acid molecule, leading to less free ligand and ultimately lower distribution ratios.
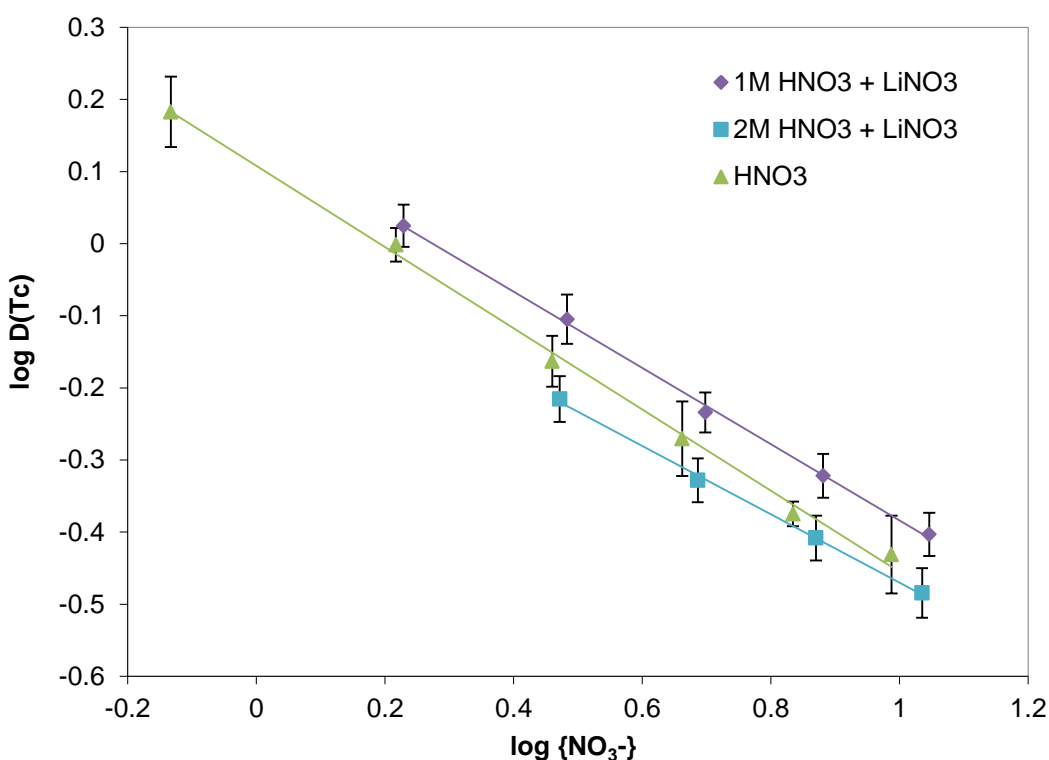
Figure 4.6: D(Tc) at constant HNO_3 and added $LiNO_3$ with 0.2 M Et(p)TDPA in FS-13

The effect of adjusting the concentration of EtTDPA is shown in

Figure 4.7. Slope analysis shows constant increasing technetium distribution ratios for all isomers of EtTDPA with solvate numbers for ortho, meta, and para also of approximately one. These solvation numbers indicate that unlike molybdenum, technetium is extracted by EtTDPA in low nitric acid conditions, but is replaced at higher

nitrate concentrations due to a lower binding affinity compared to NO_3^-. The mechanism of extraction should then be analogous to equations (4.5) and (4.6) giving:

$$TcO_4^- + H^+ + EtTDPA \leftrightharpoons [HTcO_4 \cdot EtTDPA] \tag{4.7}$$

$$[HTcO_4 \cdot EtTDPA] + NO_3^- \leftrightharpoons [HNO_3 \cdot EtTDPA] + TcO_4^- \tag{4.8}$$
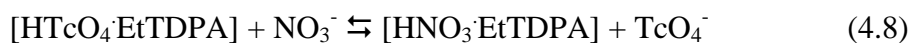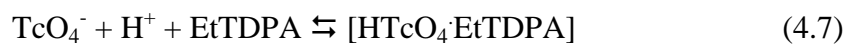
with the effect of additional nitrate driving the reaction in equation (4.8) to the right.
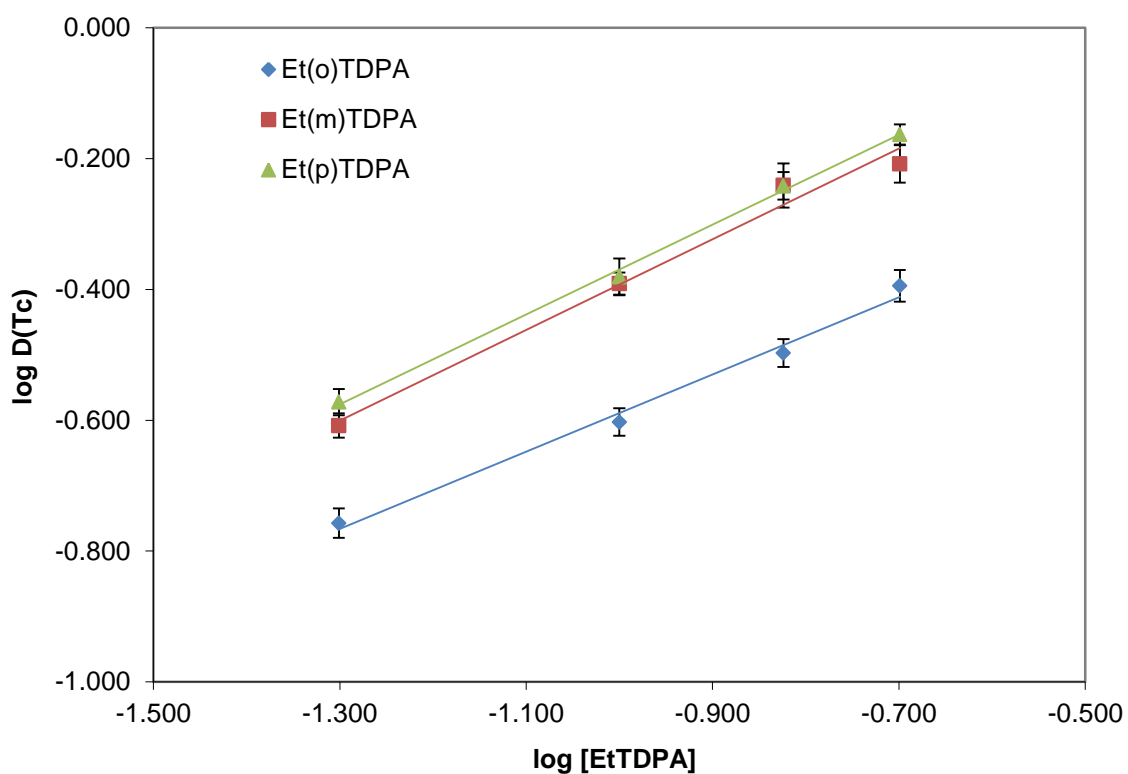
Figure 4.7: D(Tc) from 3 M HNO_3 with 0.05-0.20 M EtTDPA in FS-13

4.3. Uranium (VI)

In aqueous media, uranium(VI) primarily exists as a linear dioxocation with charge 2+ (UO_2^{2+}). The tetravalent U^{4+} cation can be produced but is of little concern in most modern fuel reprocessing schemes. The stability of the uranium-oxygen bonds constricts the geometric complexation conformations to the planar equatorial region.[137] Uranium(VI) bonding mechanisms are mostly ionic and favor complexation through oxygen donor atoms. Previous studies of monoamide extraction[138] show that at mild acidic conditions these extractants (L) complex UO_2^{2+} through the reaction mechanism:

$$UO_2^{2+} + 2\ NO_3^- + 2L \leftrightarrows [UO_2(NO_3)_2]\cdot 2L \qquad (4.9)$$
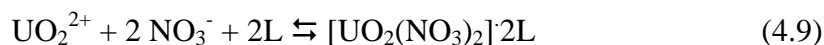
When complexation occurs, the charge of the metal cation is compensated with the anionic charge of nitrates in the extracted complex. The single carbonyl group of monoamides facilitates the extraction of the uranyl ion, requiring a charge balance from the two nitrate ions as well as two extractant molecules.

Diamides of dipicolinic acid contain two amide groups in an easily accessible geometry and thus have the ability to act as a tridentate neutral ligand extractant.[137,139] The complex is formed by two carbonyl groups and the pyridine nitrogen. The effect of varying EtTDPA concentration at constant nitric acid is shown in Figure 4.8. Ortho, meta and para isomers show similar extraction capabilities for U(VI), and log-log slope analysis gives solvation numbers of n(EtTDPA) = 1.17 ± 0.03, 1.10 ± 0.02, and 1.08 ± 0.04 for ortho, meta, and para isomers, respectively. These findings indicate that one EtTDPA molecule is suitable to perform the extraction.
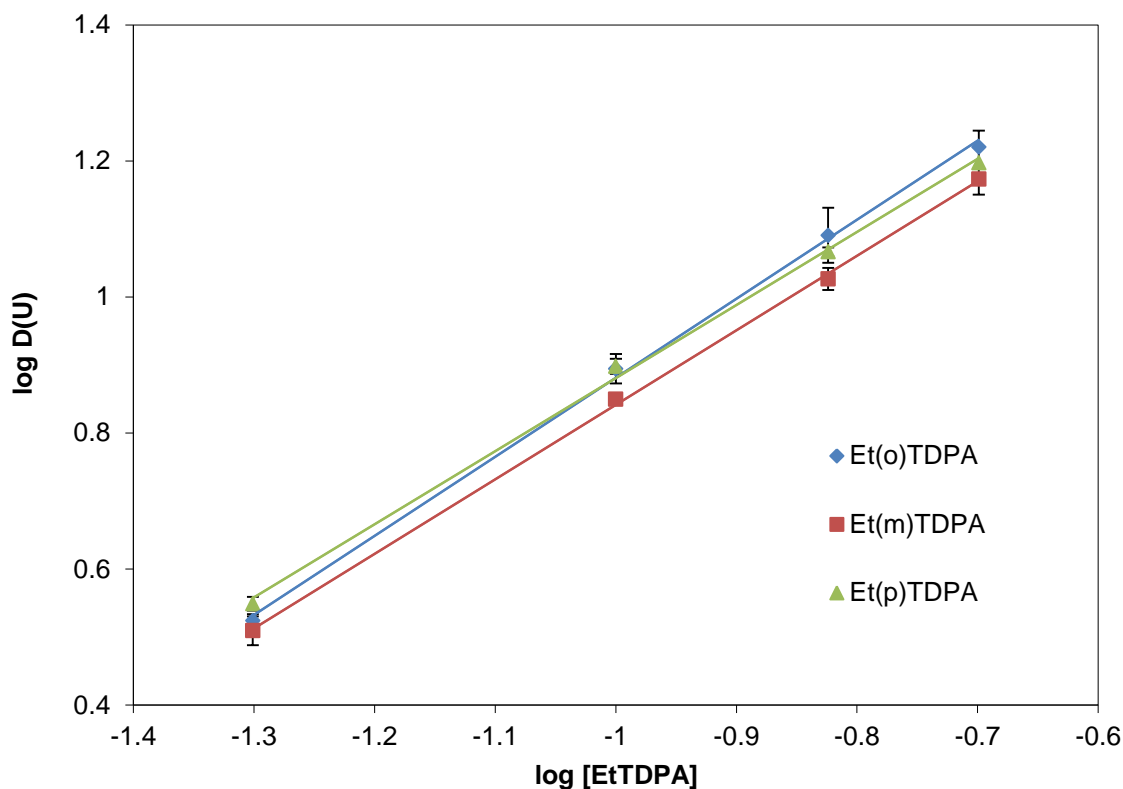
Figure 4.8: Uranium extraction from 3 M HNO_3 as a function of EtTDPA concentration

Extraction of uranium increases with HNO_3 concentration for all isomers of EtTDPA. The distribution ratios of uranium with 0.2 M EtTDPA in FS-13 are displayed in Figure 4.9 as a function of the activity of total nitrate in the extraction system. According to the reaction mechanism in Equation (4.9), it should be expected that the solvation numbers have values of close to 2. Two molecules of nitrate were found in the solid uranyl Et(p)TDPA analyzed by FTIR and single crystal XRD.[140] However, the log-log analysis of the extraction data gives a solvation numbers of $n(NO_3) = 3.27 \pm 0.13$, 2.94 ± 0.11, and 2.91 ± 0.12 for ortho, meta, and para respectively. Therefore, the three nitrate groups indicated by these plots suggest that an additional molecule of nitric acid can be solvated with diamide as well as the two nitrate ions required for charge neutrality. The extraction

of an additional molecule of nitric acid has been observed previously with N-donor ligands as well as other amidic extractants.[81,98]
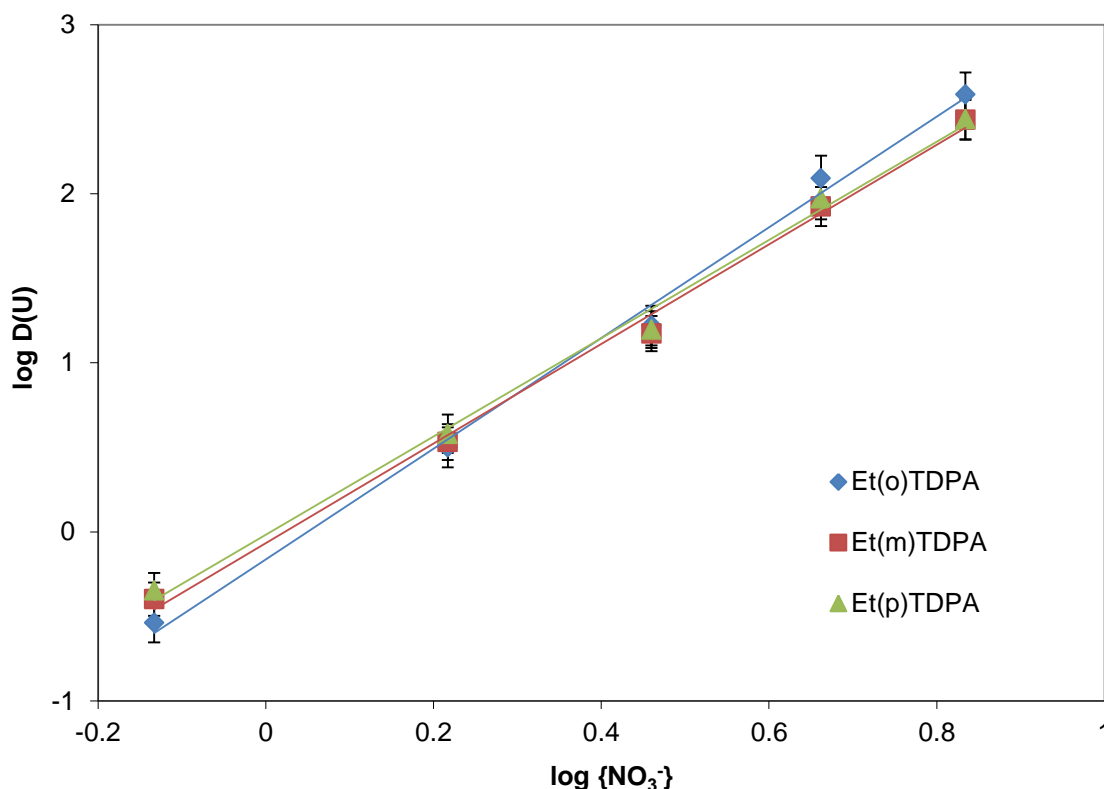
Figure 4.9: Uranium extraction with 0.2 M EtTDPA from nitric acid as a function of nitrate activity

Uranium extractions were repeated using $LiNO_3$ to adjust the total nitrate concentration, at a constant H^+ concentration, in order to determine the nitrate dependence. Since all isomers showed similar extraction capabilities for UO_2^{2+}, nitrate dependence was investigated with only the para isomer. Distribution ratios measured at a constant 1 M H^+ and varying nitrate concentrations indicate increasing values with higher NO_3^- activities as seen in Figure 4.10. Further increasing of the initial nitric acid concentration then lowers the distribution ratio due to the increased formation and

extraction of nitric acid. From these data it can be concluded that under these conditions, EtTDPA primarily extracts the uranyl ion in the form:

$$UO_2^{2+} + H^+ + 3NO_3^- + EtTDPA \leftrightarrows [UO_2(NO_3)_2(HNO_3) \cdot EtTDPA] \qquad (4.10)$$
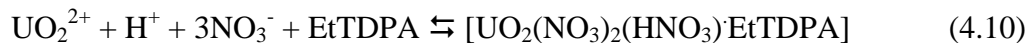
This is consistent with the preferred coordination number of six for uranium.[19] The uranium appears to only be strongly coordinated by two of the three possible donor sites of EtTDPA (one nitrogen and one oxygen atom), with the remaining site participating in the extraction of the nitric acid molecule.
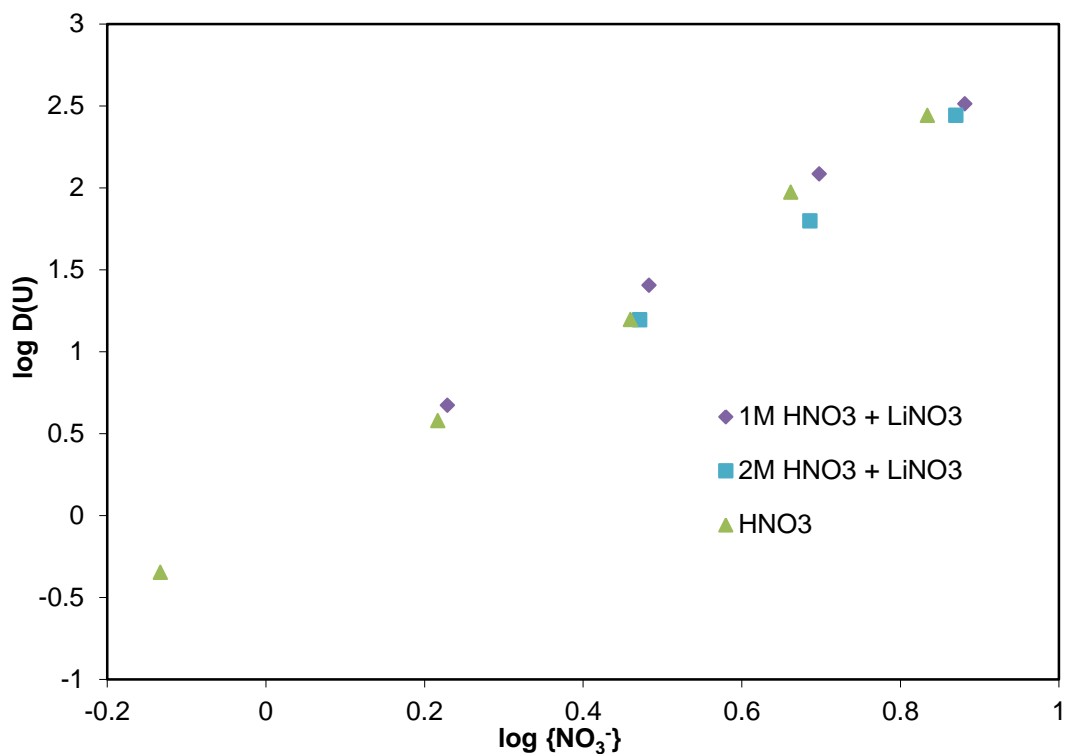
Figure 4.10: Uranium extraction with 0.2 M Et(p)TDPA from nitric acid and lithium nitrate as a function of nitrate activity

According to Musikas *et. al*. the existence of the acidic complexes can be observed as the result of competition between the amide and nitrate ions for the metal coordination sites with the amide favoring the neutral complex, and amide and NO_3^- ions for the proton.[84]   As such, metal-amide affinity also has to be considered for the formation of acidic complexes.   Extracted nitric acid coordinates with the C=O of amidic extractants through hydrogen bonding. The infrared spectra of 0.2 M Et(p)TDPA solutions in FS-13 saturated with HNO_3 and $LiNO_3$ are shown in Figure 4.11 (spectra are offset for clarity). Spectra b and c exhibit a much broader carbonyl peak about 1650 cm^{-1} compared to Et(p)TDPA prior to extraction.   At constant H$^+$ and varying $LiNO_3$, small but non-significant changes in the overall shape of this peak were observed. The widening of the carbonyl band is therefore a consequence of formation of more HNO_3 molecules by addition of H$^+$ and not simply an effect of additional NO_3^-. Thus, the IR data indeed suggests that HNO_3 interacts with the amide carbonyl group through hydrogen bonding as indicated by Equation (4.10).
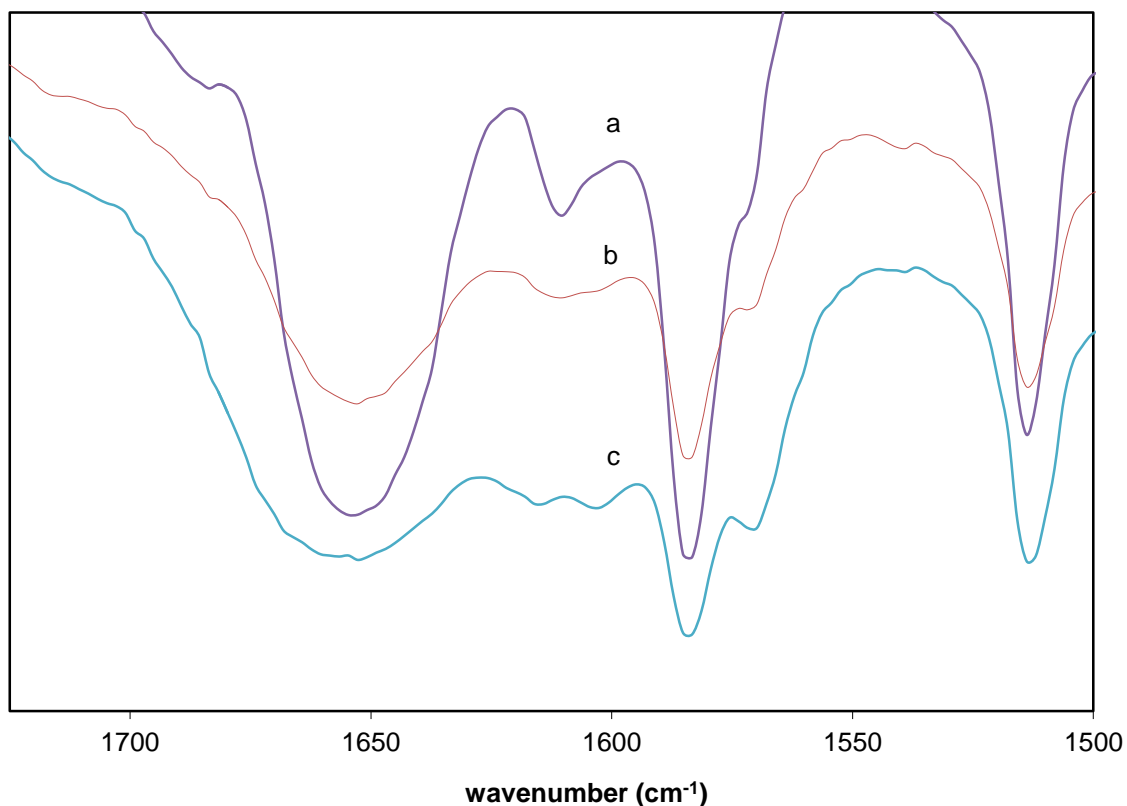
Figure 4.11: Infrared Spectra of 0.2 M Et(p)TDPA in FS-13 a. before saturation, b. saturation with 2 M HNO_3 and 1 M $LiNO_3$, c. 2 M HNO_3 and 4 M $LiNO_3$

The infrared spectrum of the uranium-diamide complex in the organic phase was also obtained. Figure 4.12 shows a comparison of the metal:ligand complex to that of pure ligand after subtraction of the solvent spectrum (again offset for clarity). As expected, a large shift is observed for the carbonyl absorption band from 1654 to 1620 cm^{-1} due to the complexation of uranium with the C=O groups of Et(p)TDPA. An absorption peak for the U=O vibrational stretch of the complexed UO_2^{2+} cation was observed at 945 cm^{-1} (not shown). These results are consistent with previously published amide extraction data.[141]
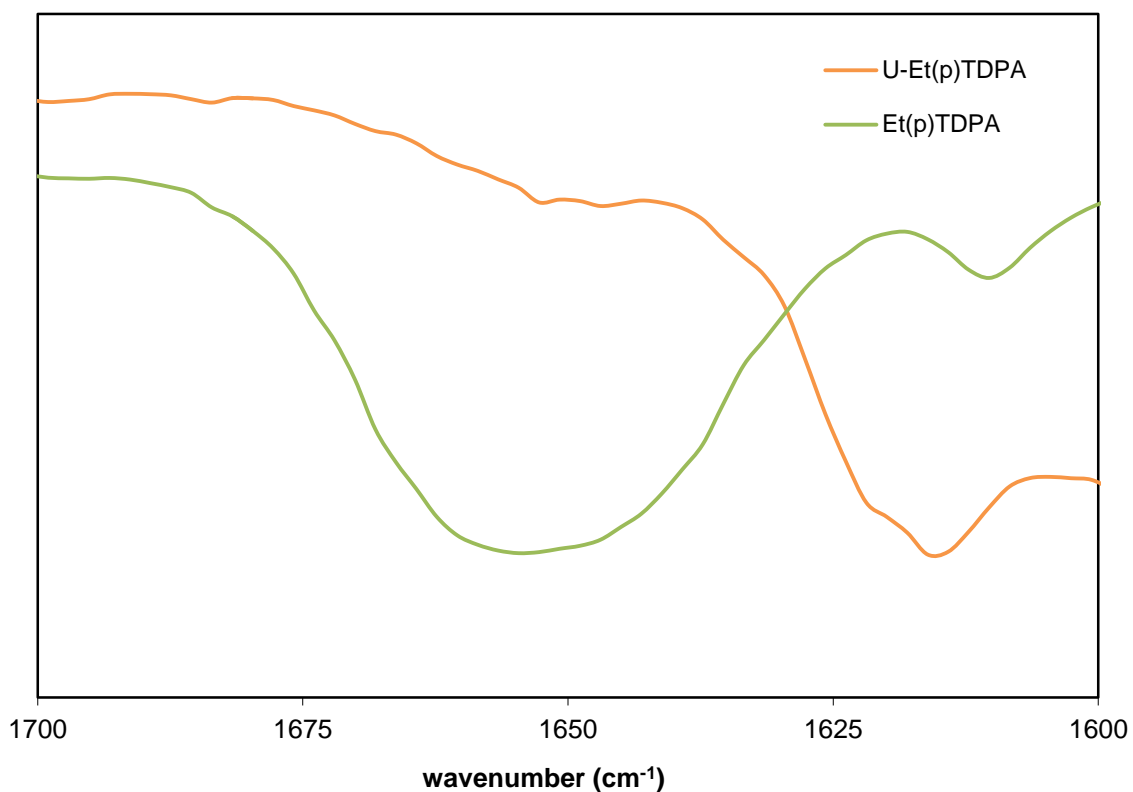
Figure 4.12: Infrared spectra of organic phase before and after UO_2^{2+} extraction with Et(p)TDPA

4.4. Neptunium(V)

Neptunium is capable of existing in three stable oxidation states when present in nitric acid media.[142] The possible three valences are Np(IV), Np(V), and Np(VI), with tetravalent neptunium existing as the bare Np^{4+} cation, while the Np(V) and Np(VI) states exist as the NpO_2^+ and NpO_2^{2+} cations respectively. Disproportionation of the pentavalent state results in the formation of both the tetra and hexavalent species with a fourth order dependence on acidity[143] as given by:

$$2NpO_2^+ + 4H^+ \leftrightarrows Np^{4+} + NpO_2^{2+} + 2\,H_2O \qquad (4.11)$$
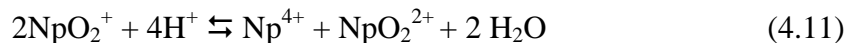
In nitric acid, tetravalent neptunium is thermodynamically unstable[144] and susceptible to oxidation to the hexavalent state by both nitric acid and the concurrent presence of nitrous acid by the mechanisms:

$$3Np^{4+} + 2HNO_3 + 2\,H_2O \leftrightarrows 3NpO_2^{2+} + 2NO + 6H^+ \qquad (4.12)$$

$$Np^{4+} + HNO_2 + H_2O \leftrightarrows NpO_2^{2+} + NO + 3H^+ \qquad (4.13)$$
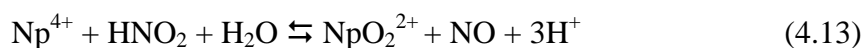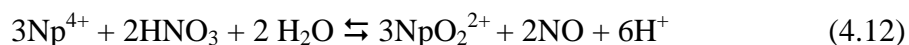
This process is generally kinetically inhibited due to the transformation of the Np^{4+} to the oxygen bearing NpO_2^{2+}. However, the spent fuel dissolution process in hot nitric acid significantly increases the kinetics of this oxidation.[5] The end result is Np(V) and Np(VI) being the more relevant forms under typical aqueous solvent extraction reprocessing conditions (3-4 M HNO_3).[24,145]

Like the hexavalent uranium UO_2^{2+} ion, the linear geometries of the penta and hexavalent states constrains the coordination environment to the planar equatorial region of these cations.[137] In typical neutral solvent extractants such as TBP, neptunium is nearly inextractable as the pentavalent form while hexavalent neptunium is extracted efficiently.[55] The expected extraction mechanisms for EtTDPA should follow as:

$$NpO_2^+ + nEtTDPA + NO_3^- \leftrightarrows [NpO_2(NO_3)]\cdot nEtTDPA \qquad (4.14)$$

$$NpO_2^{2+} + nEtTDPA + 2NO_3^- \leftrightarrows [NpO_2(NO_3)_2]\cdot nEtTDPA \qquad (4.15)$$
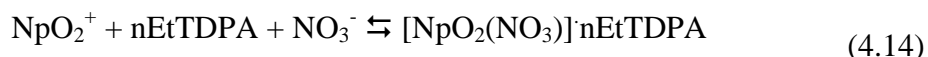
with one and two nitrate molecules being extracted per neutral complex into the organic phase for penta and hexavalent neptunium respectively.

Other ligands including diamidic complexants have been shown to cause redox changes of the neptunium speciation upon contact.[146,147] Changes in the redox chemistry could have profound effects on the distribution of neptunium in a solvent extraction scheme. To evaluate this possibility the near-IR spectra of mixed solutions of Np(V) and Np(VI) in 3 M nitric acid before and after contact with EtTDPA in FS-13 were obtained and are shown in Figure 4.13. Prior to contact with EtTDPA only Np(V) (980 nm) and Np(VI) (1225 nm) were present, with the majority of the neptunium in solution in the form of Np(VI).[148] Upon contacting with an equal volume of 0.2 M EtTDPA in FS-13 an immediate color change of the aqueous solution could be visibly seen when mixing was initiated. This reaction is extremely rapid and experiments showed that there were no further changes in the spectra after as little as 30 seconds at 20° C. Post contact analysis of the aqueous phase shows nearly all Np(VI) is reduced to Np(V) with little to no detectable Np(IV) content. Np(VI) therefore acts a strong oxidant for EtTDPA converting most to the less extractable pentavalent state, though a portion does remain in the more extractable hexavalent form. Due to these results, only the extraction of Np(V) by EtTDPA was evaluated.
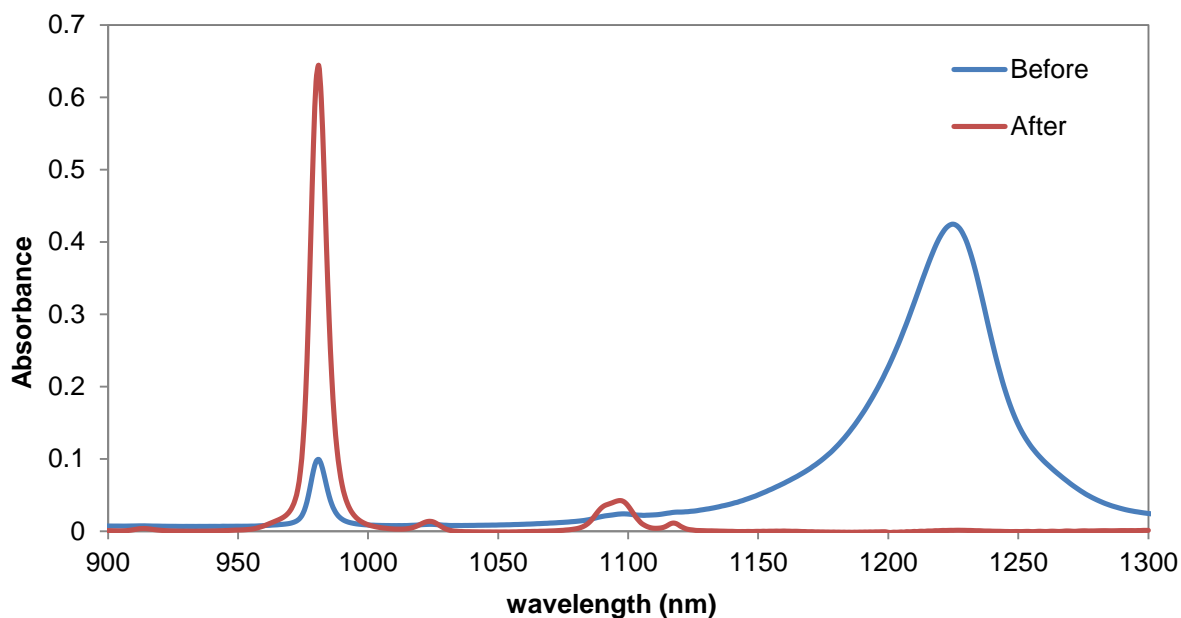
Figure 4.13: Near-IR spectra of Np solution before and after contact with Et(p)TDPA

The extraction of Np(V) by 0.2 M solutions of EtTDPA isomers in FS-13 from increasing nitric acid conditions is shown in Figure 4.14 as a function of the nitrate activity. At lower acidities the meta- isomer shows the largest distribution ratios up to 3 M HNO_3, while Et(p)TDPA is the lowest across the entire range of acidities investigated, which was also observed in a previous study on americium extraction.[106] This trend is different than that which was previously observed for uranium, where Et(p)TDPA exhibited the highest distribution ratios and Et(m)TDPA was nearly identical in extraction capability between 1-5 M nitric acid. However, in the studies of uranium (VI), neptunium (V), and americium (III), Et(o)TDPA begins with only slightly higher extraction capability than Et(p)TDPA at 1 M nitric acid but then increases at a greater rate than either Et(m)TDPA or Et(p)TDPA with increasing acidity. The distribution ratios for Et(o)TDPA surpass that of both meta- and para- isomers at greater than 3 M HNO_3.
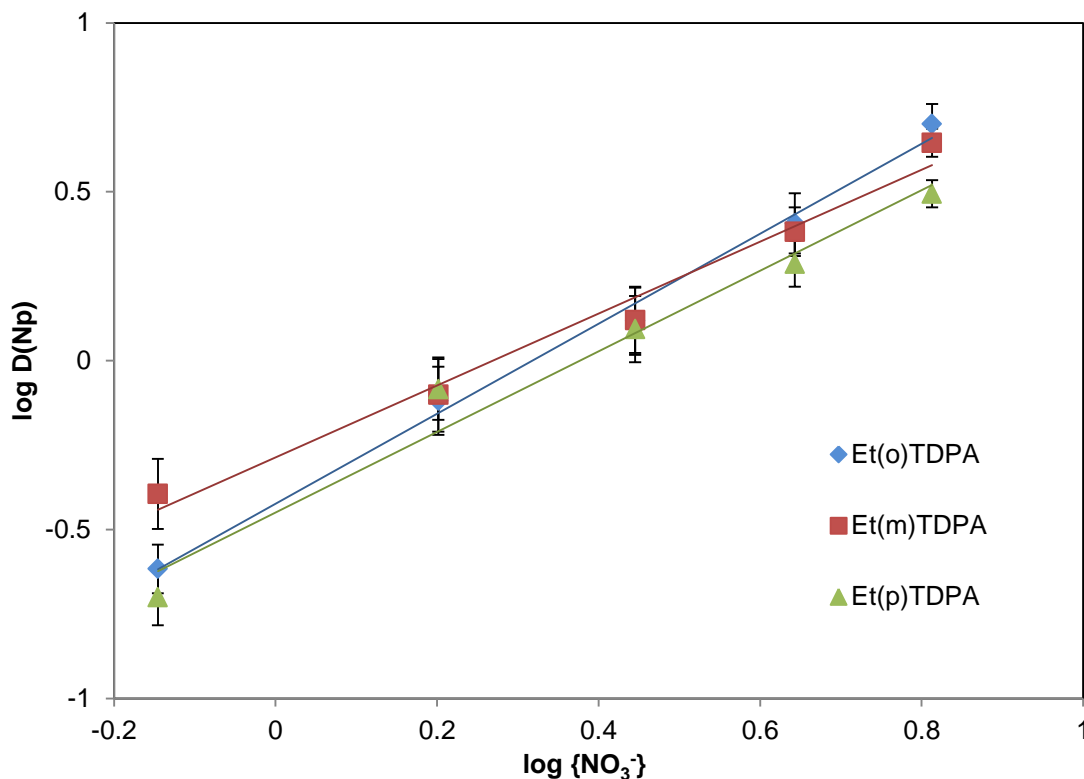
Figure 4.14: Distribution of Np(V) from nitric acid with 0.2 M EtTDPA

Using log-log analysis of the nitrate activities and $D_{Np(V)}$ values gives solvation numbers of 1.30 ± 0.05, 1.02 ± 0.07, and 1.19 ± 0.13 for ortho-, meta-, and para-EtTDPA respectively, again showcasing the greater ability of Et(o)TDPA for Np(V) extraction at higher acidities. These results confirm that which was expected from equation (4.14), where one nitrate is extracted per EtTDPA:Np(V) complex. Unlike with uranium(VI), no additional molecule of nitric acid is observed, possibly due to the lower coordination number of the pentavalent dioxocation. Spectral analysis of the organic phase does show evidence of some disproportionation of Np(V) to Np(IV) and Np(VI), with minute quantities of Np(IV) detectable at acidities greater than 3 M nitric acid, explaining the slight increase in the distribution coefficient at higher acidities. However,

Np(V) remains the dominant extracted species and no Np(VI) was observed due to the fast reduction of Np(VI) by EtTDPA. As was also expected, the distribution ratios for Np(V) were not particularly large, with nearly ten times less extraction yields than those observed for U(VI) or Am(III) at 3 M HNO$_3$.[106] In comparison to other known extraction systems, the organic solvent system based on the FS-13 diluent and any of the three EtTDPA derivatives extract Np(V) significantly better than 30% tributyl phosphate (TBP) in *n*-dodecane with D values nearly 100 times those obtained with the PUREX solvent,[55] and approximately three times more than a 0.22 M solution of the di-isobutyl form of CMPO in decane.[149]
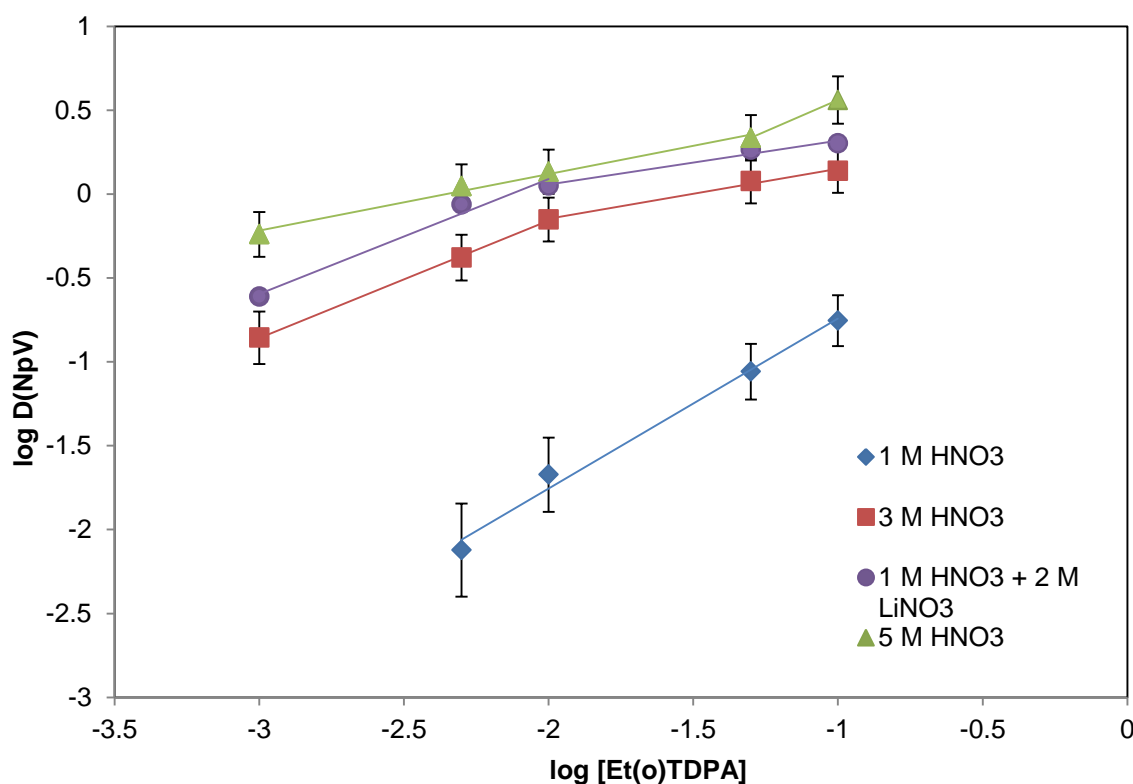
Figure 4.15: Extraction of Np(V) by variation of Et(o)TDPA concentration from various nitric acid concentrations

Figure 4.15 displays the extraction of Np(V) with increasing Et(o)TDPA concentrations at different acidities. The first point of the 1 M HNO_3 line was omitted due to the extremely low distribution of Np into the organic phase at these conditions, with count rates in the Np-237 window never being relatively larger than those observed as background. At all nitrate conditions the distribution ratios raise with increasing diamide concentration. However, what can be noticed immediately from the figure is that only the data obtained at 1 M HNO_3 consists of a straight line, with a slope of 0.98 ± 0.07. A similar slope at this concentration was also obtained for Et(p)TDPA (Figure 4.16) with a value of 0.96 ± 0.04. Beginning at 3 M HNO_3 the slope begins to decrease to a value of approximately 0.33, until the maximum concentration of EtTDPA that could be easily solvated in FS-13 was reached.
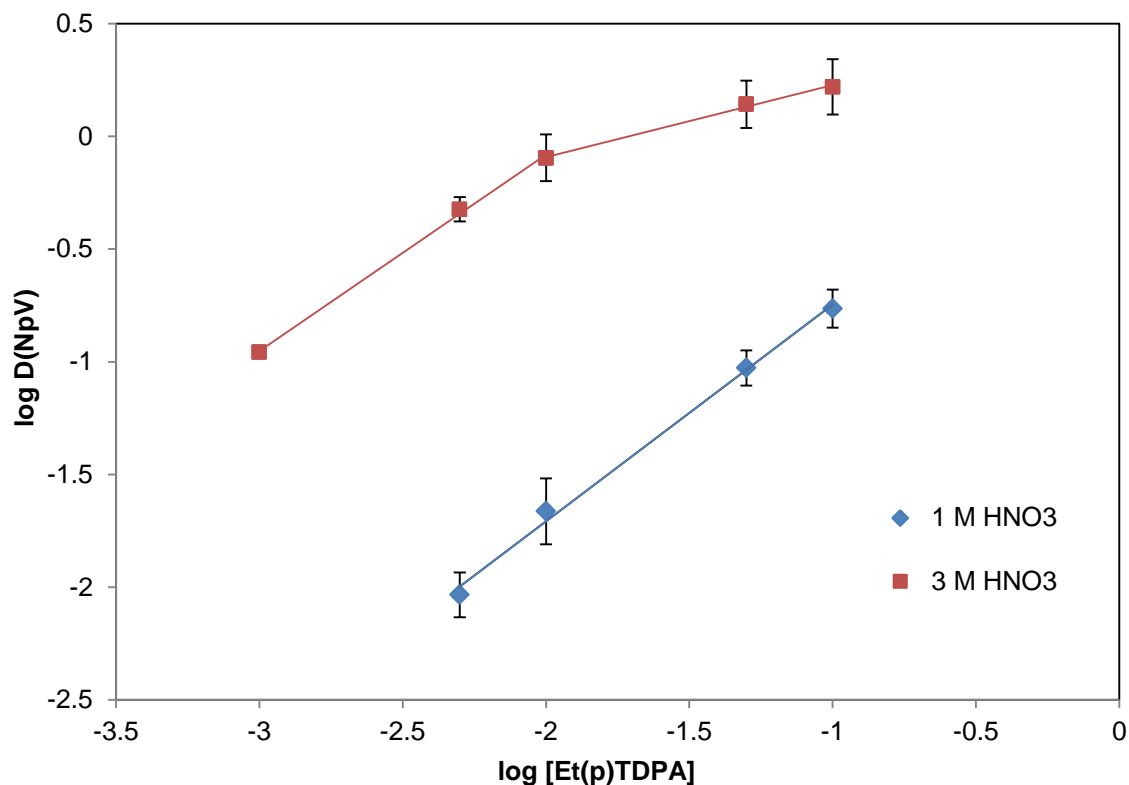
Figure 4.16: Extraction of Np(V) by variation of Et(p)TDPA concentration from various nitric acid concentrations

To determine if this was simply an effect of acidity, the extractions were also performed with 1 M HNO_3 and 2 M $LiNO_3$, also shown in Figure 4.15. The data follows the exact trend as seen with 3 M HNO_3, albeit with slightly higher distribution ratios due to the salting out effect of the lithium nitrate. It can also be assumed this is not due to a change in oxidation state of neptunium at these conditions, because as stated previously Np(V) is well known to be the least extractable species of the three nitric acid stable species of neptunium by neutral extractants. If any disproportionation or oxidation to either Np(IV) or Np(VI) was occurring then an increase in distribution ratios would be observed instead. The extraction for 5 M HNO_3 appear to begins with a similar slope as

the end of the 3 M line but then begins to show increasing distribution ratios. This is most likely disproportionation to Np(IV) and Np(VI) which is favored at higher acidities.

A similar effect to that observed in the 3 M nitrate data was also seen previously by Wisnubroto *et. al.* when varying amounts of TBP were introduced concurrently with the main extractant CMPO.[149] The effect was explained by the addition of a polar molecule like TBP lowering the activity of CMPO by causing dipole-dipole interactions between the TBP and C=O and P=O groups of CMPO, causing a decrease in affinity for the already weakly complexed Np(V). Though two extractants were not specifically used in the present work, the solvent FS-13 was chosen for its polarity among other qualities.[63] It's possible that the increasing concentration of EtTDPA lower the solvation power of FS-13 thus causing a drop in the affinity of the weakly bound neptunium ion for the organic phase. Another possibility is aggregation of the ligand due to protonation, which has been shown to occur in neutral N-donor extractants where protonation of one of the ligands in the organic phase by nitric acid is followed by aggregation of the ligands into dimer and even trimer species.[96,32] Aggregation would cause a drop in the amount of free ligand available for complexation leading to the observed decrease in ligand stoichiometric dependence.

4.5. Protactinium(V)

The literature regarding the chemistry of protactinium is filled with several discrepancies of its behavior in aqueous solution with a vast majority of the studies taking

place in the late 1950s and early 1960s.[16,150] Keller describes the difficulties in the study

of protactinium chemistry[24] as the result of "inadequacies in our handling of hydrolytic

phenomena and HF solutions." Results are not only conflicting but there are often

difficulties with reproduction of one's own findings.[151]

The most predominant oxidation state in aqueous solution is Pa(V), though Pa(IV) is

considered stable in highly acidic media.[19] It would be expected that Pa(V) would be

present as the PaO_2^+ ion as is formed by the other pentavalent actinides. However, there

is evidence that shows either this species is not formed, or has very different chemical

behavior than the rest of the actinyl ions and is more readily hydrolyzed.[152] The

prevailing belief is that in complexing mineral acids such as nitric acid of lower

concentration ($0.5 \text{ M} \leq H^+ \leq 1 \text{ M}$) protactinium is readily hydrolyzed in the form:

$$Pa^{5+} + nH_2O + mX^- \leftrightarrows [PaO(OH)_n(X)_m]^{5-n-m} + nH^+ \qquad (4.16)$$
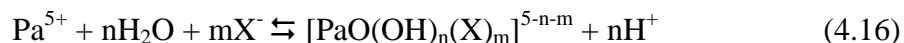
where $n \geq 2$, $m \leq 4$, and X is the singly charged conjugate base of a mineral acid. Species

such as $PaO(OH)^{2+}$, $PaO(OH)_2^+$, and $Pa(NO_3)^{4+}$ have also been reported in this acid and

nitrate concentration range with successive nitrato complexes forming upon increasing

nitrate concentrations and forming anionic complexes at greater than 4-5 M nitric acid.[152]
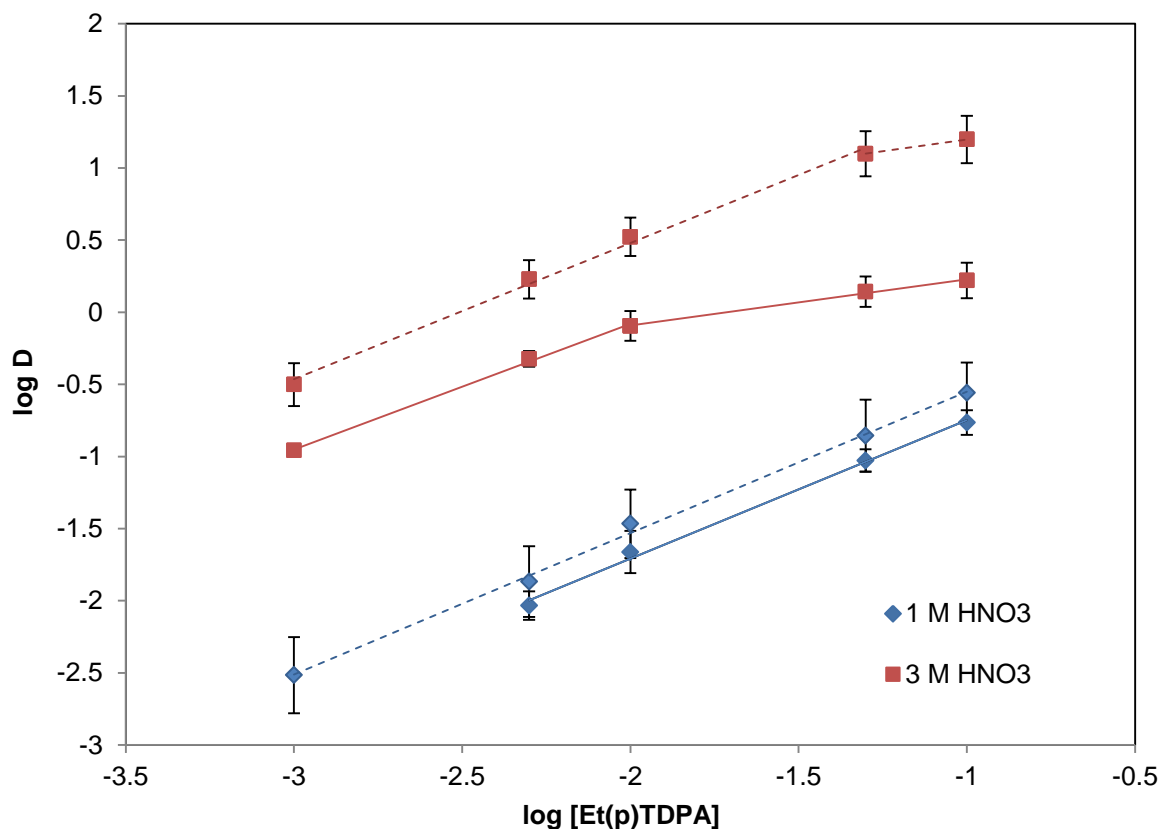
Figure 4.17: Comparison of Np (solid) and Pa (dashed) extraction by Et(p)TDPA

This hypothesis of ligand interaction seen with neptunium is supported by extraction data obtained for protactinium, which like neptunium primarily exists as the pentavalent species. A comparison of the extractions of both Np and Pa with increasing Et(p)TDPA is given in Figure 4.17. At 1 M nitric acid both metals are nearly perfect parallels within standard deviation, with a slope of 0.98 ± 0.03 for protactinium compared to the 0.98 ± 0.07 for neptunium. However, Et(p)TDPA shows higher affinity for Pa, with distribution ratios are approximately 1.5 times larger than those obtained for Np. At 3 M HNO_3 one can immediately see the deviation which appears in the Np curve particularly after the third point in the trend. The Pa curve instead remains constant much

longer, with a slope of 0.94 ± 0.06 until after the fourth point where linearity finally begins to break. If the hypothesis of ligand interactions is credible, then it should be expected that a cation for which EtTDPA has a stronger affinity would be able to resist these interactions until greater ligand concentrations, which is indeed observed in these trends.
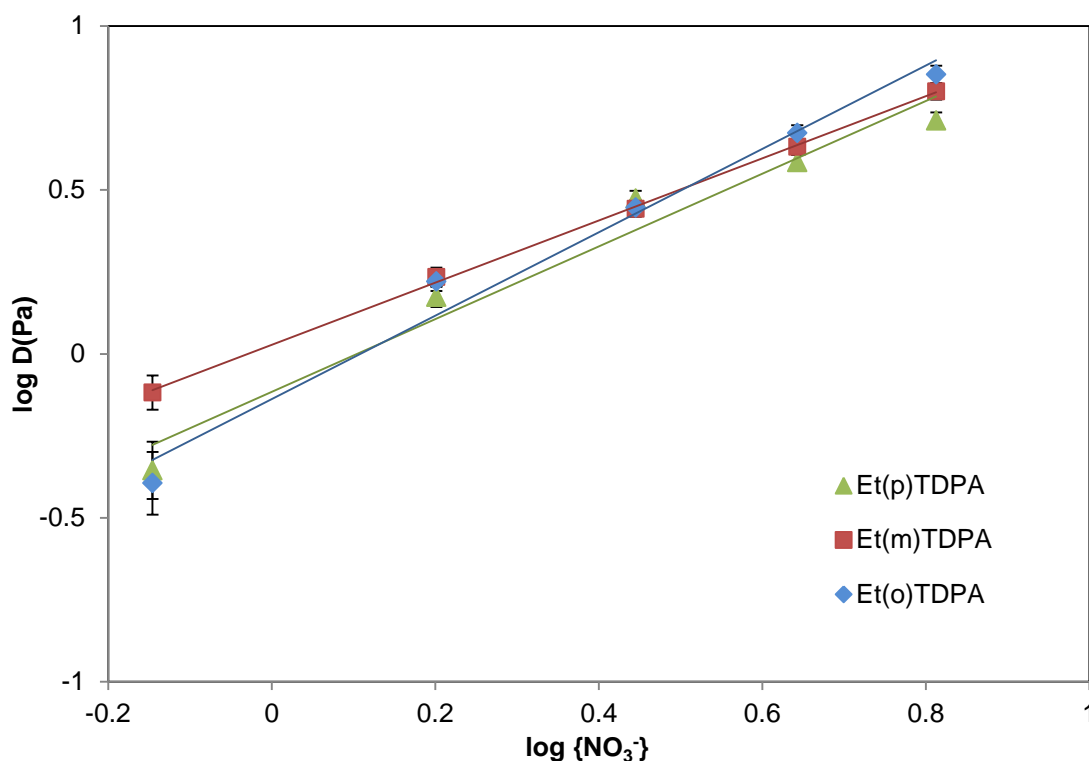
Figure 4.18: Extraction of protactinium by 0.2 M EtTDPA from nitric acid solutions

The extraction dependence of protactinium(V) on the nitric acid activity is shown in Figure 4.18. Like neptunium(V) a nitrate dependence of one was found with Et(m)TDPA and Et(p)TDPA, while the same trend in other extractions for the slightly higher nitrate dependence for Et(o)TDPA was observed but was still close to a value of one. Since

Pa(V) is considered to not form the PaO_2^+ protactinyl ion these nitrate values indicate the extracted species as the $PaO(OH)_2^+$ ion with the mechanism:

$$PaO(OH)_2^+ + EtTDPA + NO_3^- \leftrightarrows PaO(OH)_2(NO_3)^\cdot[EtTDPA] \qquad (4.17)$$

4.6. Thorium(IV)

Unlike the other actinides, the oxidation state chemistry of thorium is drastically simpler, with the only stable form in aqueous solution being the tetravalent Th^{4+} ion. Because of the large charge associated with the thorium cation, thorium is highly susceptible to hydrolysis. $Th(OH)_x^{4-x}$ species begin to form readily in appreciable amounts at pHs greater than 2, while thorium will undergo polymerization reactions above pH 3.[153] By keeping the nitric acid concentration greater than 1 M the contribution of thorium hydroxide or polymeric species should be negligible.

Thorium is known to have a strong affinity for oxygen donor atoms,[154] which should mean high extraction yields with EtTDPA with the expected mechanism of extraction:

$$Th^{4+} + nEtTDPA + xNO_3^- \leftrightarrows [(EtTDPA)_n \cdot Th(NO_3^-)_x]^{4-x} \qquad (4.18)$$

The distribution of Th into increasing EtTDPA concentrations from 3 M nitric acid is given in Figure 4.19. As expected the extraction yields are extremely high compared to those of the studied actinide cations. Thorium distribution ratios of greater than 1 are reached at 0.3 mM for both Et(m)TDPA and Et(p)TDPA compared to the least

extractable actinide neptunium(V) which requires a nearly saturated solution of EtTDPA in FS-13 to achieve this level of extraction. Et(o)TDPA shows the lowest capability for extraction, with $D_{(Th)}$ values of approximately 7-8 times less than Et(m)TDPA and 4-5 times less than Et(p)TDPA for all identical concentrations. The solvation numbers obtained from slope analysis are 1.80 ± 0.07, 1.95 ± 0.08, and 1.92 ± 0.03 for Et(o)TDPA, Et(m)TDPA, and Et(p)TDPA respectively. These numbers indicate that there are two molecules of EtTDPA extracted into the neutral ligand complex per thorium ion. This result is slightly higher than other diamidic extractants (1.31 for N,N,-dimethyl-N,N,-dihexyl-3-oxapentanediamide) however this may be a result of the more rigid structure of EtTDPA limiting the spatial conformations around the Th cation.[155]
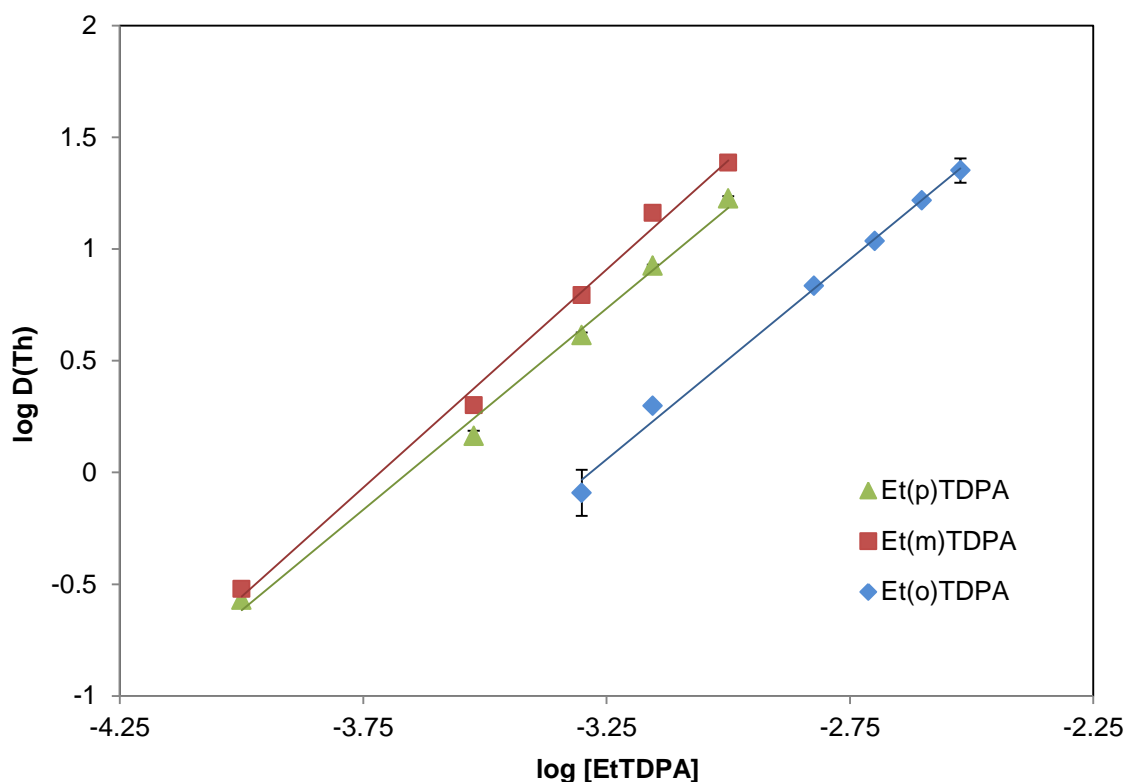
Figure 4.19: Extraction of thorium with EtTDPA from 3 M HNO$_3$ in FS-13

For determination of the nitric acid dependence, a concentration of only 0.001 M EtTDPA was used for extraction rather than the 0.2 M EtTDPA used in all previous experiments. The high extractability of thorium limited the range of conditions that could be studied, as lower amounts of EtTDPA could not contain high enough metal to ligand ratio to ensure completion of the extraction mechanism, while higher concentrations of EtTDPA led to thorium extraction beyond the sensitivity of the Arsenazo (III) spectrophotometric method. The distribution ratios obtained from these measurements are shown in Figure 4.20. After 3 M HNO_3, these values approach a maximum at 5 M HNO_3 and then begin to decline as EtTDPA begins to preferentially extract nitric acid over thorium.
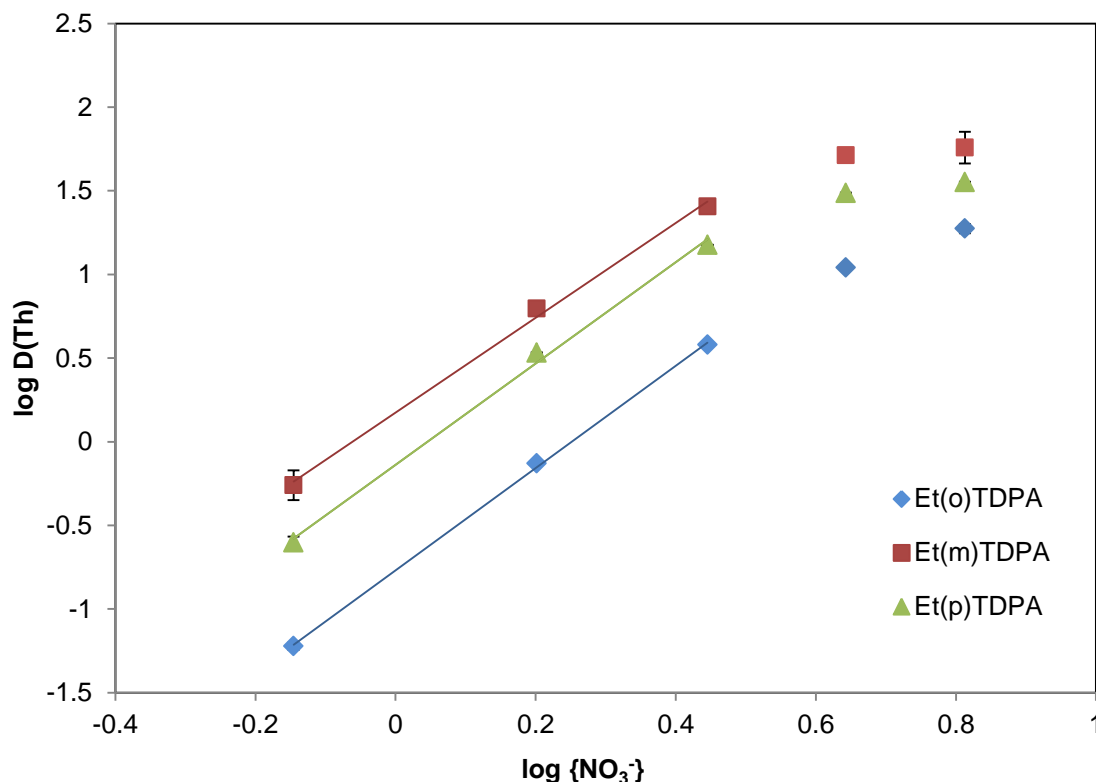
Figure 4.20: Thorium extraction with 0.001 M EtTDPA from nitric acid

As was seen in the ligand dependence experiments Et(o)TDPA again showed the lowest extraction capability for thorium. Unlike the other actinide extraction experiments, ortho did not surpass the extraction capability of meta- or para- EtTDPA at higher nitric acid conditions. The reason for this general behavior with Et(o)TDPA or why it does not occur with thorium is unknown. Based on the neutral extraction implied by Equation (4.18) it is expected that a nitrate value of approximately x = 4 should be obtained to balance the tetravalent ions charge, but this was not observed. Nitrate solvation numbers with each EtTDPA isomer are approximately 3. This non-ideality is discussed further in Section 4.8.

4.7. Plutonium(IV)

The primary oxidation state of plutonium in acidic aqueous conditions, such those during fuel reprocessing, is the 4+ tetravalent state. Like thorium, the plutonium Pu^{4+} ion is highly susceptible to hydrolysis and polymerization reactions at higher pH.[153,156] Unlike thorium the oxidation state behavior of plutonium varies greatly with possibility of having the 3+, 4+, 5+, and 6+ oxidation states existing simultaneously in solution.[157,158] The reasons for this can be seen by the Latimer diagram in Figure 4.21 where the redox potentials of the 3+ to 6+ states are all approximately 1 V vs. standard hydrogen electrode.[159]

$$+6 \qquad\qquad +5 \qquad\qquad +4 \qquad\qquad +3 \qquad\qquad 0$$

$$PuO_2{}^{2+} \xrightarrow{\;1.02\;} PuO_2{}^{+} \xrightarrow{\;1.04\;} Pu^{4+} \xrightarrow{\;1.01\;} Pu^{3+} \xrightarrow{\;-2.0\;} Pu$$
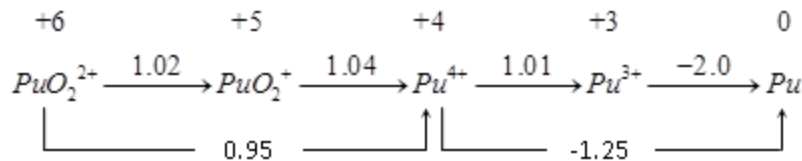
Figure 4.21: Plutonium redox potentials vs. SHE for 1 M HClO$_4$

To complicate matters further, several of the available oxidation states also undergo disproportionation depending on the conditions of the aqueous phase. The bare Pu^{4+} ion disproportionates at low acidity to form Pu(III) and Pu(V); Pu(V) will also react with Pu(IV) to form Pu(III) and Pu(VI).[158] These reactions are summarized in the following equations:

$$2Pu^{4+} + 2H_2O \leftrightarrows Pu^{3+} + PuO_2{}^{+} + 4H^{+} \tag{4.19}$$

$$PuO_2{}^{+} + Pu^{4+} \leftrightarrows PuO_2{}^{2+} + Pu^{3+} \tag{4.20}$$
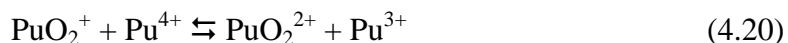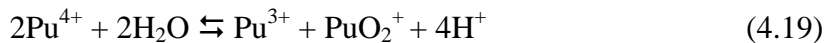
By keeping plutonium at higher acidities the tetravalent oxidation state is more stabilized, but autoradiolysis of nitric acid solutions by plutonium causes the production of hydrogen peroxide and nitrous acid which present further complications in controlling the plutonium speciation.[160,161] Since the primary oxidation state of plutonium in dissolved fuel is tetravalent, all extraction experiments where done with plutonium chemically adjusted to Pu^{4+}.
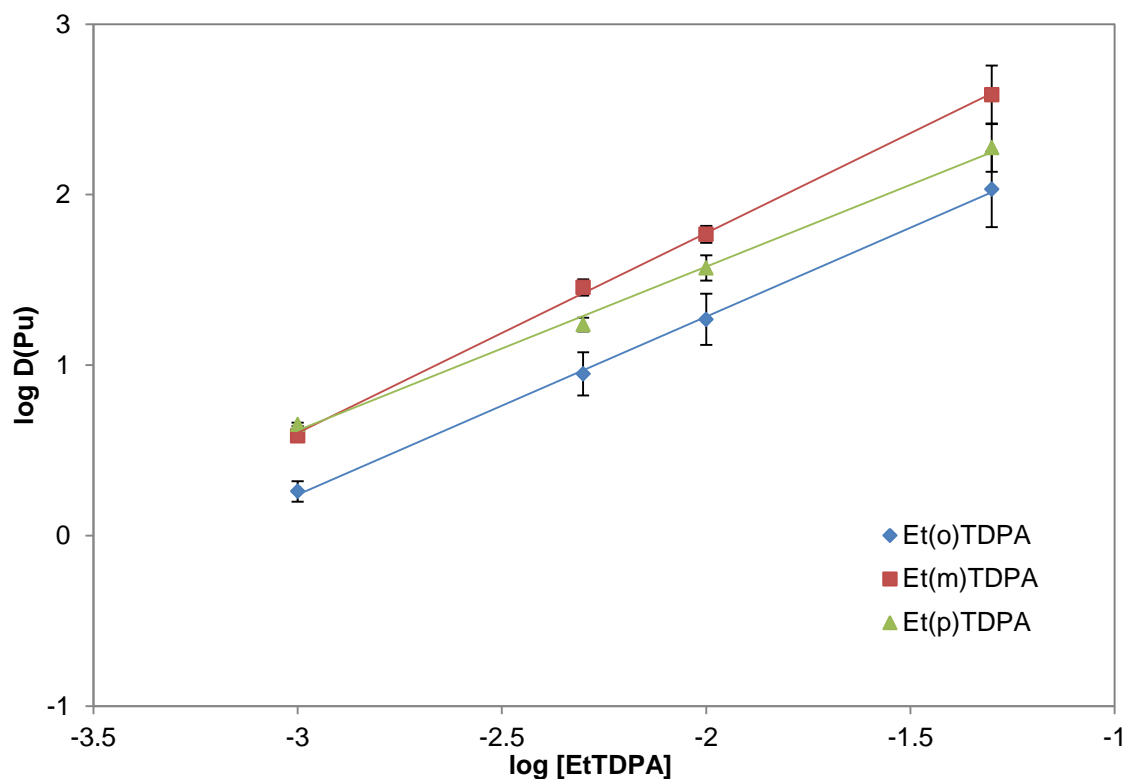
Figure 4.22: Plutonium(IV) extraction by EtTDPA from 3 M HNO$_3$ in FS-13

Extraction of plutonium(IV) by 0.001-0.05 M EtTDPA from 3 M nitric acid is shown in Figure 4.22. Slopes of approximately one were obtained for all isomers, however, as in the case with thorium, were slightly higher for Et(m)TDPA with a value of 1.10 compared to 1.05 and 0.99 for Et(o)TDPA and Et(p)TDPA respectively. These values are close enough to the integer values to consider one molecule of EtTDPA per extracted plutonium complex. This is one less EtTDPA molecule per complex than seen in extractions with the tetravalent thorium ion. The reason for this is likely attributed to the decreased ionic size of Pu^{4+} (88.7 pm) relative to Th^{4+} (97.2 pm) where the smaller Pu^{4+} ion can no longer accommodate coordination by a second EtTDPA ligand.[162]

Attempts to quantify plutonium's extraction dependency on the nitrate activity proved to be very difficult. Experiments could be reproduced when varying the nitric acid content of the aqueous phase only up to 3 M nitric acid. This is unrelated to the extraction changes seen with neptunium and protactinium, as they were only observable with variable ligand concentration. Beyond this acidity experiments were not repeatable despite holding all other variables constant. As such only points below this value were used to determine the nitrate solvation numbers and the results are discussed in Section 4.8.

It is unknown why such difficulty was seen when trying to replicate experiments. A likely reason would be oxidation state changes caused by the varying acidities required for such an investigation. Beyond 3 M nitric acid the activity dependence on the distribution ratio of the extracted complex varied from two to as much as six when a linear trend could be calculated, with the distribution ratios themselves varying by more than an order of magnitude. Since the most extractable species should correspond to the initial oxidation state of Pu(IV), any change in oxidation state should cause a decrease in the extraction rather than an increase. The stock solution of Pu(IV) was contained in 1 M nitric acid where it was found to be stable for weeks at a time. According to Equation (4.19) increasing the acidity should have promoted the formation of Pu(IV) as well. Thus although this may have been a factor it cannot be the sole cause.

Attempts were also made to hold acid strength constant and vary the total nitrate concentration by the addition of lithium nitrate. This increased the reproducibility of the extraction data and seemed to suggest coordination of nitrates similar to that with

thorium, but again the variance in distribution ratios is too large to be certain. The increasing tendency of plutonium to form the hexanitrato $Pu(NO_3)_6^{2-}$ anionic complex at greater than 3 M nitric acid could also be a cause for the unexpected extraction behavior with EtTDPA.[163] Regardless of the reason for this erratic behavior, using the standard concentration of 0.2 M EtTDPA would result in quantitative extraction of plutonium(IV) from nitric acid solutions of approximately 3 M.

4.8. Non-Ideal Extraction Behavior

Up until Section 4.6 regarding the extraction behavior of thorium, an assumption was made that the quantity D in the distribution coefficient contained only two species of metal: free hydrated ion in the aqueous phase and the metal:ligand complex in the organic phase. This assumption greatly simplifies calculations and is reasonably valid in non-complexing media or with metals which are not prone to forming complexes with the anions in the aqueous phase, such as between the uranyl or neptunyl ions and nitrate. However, the tetravalent and trivalent actinides have significantly more inner sphere complexation with nitrate and therefore a more rigorous calculation of the solvation numbers must be performed including the competition between the nitrate and ligand for the metal ion. Starting with an algebraic manipulation of Equation (2.12) and assuming the organic and water coefficients behave ideally, one can eventually arrive at the expression:

$$K = \frac{D_M(1 + \Sigma\beta_i\{NO_3^-\}^i)}{\{L\}^n\{NO_3^-\}^x} \qquad (4.21)$$

where D_M is the distribution ratio of the metal ion, and β is the stability constant of the metal anion complex up to formation of the ith species in solution.[164] Using literature stability constant values ($\beta_1 = 1.33$ and $\beta_2 = 0.88$ for Am^{3+}, $\log \beta_1 = 0.67$ for Th^{4+} and $\log \beta_1 = 0.74$ and $\log \beta_2 = 1.37$ for Pu^{4+})[118,119] the distribution of metals can be plotted as the numerator of Equation (4.21) versus nitrate activity to obtain new nitrate dependencies with values of nearly exactly 3 and 4 found for Am^{3+}, Th^{4+}, and Pu^{4+} in perfect agreement with expected values.

4.9. Separation from the Lanthanides

Because the basis for the research of EtTDPA is the separation of the elements in used nuclear fuel, it is of importance to compare the extraction of the elements studied here to other metals which consist of significant amounts, namely the trivalent actinides and lanthanides.[*] The separation of the actinides studied in this work from the lanthanides by isomers of 0.2 M EtTDPA from 3 M nitric acid are shown in Figure 4.24, Figure 4.24, and Figure 4.25 for Et(o)TDPA, Et(m)TDPA and Et(p)TDPA respectively. The separation by Et(m)TDPA is nearly identical to Et(p)TDA, with the exception of Pu(IV). In previous studies it was shown that Et(o)TDPA had the highest distribution ratio of any isomer for all of the trivalent metals when extracting from 3 M nitric acid.[106]

[**] Data for the trivalent f-metals obtained from reference [106] and used with permission

This is not always the case for the other actinide elements and as a result the separation factors are generally slightly lower for Et(o)TDPA, and significantly lower in the case of thorium. However, the separation factors for thorium with any EtTDPA isomer are still well above what is needed to perform an efficient separation from any of the trivalent lanthanides.
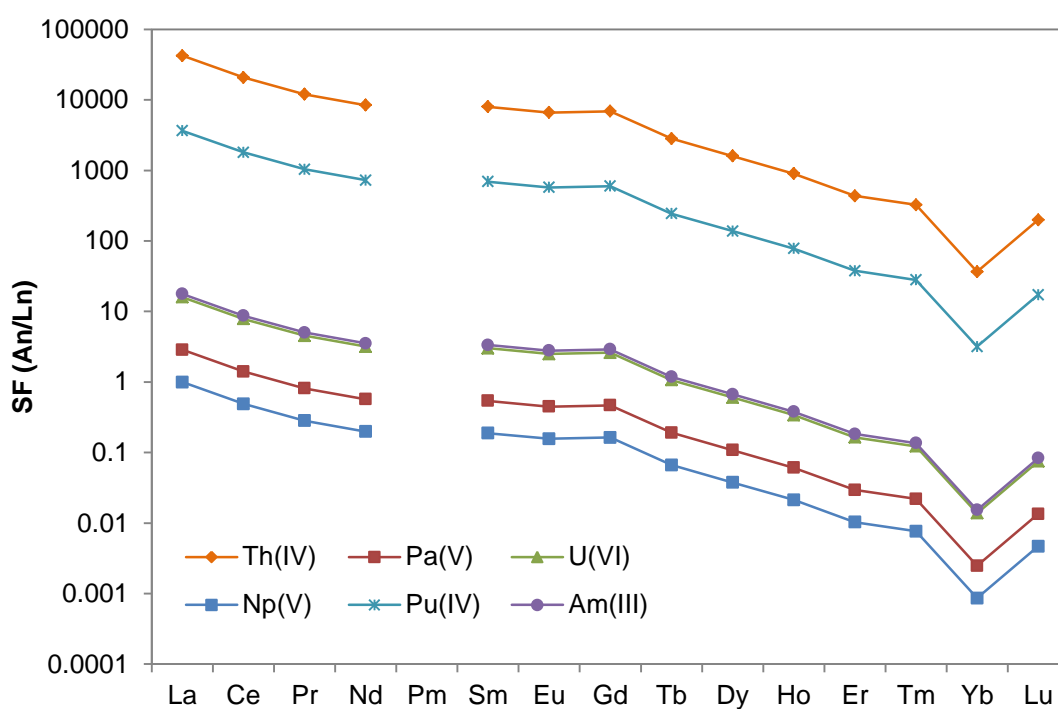
Figure 4.23: Separation of the actinides from trivalent lanthanides at 3 M nitric acid with 0.2M Et(o)TDPA
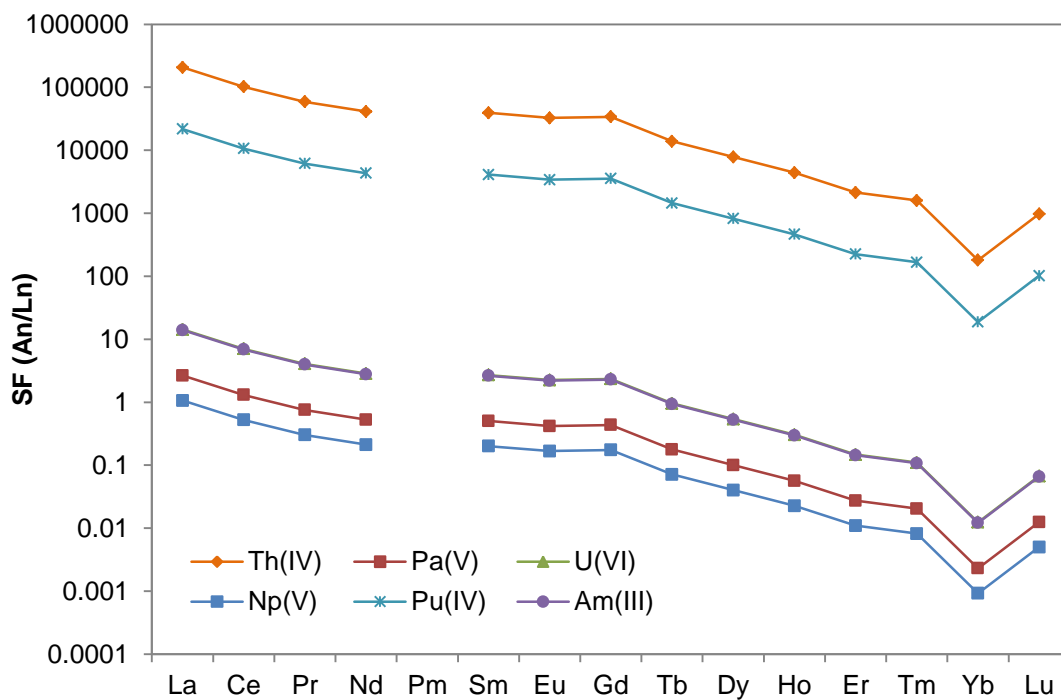
Figure 4.24: Separation of the actinides from trivalent lanthanides at 3 M nitric acid with 0.2 M Et(m)TDPA
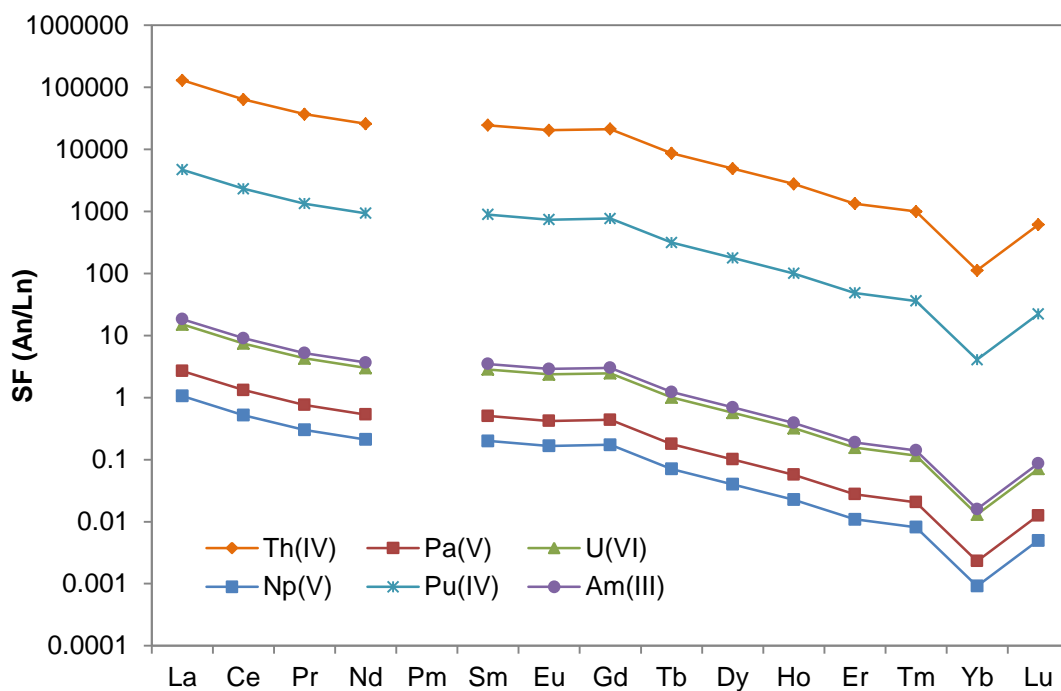
Figure 4.25: Separation of the actinides from trivalent lanthanides at 3 M nitric acid with 0.2 M Et(p)TDPA

From the figures it can be seen that the extraction order of the actinides does follow as the effective cationic charge: $An^{4+} > AnO_2^{2+} \sim An^{3+} > AnO_2^+$ as expected. Most actinides are able to achieve good separation from the majority of the lanthanides with a few exceptions. The most poorly separated metals when extracting from 3 M nitric acid are pentavalent neptunium and protactinium and the light lanthanides, with separation factors close to a value of one for gadolinium from protactinium. Neptunium is able to achieve a reasonable

separation from all the lanthanides after cerium, but would require the neptunium to be stripped from the lanthanides, rather than stripping the lanthanides first. The heavier middle lanthanides are also poorly separated from americium and uranium. Of most concern is the little separation of uranium from americium, however this small separation is only seen when extracting from 3 M nitric acid and is also aided by the fact that only trace amounts uranium should be in the raffinate from the uranium reprocessing step.

5. DEGRADATION OF ETTDPA AND ITS EFFECT ON EXTRACTION CAPABILITY

5.1. Radiolysis

$$H_2O$$

$$H_2O^* \qquad\qquad H_2O^+ + e^-$$

$$\downarrow H_2O$$

$$\cdot OH + H_3O^+$$

$$\cdot H + \cdot OH \qquad H_2 + \cdot O$$

$$e^-_{aq}$$

$$e^-_{aq}, \cdot H, \cdot OH, H_2, H_2O_2, H_3O^+$$

Time (s)

10^{-16}

10^{-14}

10^{-13}

10^{-7}
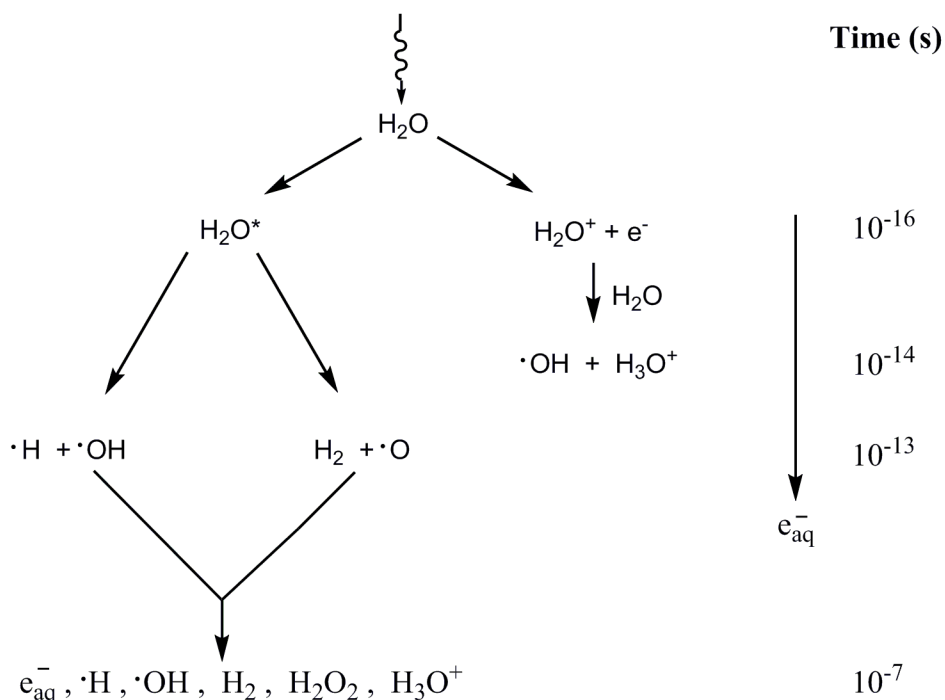
Figure 5.1: Event timeline during radiolysis of neutral water (adapted from Radiochemistry and Nuclear Chemistry 3rd Edition, Choppin)[9]

The primary source of radiolytic damage to the organic ligands used in fuel reprocessing is through indirect reactions rather than from direct energy deposition into the ligand itself.[100] Aqueous and organic soluble ligands are typically present in significantly lower concentrations compared to that of their respective diluents and as a result the most probable interaction of ionizing radiation is with the diluent. Radiolytic damage of the diluent forms a wide variety of molecular and radical species which then

98

facilitate degradation of the organic ligands through chemical rather than radiolytic reactions.

One of the most important radiolytic reactions is the radiolysis of water which is pictured in Figure 5.1. Initial deposition of energy into the water molecule results in either the excitation of molecular water to a higher energy state or the formation of an electron-water ion pair. Due to the high concentration of neighboring water molecules the ionized water will interact on extremely short time scales to form the hydronium ion as well as the reactive hydroxyl radical.[9] The free electron will continue to cause further ionizations until its energy reaches that of the ionization potential of water (12.6 eV) when it then becomes the highly reducing solvated electron species. Molecular excited species will dissociate on the time scale of molecular vibrations (10^{13}-10^{14} s) forming further radical species. The distribution of products from radiolysis of water is highly dependent on the energy and type of incoming ionizing radiation. Low linear energy transfer (LET) interactions (β, γ) result in higher amounts of radical species being formed. High LET radiation such as α-particles deposit their energies in much shorter paths than low LET radiation, resulting in more recombination of radical species and thereby higher yields of molecular products relative to low LET interactions.[165]

Irradiation of more concentrated solutions of nitric acid which are aerated produce an oxidizing environment due to electron and radical scavenger reactions,[166] namely capture of the solvated electrons by dissociated nitric acid and dissolved oxygen gas in the forms:

$$e^-_{(aq)} + H^+ \rightarrow H \cdot \qquad (5.1)$$

$$e^{-}_{(aq)} + NO_3^{-} \rightarrow \cdot NO_3^{2-} \tag{5.2}$$

$$e^{-}_{(aq)} + O_2 \rightarrow \cdot O_2^{-} \tag{5.3}$$

$$\cdot H + O_2 \rightarrow \cdot HO_2 \tag{5.4}$$

$$\cdot HO_2 \leftrightarrows H^{+} + \cdot O_2^{-} \tag{5.5}$$
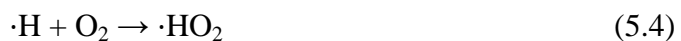
The end result is the predominance of the reactive hydrogen peroxide and hydroxyl radical species in solution, which readily oxidize organic molecules.[100]

It is well known that under radiolysis nitric acid produces radical nitrogen groups by the mechanisms:

$$NO_3^{-} \vee\!\!\wedge\!\!\vee\!\!\wedge \rightarrow e^{-} + \cdot NO_3 \tag{5.6}$$

$$\cdot NO_3^{2-} + H^{+} \rightarrow \cdot NO_2 + OH^{-} \tag{5.7}$$

$$\cdot OH + HNO_3 \rightarrow \cdot NO_3 + H_2O \tag{5.8}$$

in addition to Equation (5.2). Successive protonations of the $\cdot NO_3^{2-}$ radical species will form $H_2NO_3\cdot$ which will then decay by loss of water in a dehydration reaction[167]:

$$H_2NO_3\cdot \rightarrow \cdot NO_2 + H_2O \tag{5.9}$$

The $\cdot NO_2$ radicals are capable of hydrogen abstraction as well as nitration of unsaturated

100

carbon bonds such as aromatics.[168] Nitration of aromatics by ·NO$_2$ radicals is a non-regioselective process, generally resulting in a distribution of species at the ortho, meta, and para position in a monosubstituted aromatic.[169] The para substitution generally appears as the least abundant species, while addition at the ortho position can be impeded by steric effects due to a bulky original substituent, ultimately leading to relative enhancement in the production of the meta isomer.[170] This mechanism of nitration is more predominant at higher pH levels.

Aromatic nitration also proceeds by formation of the NO$_2^+$ nitronium ion. Nitronium can be produced in more concentrated nitric acid solutions by the disproportionation reaction:

$$HNO_3 \rightarrow NO_2^+ + NO_3^- + H_2O \tag{5.10}$$

and along with a sulfuric acid catalyst is the common method of industrial nitration of aromatics.[171,172] Radiolytically, nitronium is produced by the combination of ·NO$_2$ and ·NO$_3$ radicals and direct radiolysis of undissociated nitric acid[165]:

$$\cdot NO_3 + \cdot NO_2 \rightarrow N_2O_5 \rightarrow NO_3^- + NO_2^+ \tag{5.11}$$

$$HNO_3 \; \backslash\!\backslash\!\backslash\!\backslash \rightarrow HNO_3^+ + e^-_{(aq)} \tag{5.12}$$

$$HNO_3^+ \rightarrow NO_2^+ + \cdot OH \tag{5.13}$$
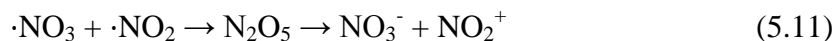
Unlike aromatic nitration by the less powerful ·NO$_2$ radical, nitronium induced reactions are due to electrophilic attack of the positively charged nitronium to the π-orbital of the

aromatic ring system. Nitration is directed by the original substitution group to either the ortho and para direction by electron donating activating groups, or to the meta position by electron withdrawing deactivating groups. This process is more predominant at higher concentrations of nitric acid.[165]

In solvent extraction, radiolysis of the organic phase used as the diluent also plays an important role in determining the possible radiolytic reactions a ligand might undergo. For the solvent extraction reported in this work the diluent trifluoromethylphenyl sulfone (FS-13) was primarily used. The radiolysis of FS-13 has been previously investigated with regards to the CCD-PEG process for removal of cesium and strontium from waste raffinates.[173] Direct radiolytic damage of the diluent is highly probable due to the large amount of solvent molecules present compared to that of any organic phase solutes. Radiolysis of FS-13 results in the ejection of an electron giving a charged radical species which then decays to the benzenesulfonyl ion and the trifluoromethyl radical:

$$C_6H_5SO_2CF_3 \rightsquigarrow C_6H_5SO_2^+ \cdot CF_3 + e^-_{(aq)} \tag{5.14}$$

$$C_6H_5SO_2^+ \cdot CF_3 \rightarrow C_6H_5SO_2^+ + \cdot CF_3 \tag{5.15}$$
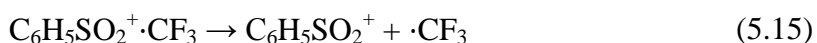
The benzenesulfonyl ion is most readily hydrolyzed by dissolved water in the organic phase to benzenesulfonic acid:

$$C_6H_5SO_2^+ + H_2O \rightarrow C_6H_5SO_2OH + H^+ \tag{5.16}$$

while the trifluoromethyl radical can either undergo radical substitution of aromatics similar to the $\cdot NO_2$ radical or recombine with other trifluoromethyl radicals forming

102

hexafluoroethane[174]:

$$2 \cdot CF_3 \rightarrow C_2F_6 \tag{5.17}$$

Trifluoromethyl ion groups can also cause aromatic substitution by both electrophilic and nucleophilic attack; however these reactions typically have much lower yields, particularly electrophilic attack due to the difficulty to producing the CF_3^+ ion.[175] FS-13 has been previously studied as a direct source of aromatic nucleophilic trifluoromethyl substitution by generation of the CF_3^- group.[176,177]

Mowafy recently reported that symmetrical diamides are the most stable over unsymmetrical and branched amides.[178,179] Furthermore, shorter branching substituents on the amide nitrogen led to higher stability as well. EtTDPA has both of these characteristics indicating that some stability against radiation damage is expected. Et(o)TDPA, Et(m)TDPA, and Et(p)TDPA show strong carbonyl absorptions at 1650, 1651, and 1654 cm^{-1} respectively with concentrations of 0.2 M. These functional groups play a strong role in the mechanism of neutral ligand extractions and thus it is important that they remain mostly intact in order to be of use in waste raffinates. In addition, one of the radiolysis products of FS-13 is sulfuric acid which acts as a catalyst for the electrophilic nitration of aromatic groups.[173] Thus is highly likely that EtTDPA will undergo some form of aromatic nitration in addition to other radiolytic mechanisms such as trifluoromethylation during irradiation. While these reactions would not result in a change in the functional group participating in the extraction process, the addition of electron withdrawing groups such as $\cdot NO_2$ or $\cdot CF_3$ radicals could alter the basicity the

carbonyl groups of EtTDPA, affecting the complexation ability of EtTDPA for the metals of interest.

5.2. Hydrolysis

One of the other primary mechanisms of ligand degradation during the solvent extraction step of used fuel reprocessing is acidic hydrolysis.[180] Some of the more common neutral extractants consist of oxygen containing functional groups such as carbonyls, phosphates, or sulfones, all of which are susceptible to nucleophilic attack by water in the presence of an acid catalyst. Amides are particularly resilient towards acidic hydrolysis when compared to other carbonyl based functional groups such as esters.[181] The chemistry of amides is strongly influenced by the fact that in acidic solution the amide nitrogen is almost completely unprotonated and it is the carbonyl oxygen that acts as the basic site.[182]
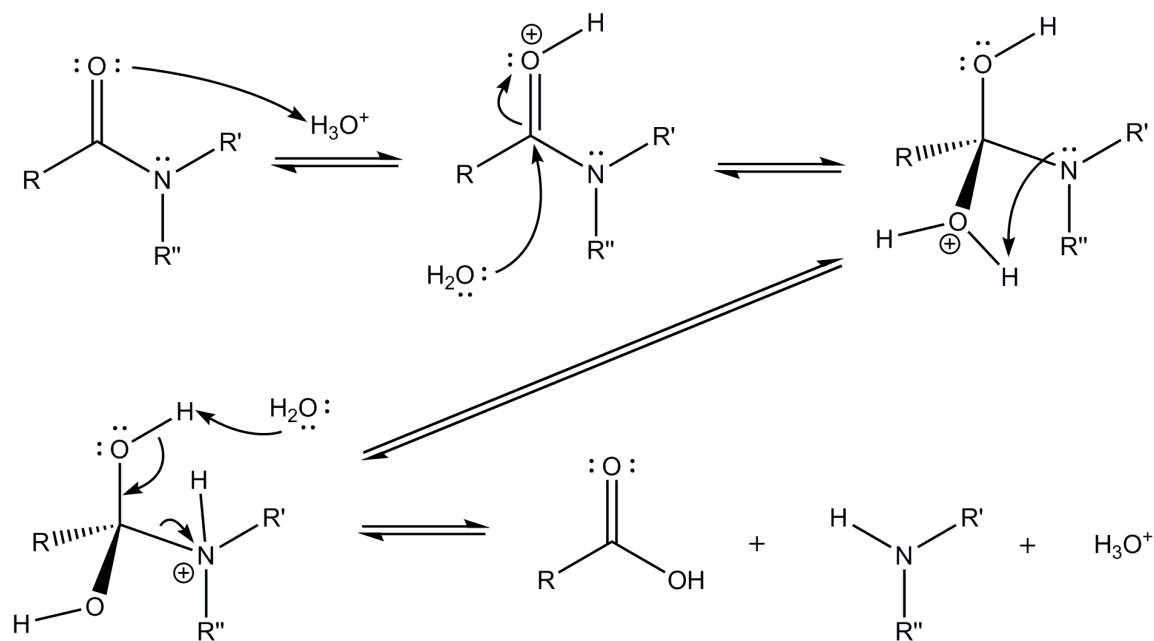
Figure 5.2: Acid-catalyzed hydrolysis mechanism of a generic amide

A diagram of the steps involved in a hydrolysis reaction is shown in Figure 5.2. Acid catalyzed hydrolysis of amides begins with the protonation of the carbonyl oxygen. The pK$_a$s of amides are generally in the range of 0-2 and thus require fairly acidic conditions in order for hydrolysis to proceed by this mechanism.[183] Once this oxygen has been protonated enough electron density is withdrawn away from the carbon atom for it to undergo nucleophilic attack by water. This process forms a tetrahedral intermediate where the previously amidic nitrogen is now an amine, which is far more basic. The amine then removes a proton from the attached water group, forming a carbon center with two hydroxyl groups and a protonated amine attached. The amine is a much better leaving group and is dislodged, while a free water removes the hydrogen from one of the protonated oxygens resulting in the reformation of a carbonyl group and the acid catalyst.

A carboxylic acid and amine is the end result of this process.

5.3. Infrared Spectra of Organic Phase
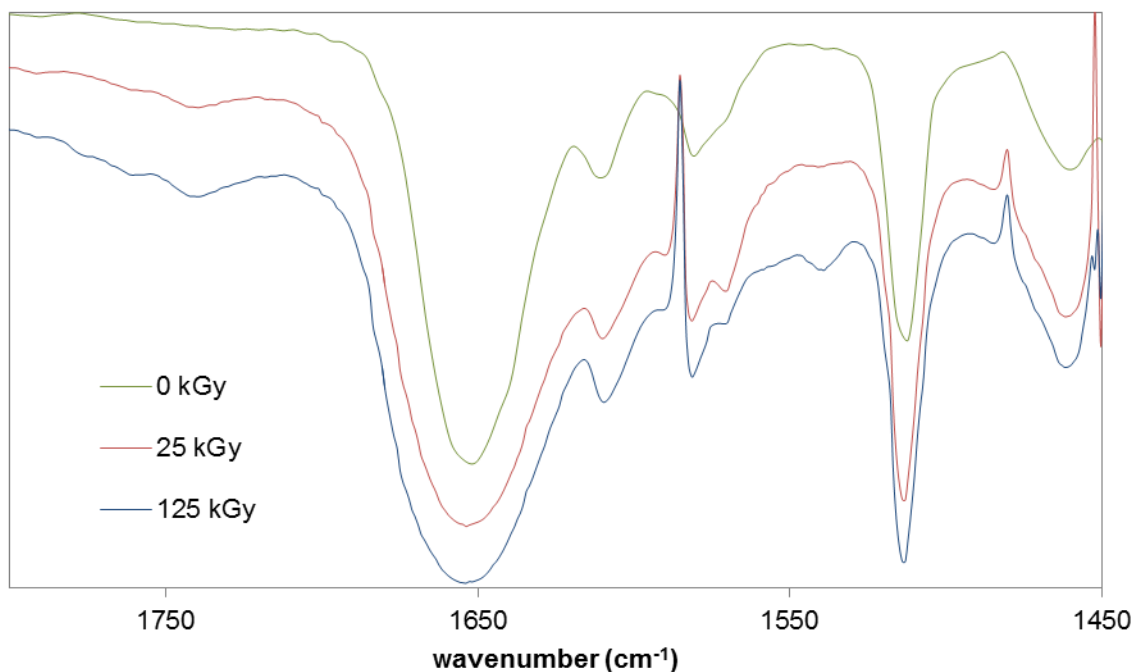
Figure 5.3: IR spectra of carbonyl the region of acid saturated Et(p)TDPA at varying absorbed dose

Infrared absorption analysis of irradiated EtTDPA shows a small decrease in absorption of the amidic nitrogen absorption bands around 3200 cm^{-1} as well as the amide carbonyl stretches in all isomers, though there was not a significant change in the intensities of any of these peaks. The carbonyl spectrum of Et(p)TDPA can be seen in Figure 5.3. The various doses have been off set on the y-axis for clarity, and the spikes at 1590 and 1480 cm^{-1} are artifacts of the solvent spectrum subtraction. At 125 kGy the

carbonyl peak for Et(p)TDPA is slightly broadened at 1654 cm^{-1} at the half-width by less than 2 cm^{-1} compared to that at 25 kGy. With increasing absorbed dose two new peaks begin to grow in at 1537 and 1738 cm^{-1}. Ingrowth of the peak at 1738 cm^{-1} is consistent with the higher vibrational energy of a carboxylic acid moiety.[184] However, the relatively small change in transmittance between the 25 kGy and 125 kGy data suggests that production of this moiety is mostly a result of hydrolysis from the extensive times required to achieved the desired dose rather than due to radiolytic damage. Subsequent investigations of hydrolyzed EtTDPA saw identical products indicating that the radiolytic products are in too small yield with these doses to be determined by infrared spectroscopy.

5.4. Determination of Radiolytic Products by Gas Chromatography-Mass Spectroscopy

In order to determine the exact degradation products of EtTDPA, gas chromatography mass spectroscopy was performed using solutions that had been contacted both with water and nitric acid and irradiated using a cobalt-60 gamma irradiator. Initially solutions of the ortho, meta, and para isomer were individually irradiated after contact with 3 M nitric acid up to a dose of 80 kGy. Chromatographs of these solutions showed almost no peaks associated with degradation products at sufficient intensity to determine their exact structure. It could be determined, however, that the elution times of these products were similar across all three isomers and were determined to be the result of the

slightly different isomeric forms of the parent EtTDPA molecule. Because of this similarity between EtTDPA isomers and lack of irradiator space, only the ortho isomer was irradiated up to a dose of 200 kGy. Quantitative determinations of degradation product yields from similar amidic ligands have required doses in excess of 1 MGy.[185] Quantification of degradation products was not feasible due to the low dose rate available and thus only a qualitative assessment of degradation products was performed.

Some particular degradation products were expected from known reaction pathways by either radiolytic or hydrolytic mechanisms, generally organic acid products, but these could not be seen in the resulting chromatographs. Solutions were then reacted with trimethylsulfonium hydroxide in order to convert the organic acids into their more volatile methylized derivatives. In all cases the detector was disabled from approximately 23-30 minutes to avoid overloading and damaging the detector filament from the evolution of the much more volatile and more than thirty-fold mole excess of FS-13 in each solution which is why no signal is shown for these timeframes.

5.4.1. EtTDPA in FS-13
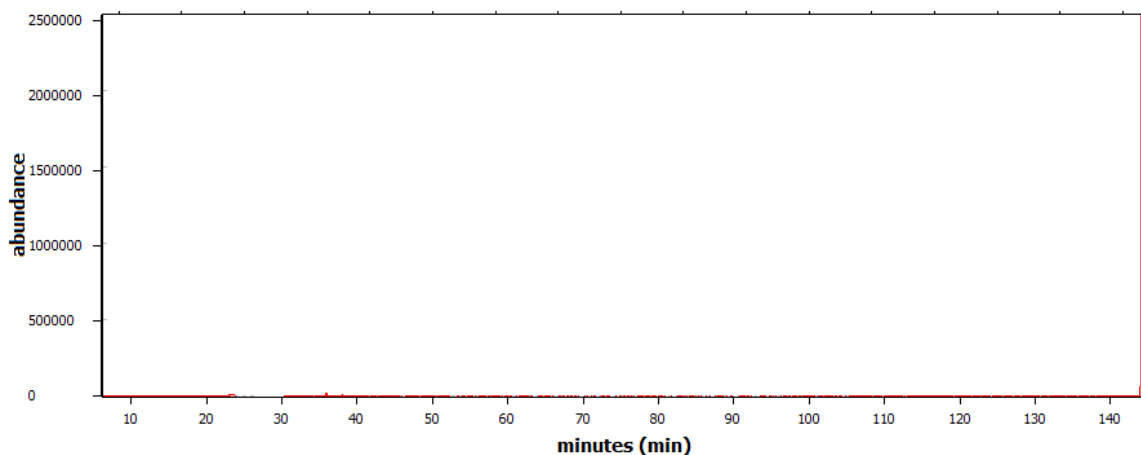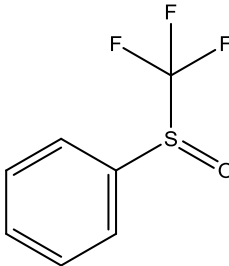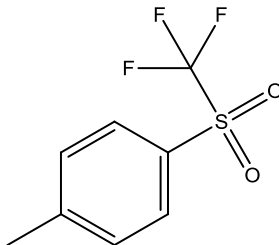
Figure 5.4: Gas chromatograph of Et(o)TDPA in FS-13

The chromatograph of neat Et(o)TDPA dissolved in FS-13 is shown in Figure 5.4 with the detected products shown with their retention times, base peak, and molecular ion in Table 5.1. Elution of Et(o)TDPA corresponds to the large peak at 144 minutes. The only other detectable compounds in the original chromatograph are impurities from the synthesis of FS-13, including the sulfoxide at 23.2 minutes from incomplete oxidation of the sulfur group to a sulfone moiety, and from 33.9-37.9 minutes the tolyl isomer analogs of FS-13. Each of these compounds appear in the chromatographs of the other studied solutions and thus are omitted from the following tables of degradation products. No by-products or unreacted components from synthesis of EtTDPA are detected under these conditions.

Table 5.1: Identified compounds in Et(o)TDPA dissolved in FS-13

Retention Time (min)	Base Peak	Molecular Ion	Structure
23.2	124.9	193.8	
33.9-37.9	91.0	223.8	isomers
144.1	134.1	401.1	Et(o)TDPA

5.4.2. *Hydrolysis of non-irradiated EtTDPA*
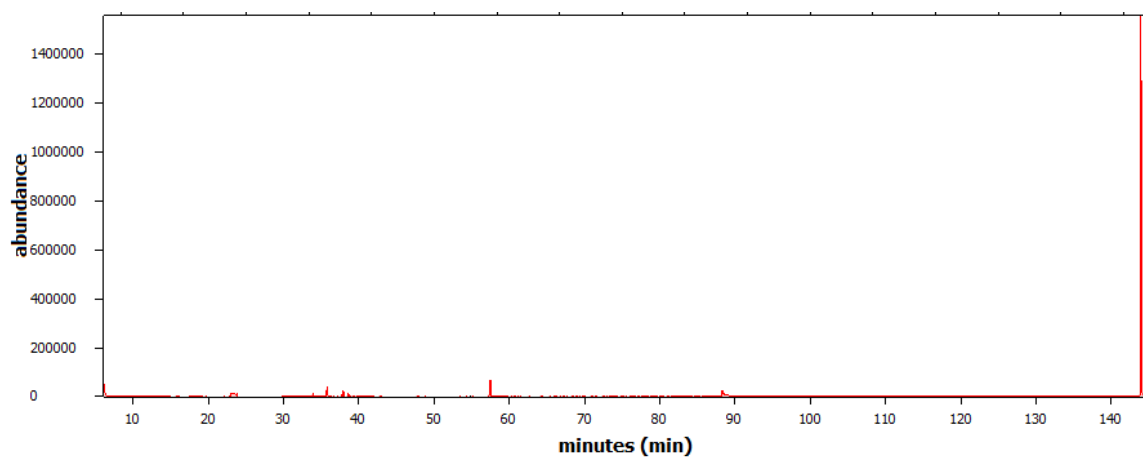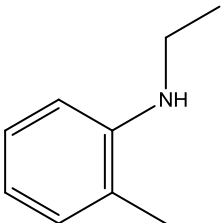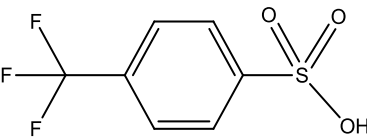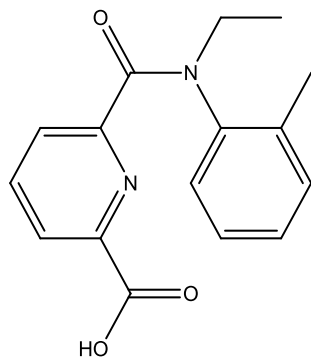
Figure 5.5: Chromatograph of derivatized Et(o)TDPA saturated with 3 M HNO_3 for 3 months

Due to long periods of time required to achieve a specific dose in the cobalt irradiator (dose rate ~0.3 kGy/hr) and the fact that samples could not be analyzed directly after radiolysis due to instrumentation scheduling, it was necessary to determine the degradation of EtTDPA by hydrolytic processes over this large time span between irradiation and analysis. The most probable reaction is the cleavage of the C-N amide bond forming the synthesis reactant N-ethyltoluidine and its complimentary carboxylic acid by the mechanism shown in Figure 5.2. Indeed, N-ethyl o-toluidene is seen as a hydrolysis product at 38.5 minutes in

Figure 5.5 and listed in Table 5.2. This peak is less intense after derivatization due to some of the secondary amine reacting with the trimethylsulfonium hydroxide to form the slightly less volatile tertiary amine. The carboxylic acid compliment is not detected until after methylation with trimethylsulfonium hydroxide, but is too small to be seen on the scale of the graph. This result is somewhat expected though as the N-ethyltoluidine is nearly unidentifiable and more volatile than the ester form of that acid, meaning it would have a lower detection efficiency and thus lower detectable signal.

Hydrolysis of FS-13 from nitric acid also results in the production of benzenesulfonic acid and elutes in methylized form at 57.7 minutes, the other product of this reaction is likely fluoroform and dissolved gas released either upon opening of the vial or early in the chromatogram along with the dichloromethane solvent. A peak can also be seen at 88 minutes, however this peak is the result of impurities inherent to the GC instrument used and is seen along with other impurities in the span of 90-96 minutes in other runs as well.

Table 5.2: Hydrolysis products after contact with 3 M HNO$_3$

Retention Time (min)	Base Peak	Molecular Ion	Structure
39.5	120.0	134.9	
57.7	77.0	172.0 methyl sulfinate	
115.8	134.0	298.1 methyl ester	
144.1	134.1	401.1	Et(o)TDPA

5.4.3. Radiolysis of water contacted EtTDPA

Water saturated solutions of EtTDPA which have been irradiated show some of the same products observed during acidic hydrolysis of EtTDPA with nitric acid, but are produced through the radical reactions described earlier. These reactions include cleavage of the amide C-N and sulfone S-C bonds during radiolysis of organic phase partitioned water, forming N-ethyltoluidine and its carboxylic acid compliment and benzenesulfonic acid. All of these compounds are produced in higher relative yields through radical reactions through radiolysis than observed through acidic hydrolysis. The

112

previously seen trifluoromethylphenyl sulfoxide in neat FS-13 has undergone oxidation by hydroxyl radicals forming phenylsulfinic acid and is seen as the methylized derivative at 60.4 minutes in Figure 5.6and listed in Table 5.3.
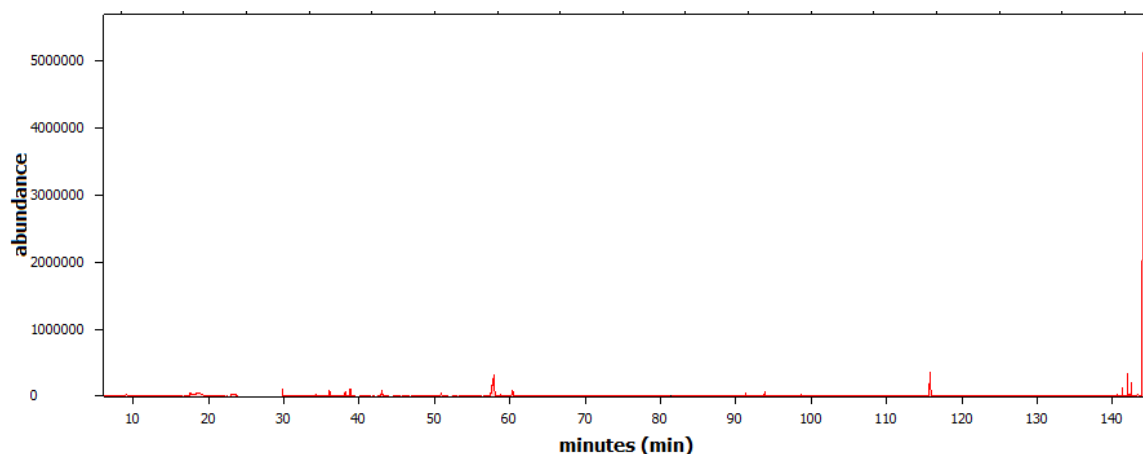
Figure 5.6: Gas chromatograph of water saturated derivatized Et(o)TDPA in FS-13 at 200 kGy

In addition to those already seen during acid hydrolysis, two new major types of products are observed in irradiated solution. First is a peak at 143.4 minutes corresponding to the loss of a methyl group from one of the outer tolyl rings, converting one half of the molecule into an ethyl-phenyl amide derivative. This lost methyl radical reacts with other species in solution, and, in fact, both the methyl sulfinate forms of benzenesulfonic acid and phenylsulfinic acid can be detected in small quantities even when no additional methylating reagent is added.
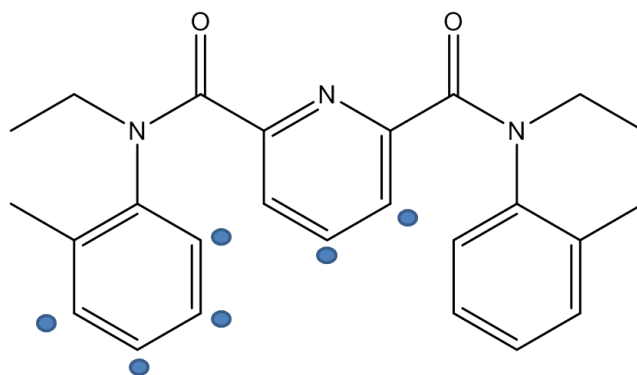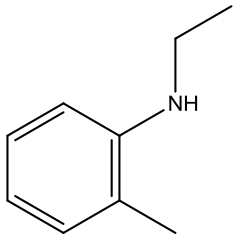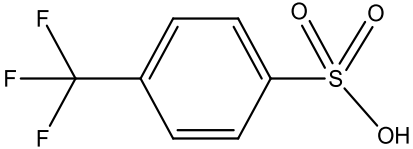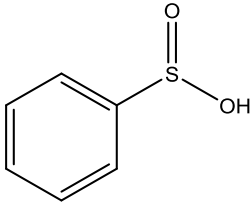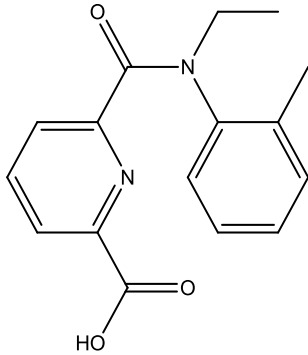
Figure 5.7: Aromatic substitution positions of Et(o)TDPA by CF_3 radicals

The second and most prominent new feature is a group of peaks ranging from 138.5-143.5 minutes. These six peaks are isomers in which EtTDPA molecules have undergone radical substitution reaction of C-H bonds with the trifluoromethyl radical, giving a molecular ion of 469.1 mass units. These substitutions occur at all possible aromatic C-H sites as despite EtTDPA's eleven C-H aromatic positions, symmetry reduces this to only six unique positions for a monosubstituted species as shown in Figure 5.7. This substitution pattern will be discussed further in the next section. No fragmentation patterns are seen which would correspond with substitution on the amide-branching ethyl chains in any of these peaks.

Table 5.3: Water saturated radiolysis products

Retention Time (min)	Base Peak	Molecular Ion	Structure
39.5	120.0	134.9	
57.7	77.0	172.0 methyl sulfinate	
60.4	77.0	156.2 methyl sulfinate	
115.8	134.0	298.1 methyl ester	
143.4	134.0	387.1	Et(o)TDPA − CH$_3$ + H
144.0	134.0	401.1	Et(o)TDPA
138.5-143.5	134.0	469.2	Et(o)TDPA − H + CF$_3$ isomers

5.4.4. Radiolysis of EtTDPA Saturated with Nitric Acid

Derivatization of irradiated nitric acid saturated EtTDPA solutions did not reveal the production of any new species capable of undergoing methylation by trimethylsulfonium hydroxide. Since methylation caused multiple incomplete reactions with some of the already detectable secondary amines produced during radiolytic and hydrolytic reactions, solutions were also injected into the GC-MS without undergoing any additional methylation step such as the chromatograph displayed in Figure 5.8.
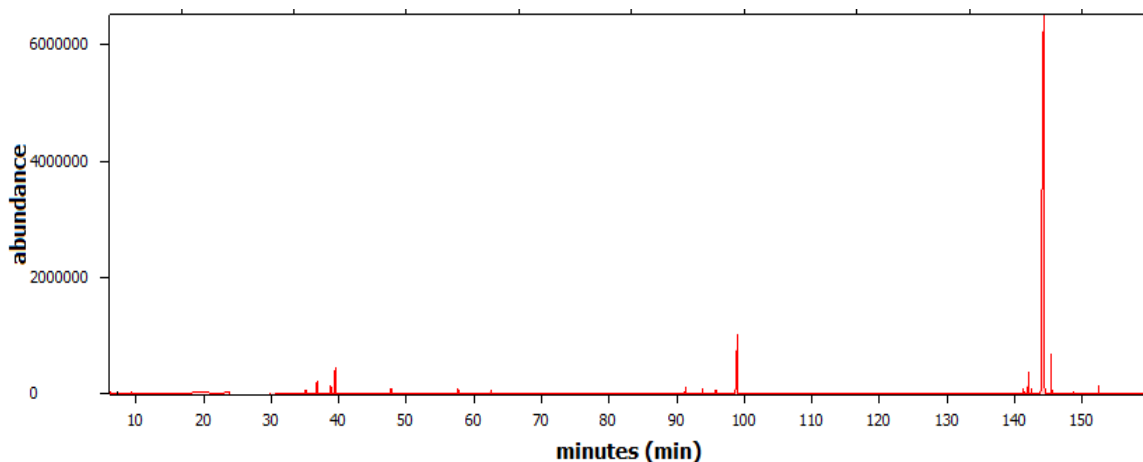
Figure 5.8: Chromatograph of acid saturated Et(o)TDPA in FS-13 at 200 kGy

The radiolytic products of nitric acid contacted EtTDPA are almost identical to those seen in water-contacted solutions and are listed in Table 5.4. Since this chromatograph did not undergo methylation there is a new peak at 98.8 minutes which corresponds to the same carboxylic acid seen at 115.8 minutes in Table 5.2 and Table 5.3. While in the GC column this carboxylic acid degrades by loss of CO_2 and elutes as the N-ethyl o-tolyl amidic derivative of picolinic acid. Benzenesulfonic acid is not seen in nearly as much abundance again from lack of derivatization though small amounts of this molecule and

the carboxylic acid previously mentioned are methylized by CH_3 radicals, as also seen in the water-contacted irradiated solutions, albeit in very small quantities.

After Et(o)TDPA elutes at 144 minutes a new peak related to EtTDPA elutes at 145.4 minutes. The fragmentation pattern of this isomer is different than those of either the ortho, meta, or para EtTDPA isomers. Though it appears as one peak in the chromatogram using selective ion monitoring of 401 m/z shows that it is in fact a series of different peaks which overlap when viewing the total ion current. This indicates that a methyl group which was previously lost by energy deposition underwent recombination with its parent molecule forming an isomer that exists as a combination of both ortho and either meta or para methyl positions.

Two new peaks appear at 95.8 and 152.4 minutes which are the result of aromatics undergoing radical nitration. The molecule at 95.8 minutes is nitrated N-ethyl-toluidene while nitrated EtTDPA appears at 152.4. In both cases substitution only is seen at the 2-position relative to the carbon-nitrogen bond on the tolyl ring and no other isomers are detected. If this reaction proceeded by electrophilic substitution there would be direction of the nitronium ion to the ortho and para positions relative to the nitrogen and methyl substituents due to their electron donating character. This would correspond to a mix of the hydrogens at both the 2 and 3-positions being substituted by nitro groups. Instead, the result of substitution only at the 2-position is consistent with the predominantly meta-substitution of aromatics by NO_2 radicals.[170] No observance at the 3-position is likely due to sterics. However, this result is most likely a consequence of the design of the batch irradiation experiments which used pre-equilibrated organic phases. In a true

reprocessing scheme the organic phase would be in continuous contact with the aqueous phase while being thoroughly mixed during irradiation, most likely leading to nitration by predominantly electrophilic substitution.
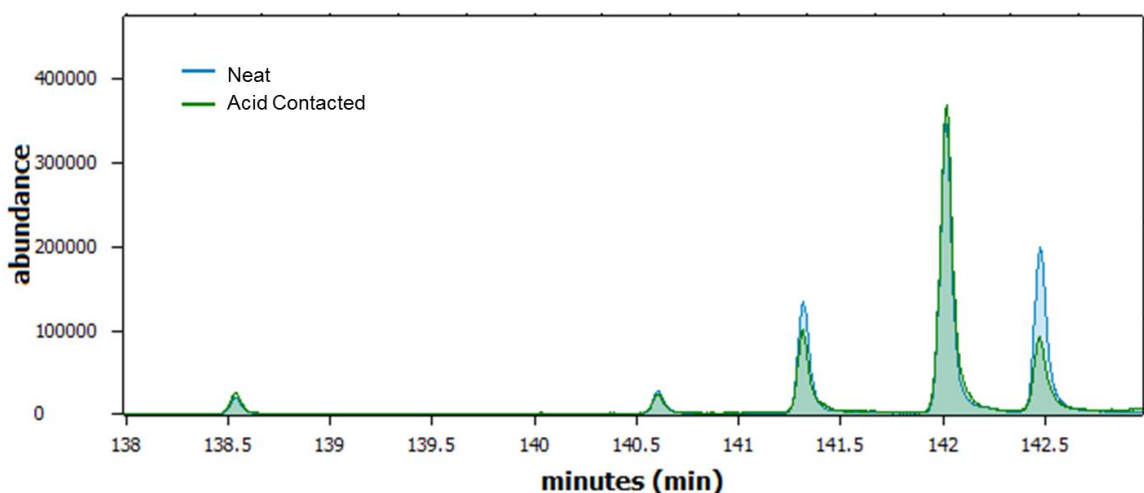
Figure 5.9: Effect of organic phase nitric acid content on CF_3 radical substitution
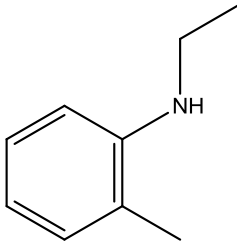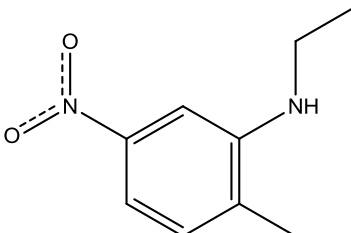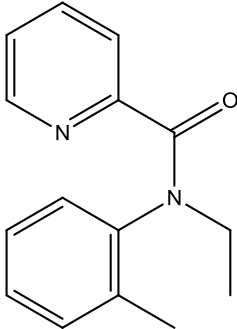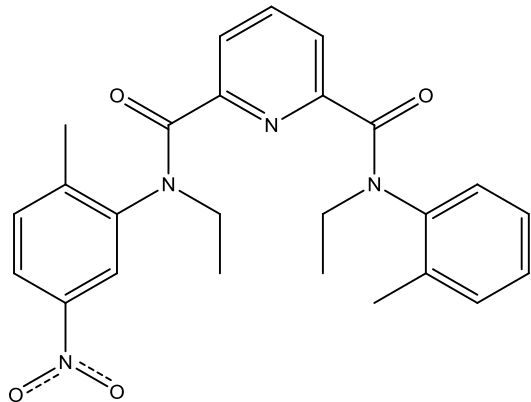
Nitric acid saturated solutions of EtTDPA also undergo substitution by trifluoromethyl radicals as discussed regarding water saturated solutions in Section 5.4.3. The same six isomers produced during irradiation of the organic phase of water saturated solutions are seen when the solutions are saturated with 3 M nitric acid and elute at identical times as seen in Figure 5.9. The sixth peak elutes at 143.5 minutes but is masked by the much larger Et(o)TDPA signal and can only be resolved when using selective ion monitoring. Four of these peaks have virtually identical relative intensities when saturated with water or nitric acid, while the two peaks at 141.4 and 142.5 minutes show a noticeable reduction in their yields from being irradiated in the presence of nitric acid. Since only two positions are affected by this change it can be reasoned that these

two peaks belong to the β and γ positions of the central pyridine ring of EtTDPA.

A possible cause of this decreased yield is that not only are ·CF_3 radicals produced during irradiation of the FS-13 solvent but also nucleophilic CF_3^- ions. The very basic CF_3^- ion would react very quickly with any acidic proton in the organic phase to form fluoroform. In acid saturated solutions this is a much more probable reaction than when the solution is saturated with water. The pyridine ring is far more susceptible to nucleophilic attack due to its lower electron density within the ring relative to the tolyl moieties which contain groups donating electron density. This is consistent with the hypothesis of why the tolyl rings remain largely unaffected by this change in acidity while a decrease in yield is seen for the pyridine substituted positions.

In all experiments performed using GC-MS, the amount of degradation is very small compared to that of the unreacted ligand in solution. In all cases the total peak areas of the degradation products were much less than 1% of the total area of the unreacted ligand. Assuming that the relative detection efficiencies for each degradation product are similar to or greater than that of EtTDPA this means that these products are not in sufficient concentration to significantly alter the extraction chemistry under the studied conditions.

Table 5.4: Nitric acid saturated radiolysis products

Retention Time (min)	Base Peak	Molecular Ion	Structure
39.5	120.0	134.9	
95.8	165.0	180.0	
98.8	134.0	240.1	
138.5-143.5	134.0	469.2	Et(o)TDPA − H + CF$_3$ isomers
144.0	134.0	401.1	Et(o)TDPA
145.4	134.0	401.1	EtTDPA new isomer
152.4	134.0	446.1	

5.5. Thermal Stability
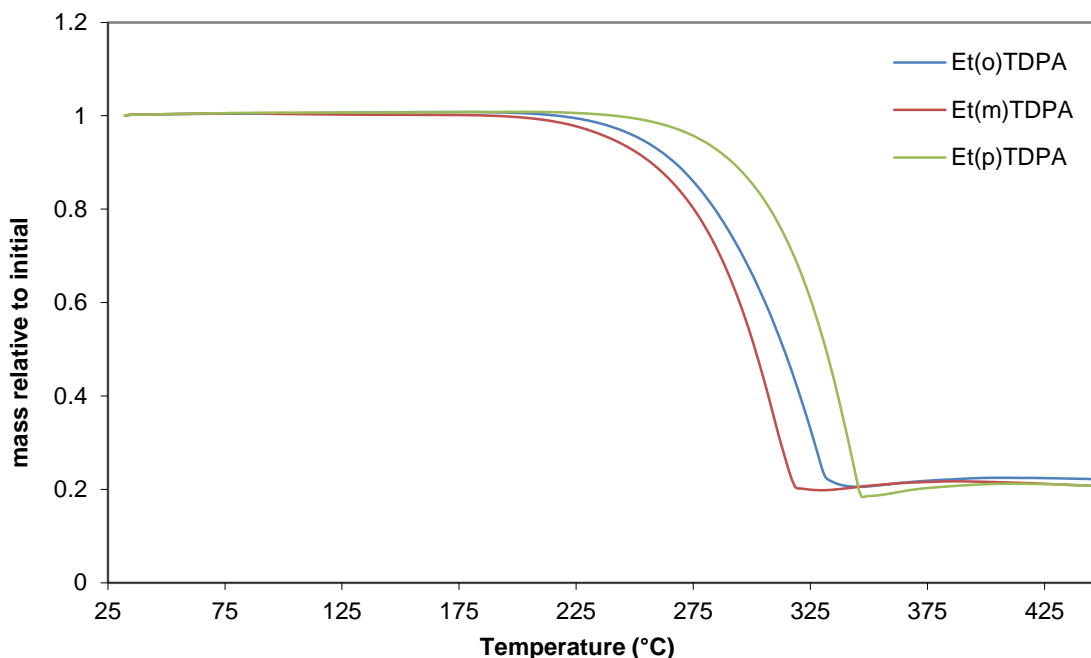
Figure 5.10:Thermogravimetric analysis of solid EtTDPA isomers

Crystallized samples of EtTDPA were evaluated for their thermal stability by thermogravimetric analysis. Et(m)TDPA showed weight loss beginning slightly after 180 °C, Et(o)TDPA at 200 °C, and finally Et(p)TDPA after 220 °C as shown in Figure 5.10. During heating no plateaus were seen corresponding to the formation of a stable intermediate during decomposition. Complete evaporation of all isomers occurred by 360 °C with the meta isomer completing first followed by ortho and then para. After ending the analysis at a temperature at 450 °C only a slight layer of black char residue remained in the pan. The lack of any plateauing in the thermograph until after evaporation of the ligand had begun indicates that EtTDPA is stable with respect to direct thermolysis under temperatures which would be present in a typical reprocessing system.

This result is consistent with results previously obtained for analyses of other amidic extractants.[186]

5.6. Effects on Extraction of Americium and Europium

5.6.1. Radioylsis

Previous experiments have shown that a significant extraction (D > 1) of Am and Eu with EtTDPA begins at 3 M nitric acid; therefore, all extraction experiments were performed from this nitric acid concentration for each isomer of EtTDPA.[107] The dependence of the post-irradiation distribution ratios for Am with 0.2 M EtTDPA on absorbed dose up to 125 kGy is shown in Figure 5.11. There was little to no effect of increasing absorbed dose observed for extraction of Am with the irradiated phase of EtTDPA in FS-13. In previous extraction studies americium was shown to be most extracted by Et(m)TDPA followed closely by Et(o)TDPA in 3 M nitric acid with Et(p)TDPA last. This trend is continued for EtTDPA irradiated with doses from 0-125 kGy.[106] Though the average of the initial 0 kGy Et(m)TDPA data point is lower than that of Et(o)TDPA, each isomer remains relatively constant within the measurement errors.
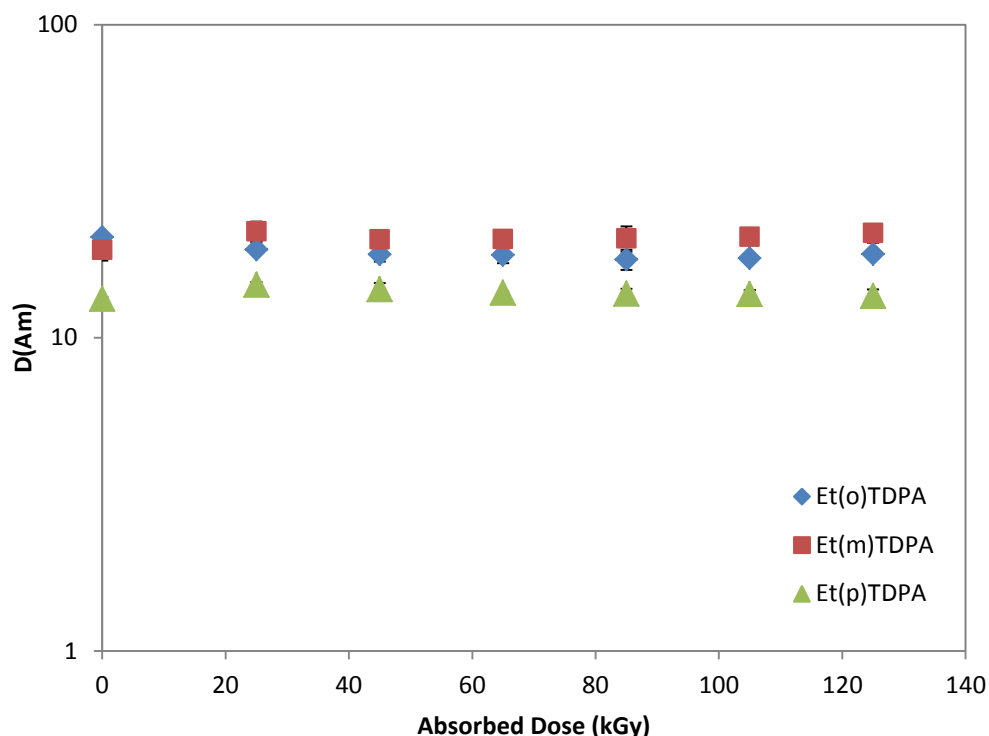
Figure 5.11: Extraction of americium from 3 M HNO_3 with 0.2 M EtTDPA

The extraction of europium (Figure 5.12) behaved in a similar manner to americium, though with significantly lower distribution values. Et(o)TDPA and Et(m)TDPA are reversed in extractability of europium compared to americium and Et(p)TDPA remains the lowest for extractability throughout each absorbed dose. Initially no substantial changes are seen in the distribution ratios as the absorbed dose is increased. Around 100 kGy an inversion in the average distribution ratio between Et(o)TDPA and Et(m)TDPA is seen, though this may be an artifact from the larger error in those data sets.
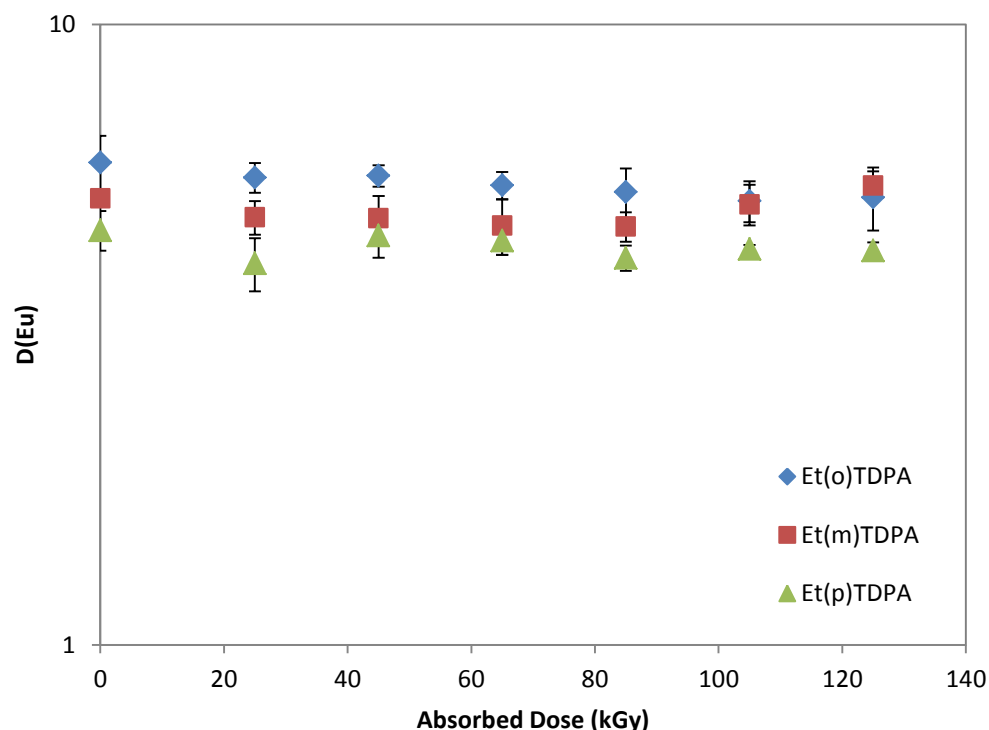
Figure 5.12: Distribution ratios of europium after extraction from 3 M HNO_3 with 0.2 M EtTDPA

The lack of changes in the distribution ratio from forward extraction of EtTDPA is consistent with the infrared spectra, which show little disruption of the carbonyl region through where, along with the pyridine nitrogen, neutral complexation occurs. Though GC analysis does confirm that there are other products such as carboxylic acids present in the irradiated solution, these species would be protonated in acidic solution and would not compete with EtTDPA for extraction more through more powerful ionic interactions. Small variances in distribution ratios were also previously seen with similar amidic extractants with trivalent metals.[187] Fe(III) with irradiated tetra-octyl-DPA as reported by Mowafy shows a slight fluctuation in distribution ratios with increased absorbed dose (above 40 kGy), and is similar to the extraction of Am and Eu with irradiated EtTDPA as

presented here.[179]
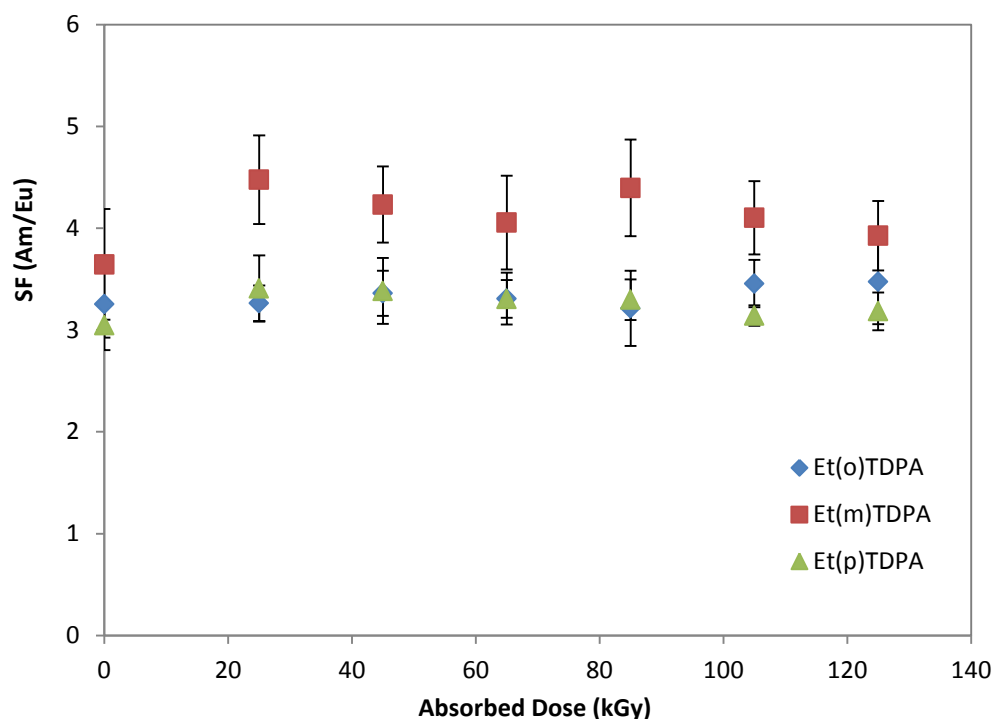
Figure 5.13: Separation factors of Am/Eu after radiolysis

The effect of radiolysis on Am/Eu separation factors are shown in Figure 5.13. At 0 kGy a reasonable separation factor of greater than three is obtained for all extraction mixtures and is maintained relatively constant throughout the studied dose ranges. Et(m)TDPA does show a small increase in separation factor once an initial dose is received. A possible explanation of this effect is that as seen in GC-MS analysis, nitro groups undergo electrophilic substitution with the outer aromatic rings in EtTDPA at one of the meta positions relative to the C-N bond. In the case of Et(m)TDPA both the C-N and methyl group have the same meta position in common relative to each other, thereby enhancing the amount of nitration occurring at this position. Since the nitro group is electron withdrawing it is possible for it to lower the basicity of the carbonyl groups,

lowering the harder oxygen donor's affinity for metal ions in solution. This causes an enhancement in the selectivity from the less effected nitrogen soft donor. The enhancement begins to fade as the irradiation continues and other interfering species are produced. However, none of the separation factors deviated by more than 10% of the average for each isomer, with Et(m)TDPA giving the best separation factors at all observed doses. This result was identical to the separation factor order for americium and europium obtained for these three isomers from nitric acid in previous work without radiolysis.[106] Therefore, regardless of the methyl position the extractions remain relatively unaffected under the studied dose ranges.

5.6.2. *Hydrolysis*
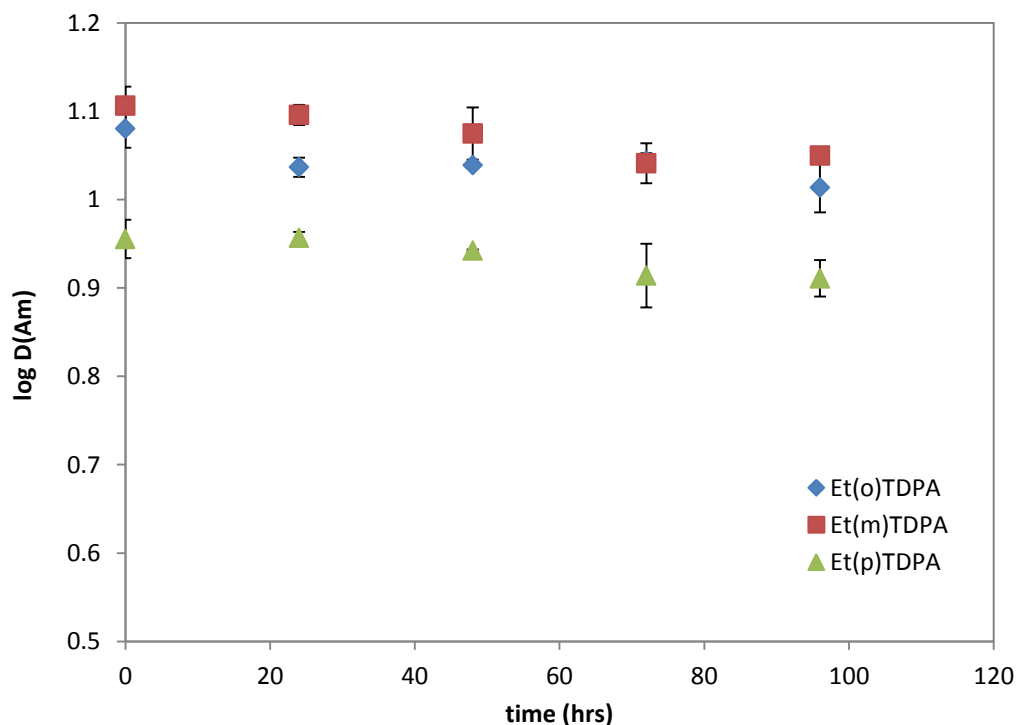
Figure 5.14: Distribution of Am with EtTDPA from 3 M HNO_3 after hydrolysis at 50 °C

While radiolysis of EtTDPA in FS-13 produces both new species of neutral and acidic extractants, hydrolysis results in the production of only products which will interfere with stripping of metals from the organic phase. Both the amine and carboxylic acid would be protonated during the more acidic forward extraction phase and generally not interfere with complexation. The protonated amine (pKas of N-ethyl-toluidene isomers are generally ~ 4.5) should be partitioned to the aqueous phase as an ammonium salt whereas the carboxylic acid can still form metal complexes through the uncleaved amide group.
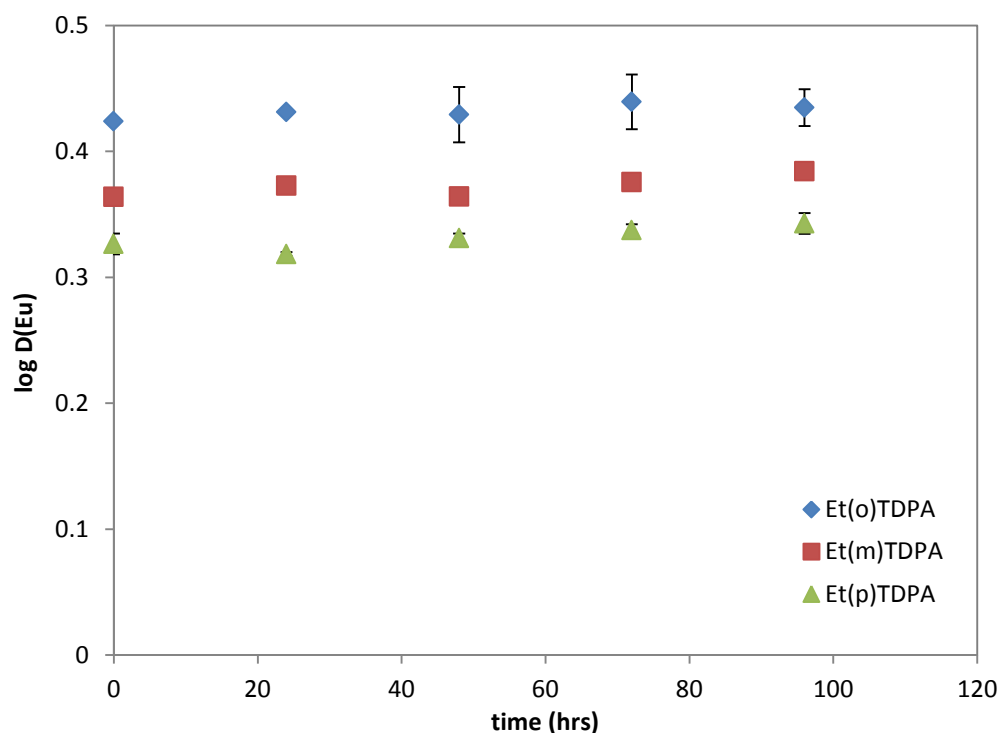
Figure 5.15: Distribution of Eu from 3 M HNO_3 after hydrolysis at 50 °C

The effect of hydrolysis at 50 °C on the distribution of americium and europium from 3 M nitric acid is shown in Figure 5.14 and Figure 5.15 respectively. A small but

noticeable decline in the distribution of americium can be seen as the hydrolysis continues up to 96 hours of total contact time with 3 M nitric acid. Distribution of europium does not appear to exhibit this decline and remains fairly constant within the error of the experiment, with a possible slight increase. In comparison the extractant dimethyl dioctyl hexylethoxymalonamide (DMDOHEMA), used in the French DIAMEX trivalent metal reprocessing scheme, saw a factor of 5 decrease in the distribution of both americium and europium after approximately 100 hours of hydrolysis time with 3 M HNO_3 at 60 °C.[188]

Conversion of the amide group to a carboxylic acid causes withdrawal of electron density from the soft donor pyridine nitrogen thereby lowering its affinity for the softer americium ion. Europium complexation remains largely unaffected by this effect and more electron density at the carbonyl oxygens is consistent with the possible slight increase in distribution ratios. The ultimate result is a decrease in the separation factor between americium and europium for their extraction into the organic phase as illustrated in Figure 5.16.
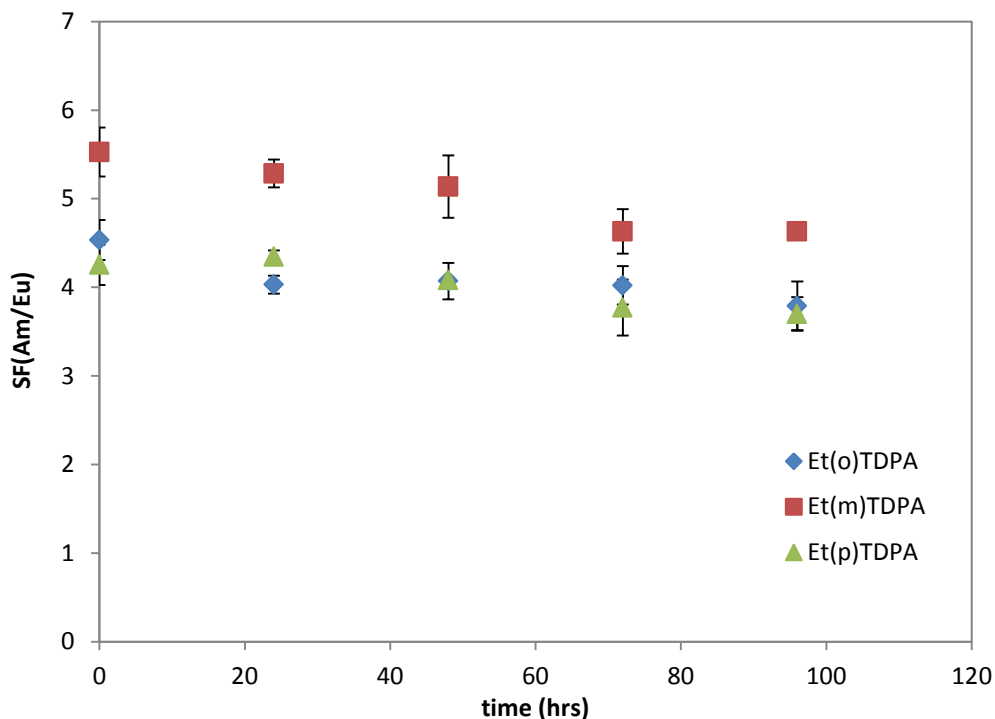
Figure 5.16: Separation factors of Am and Eu after hydrolysis at 50 °C

Back extraction of neutral extractants requires decreasing the metal counter anion concentration. Generally, this counter ion is nitrate from nitric acid, and thus it is necessary to lower the acidity levels into the higher pH range (pH > 2). In a fresh neutral ligand solvent extraction system this generally presents no problem other than possible kinetic issues. However it is in the pH region where organic acids tend to more easily deprotonate and become available to form complexes with metal ions, partitioning them to the organic phase. This is the basis for trivalent metal separation processes such as TALSPEAK which uses a combination of organophosphoric and carboxylic acids.[64] This is problematic in a neutral extractant system as the acidic degradation products of both hydrolysis and radiolysis can start to act as complexants in this pH region, limiting the ability to back extract these metals into the aqueous phase.
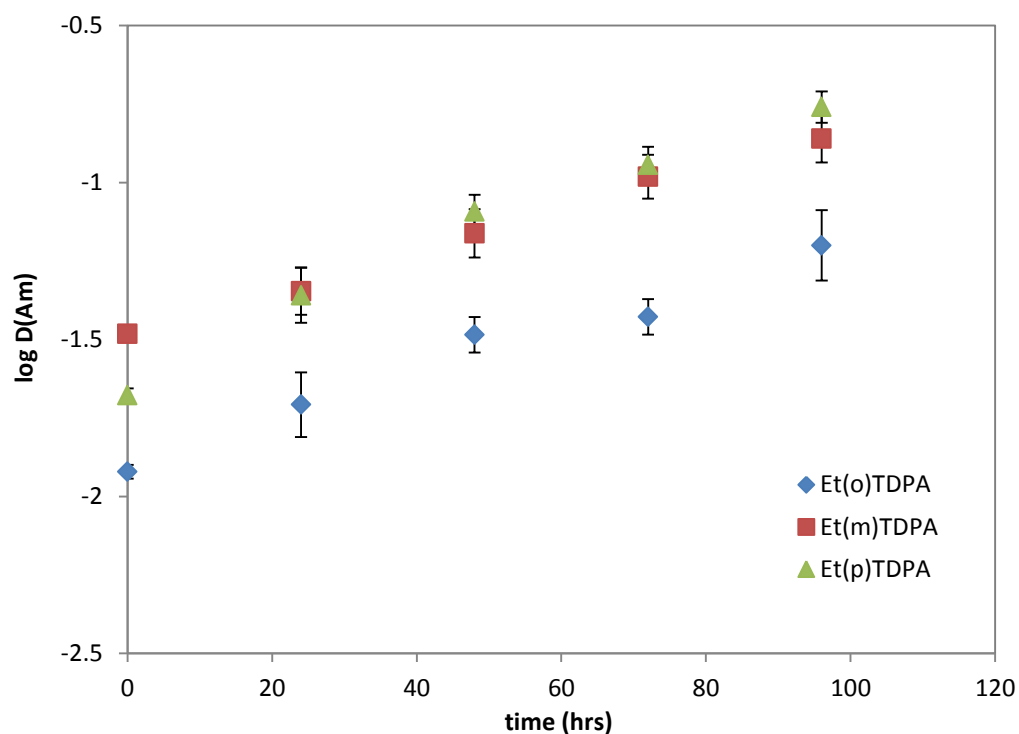
Figure 5.17: Stripping of Am with 0.01 M HNO$_3$ after hydrolysis

Although benzenesulfonic acid is also produced during these experiments, it generally considered a strong acid in aqueous solution (literature is inconsistent on the exact value but tabulated values tend to agree on a pK$_a$ < 1 and as low as pK$_a$ = -6)[189] and unlikely to form strong complexes in the organic phase compared to those formed by carboxylic acids. Thus any changes in the extraction behavior are attributed to products of only EtTDPA degradation.
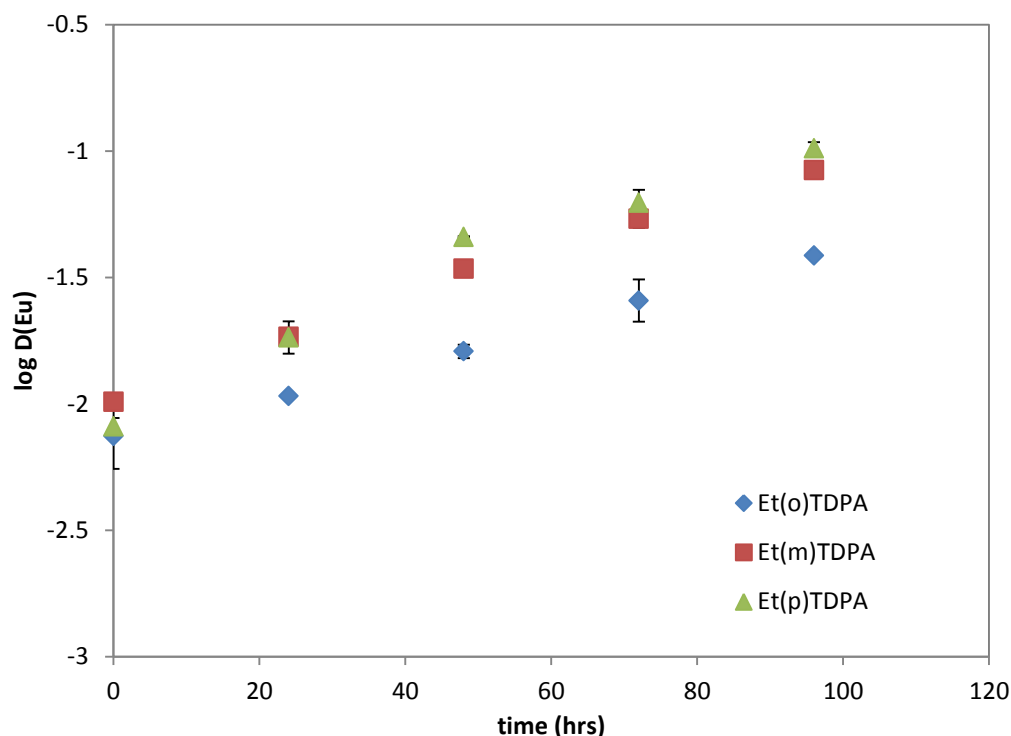
Figure 5.18: Stripping of Eu with 0.01 M HNO$_3$ after hydrolysis

The same solutions investigated for hydrolysis effects in the forward extraction of americium and europium from 3 M nitric acid were then analyzed for the ability to strip these metal ions from the loaded organic phase using 0.01 M nitric acid. These results are shown in Figure 5.17 and Figure 5.18. In the americium solutions Et(o)TDPA shows the least amount of difficulty in stripping from the organic phase which is consistent with previous literature showing it to be a weaker extractant at low ionic strengths relative to Et(m)TDPA and Et(p)TDPA.[106] A positive linear dependence is seen for the logarithm of the distribution coefficient versus the acid contact time, corresponding to a first order production of the interfering carboxylic acid. Et(p)TDPA appears to be the most susceptible to acidic hydrolysis as it has a larger rate of carboxylic acid production and distribution ratios of both americium and europium eventually overtake Et(m)TDPA.

131

The decontamination factor can be defined as the concentration of metal initially present in the organic phase divided by the amount remaining after back extraction. This can be expressed in terms of the distribution ratio after mathematical manipulation by the equations:

$$DF = \frac{[Org]_i}{[Org]} \tag{5.18}$$

$$[Org]_i = [Org] + [Aq] \tag{5.19}$$

$$DF = \frac{[Org] + [Aq]}{[Org]} \tag{5.20}$$

$$DF = 1 + \frac{1}{D} \tag{5.21}$$

The decontamination factors from the back extraction of americium and europium from hydrolyzed EtTDPA solutions with 0.01 M nitric acid are listed in Table 5.5. All solutions of EtTDPA isomers exhibit a significant decrease in the ability of americium and europium to be removed from the organic phase. This is expected from the increasing D values with hydrolysis time as per Equation (5.21).

More importantly from a reprocessing standpoint is the effect on separation of these two elements. Initially a moderate separation of americium and europium is obtained with Et(m)TDPA (SF > 3) which decays rapidly until there is no distinction in the separation between any isomers as seen in Figure 5.19. From this it can be seen that once a sufficient amount of hydrolysis has occurred, the position of the methyl group is largely

irrelevant on the separation behavior. The increasingly prevalent carboxyl group and its

hard donor character does lower the separation factor of these two elements, but a slight

preference for americium is maintained from the softer donor pyridine nitrogen.

Table 5.5: Decontamination factors after extraction with 3 M HNO_3 and stripping with 0.01 M HNO_3

Time	Am			Eu		
(hrs)	Et(o)TDPA	Et(m)TDPA	Et(p)TDPA	Et(o)TDPA	Et(m)TDPA	Et(p)TDPA
0	84	31	49	135	99	125
24	52	23	24	94	55	56
48	32	16	13	63	30	23
72	28	11	10	40	20	17
96	17	8	7	27	13	11
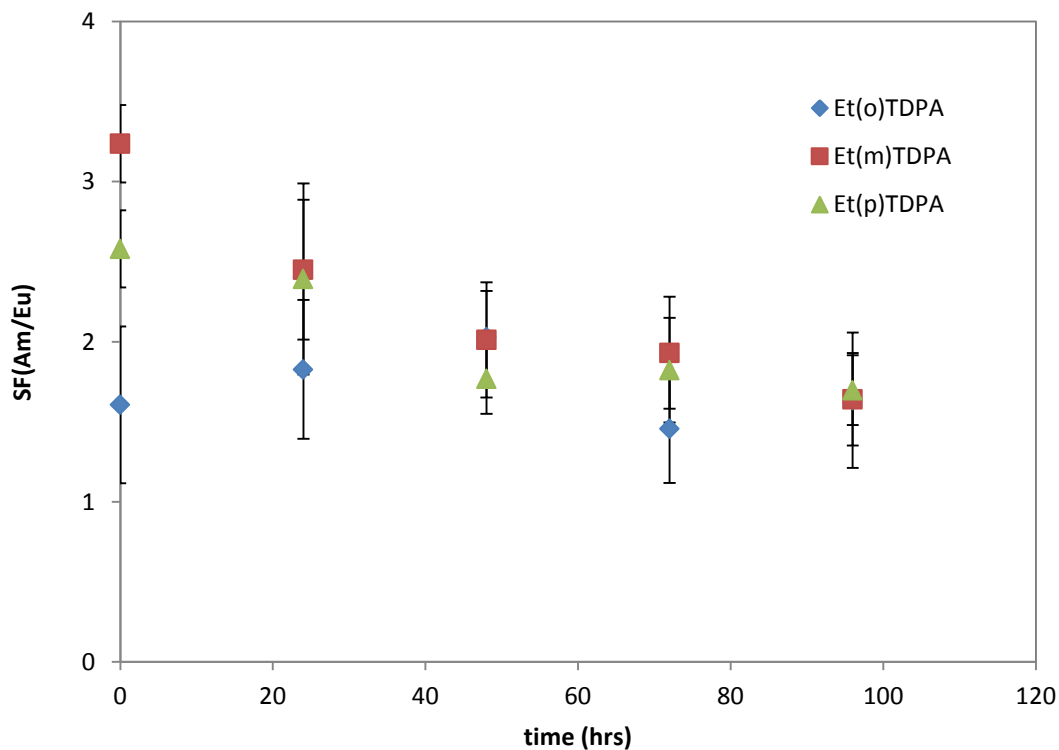
Figure 5.19: Separation of Am/Eu after stripping with 0.01 M HNO_3

Despite this decrease in separation it can be rectified by scrubbing the organic phase

prior to metal loading with a 0.5 M sodium carbonate solution. Sodium carbonate neutralizes the organic acids and converts them to their sodium salt. The sodium salts are much more soluble in water and are partitioned out of the organic phase which can then be discarded. After scrubbing the organic phase hydrolyzed at 96 hours with 0.5 M sodium carbonate the distribution ratios and separation factors then returned to their initial values within experimental error.

6. THERMODYNAMICS OF COMPLEXATION OF METALS BY EtTDPA

In order to better understand the mechanisms behind solvent extraction behavior, it is essential to study the thermodynamics of complexation. Knowledge of parameters such as the stability constant β between two species leads to the development of new ligands which minimize unwanted effects caused by competitive reactions, sterics or conformational barriers.[190] Determination of stability constants is most often performed by spectrophotometric or potentiometric methods when applicable.[119,191–194] Calorimetric titrations have also been shown to be a powerful tool for comparison of stability constants obtained by other titration methods.[195–197] Having knowledge of the signs of the thermodynamic parameters ΔG, ΔH, and ΔS indicates the nature of the complexation and is important when elucidating the chemical interaction between the species in solution.

One of the most basic thermodynamic equations is the relation between ΔG the Gibb's free energy, ΔH the enthalpy, and ΔS the entropy:

$$\Delta G = \Delta H - T\Delta S$$

(6.1)

ΔG of course is related to the equilibrium constant *K* by a factor of *–RT,* with a *K* greater than one resulting in a spontaneous process. More important for interpretation of the nature of complexation are the ΔH and ΔS terms.[127] Generally, a large negative ΔH is the result of inner sphere coordination. In aqueous systems the hydration energy from the 8-9 coordinated waters for lanthanides in the inner sphere is extremely large, requiring

significant energy to disengage them from the metal ion which is much larger than the formation energy of the new metal ligand complex.[19] This is not always true however, as metal salts in organic systems are often poorly solvated. For solutions with poor solvating power, a net release of heat is observed when complexing with a more powerful donor ligand resulting in a more thermodynamically stable complex.

The sign of ΔS is more independent of the solvent system. A positive ΔS means a more disordered system; a negative ΔS represents a system has become a more ordered one. Regardless of the solvent system, if a complex occurs in the inner sphere, the ligands that were previously coordinating will be removed. Complexation by multidentate ligands will result in the displacement of multiple solvating molecules. If one considers the original metal and its inner coordination sphere as a "single" particle, then removal of multiple solvating molecules leads to a net increase in the total number of particles in the system which is an increase in entropy.

Diamides of dipicolinic acid have been previously shown to coordinate metal ions as tridentate neutral ligands.[106] This ability is owed to the positioning of the two carbonyl group oxygens, common among many proposed neutral solvent extraction ligands, as well as the lone pair electrons from the central pyridine nitrogen. This configuration allows for EtTDPA to efficiently extract lanthanides and actinides from acidic aqueous solutions, with a preference for actinides due to their relatively softer character as electron acceptors with the softer nitrogen atom. Coordination of EtTDPA with the metal ion takes place as shown in Equation (6.2) by forming neutral adducts where n = 1-3 while the stability constant β_n is given in Equation (6.3):

$$Nd^{3+} + nEtTDPA \longrightarrow [Nd(EtTDPA)_n]^{3+} \qquad (6.2)$$

$$\beta_n = \frac{[Nd(EtTDPA)_n]}{[Nd][EtTDPA]^n} \qquad (6.3)$$

6.1. Spectrophotometric Titrations

Stability constant determinations of metal complexes with non-aqueous soluble organic ligands are typically performed by dissolution of a metal nitrate or chloride in either acetonitrile or methanol/water mixtures and analyzing spectral changes in the $\pi \rightarrow \pi^*$ and n $\rightarrow \pi^*$ transition regions of the UV spectrum from the small degree of back bonding by 4f orbital electrons, particularly in the complexes of the lanthanides which exhibit weak or no visible region absorptions.[43,44,105,139] It is possible to monitor shifts of the metal f-f transitions for select lanthanides such as neodymium which is typically done in a mixed methanol/water solution as well.[193] Neodymium has particularly sharp peaks especially the $^4I_{9/2} \rightarrow {}^4G_{7/2}, {}^4G_{5/2}$ transition at approximately 576 nm. This transition is an f-f transition and as such is forbidden by the Laporte rule.[198] The weak intensity of this transition means significantly higher concentrations of both the metal and ligand are required experimentally as compared to monitoring the ligand spectrum. In either system conditions are chosen in order to limit competitive inner sphere complexation reactions for the metal ion between the ligand of interest and anions (NO_3^-, Cl^-, etc.) in solution.

Despite the significant absorption of EtTDPA in the UV region from its extended π system conjugation ($\epsilon > 6{,}000$ L/mol·cm), initial instrument limitations prevented

spectroscopic investigations below 300 nm in the current work. In addition, the almost complete insolubility of EtTDPA in water prevented the use of water/alcohol mixtures (mixtures of 10^{-4} M EtTDPA in 75/25% methanol/water caused formation of a fine suspension). Therefore spectroscopic titrations were performed in acetonitrile using the perchlorate salt of neodymium in order to limit inner sphere anionic complexation of the metal cation. The complexation occurring between neodymium and the perchlorate anion was accounted for using known literature stability constants in acetonitrile.[199,200]
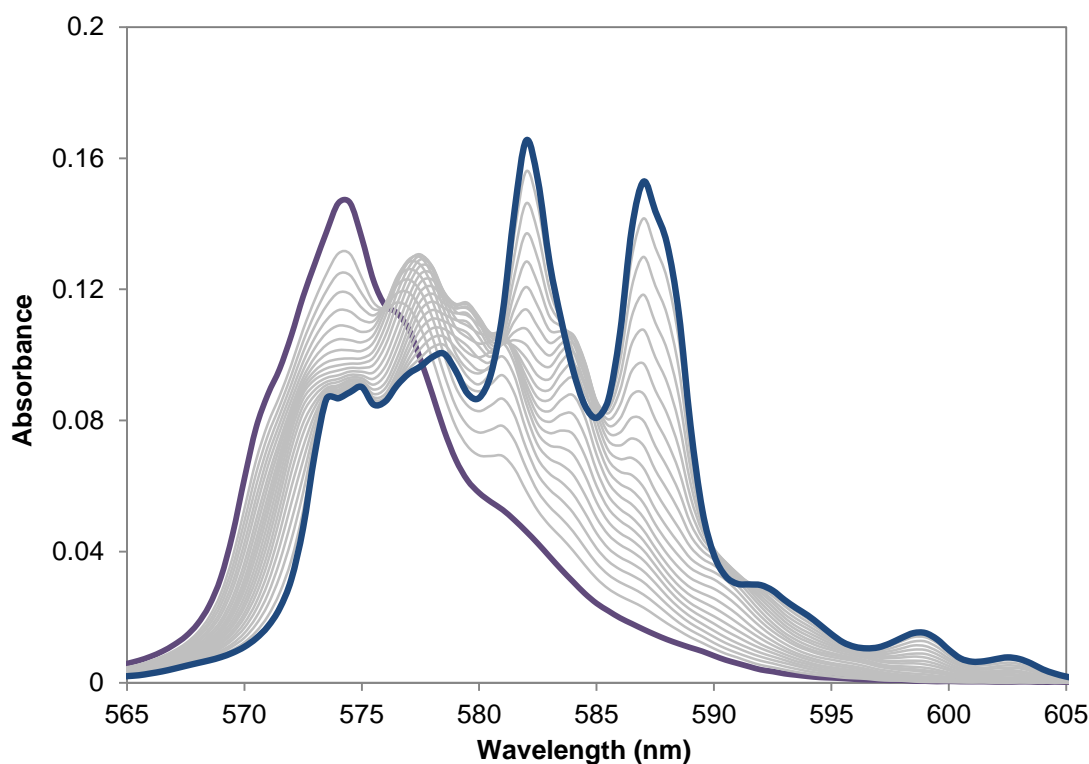
Figure 6.1: Spectrophotometric titration of Nd^{3+} with Et(o)TDPA in acetonitrile

The spectroscopic titration on Nd^{3+} with Et(o)TDPA is shown in Figure 6.1. The initial peak at 575 nm (shown in purple) corresponding to the $^{4}I_{9/2} \rightarrow {}^{4}G_{7/2}, {}^{4}G_{5/2}$

transition was consistent with previously published data of neodymium perchlorates in acetonitrile solution.[21]   All isomers of EtTDPA showed similar spectral changes upon being titrated into Nd^{3+}. Initially an isosbestic point from the red shifted complex can be seen before the growth of the second metal:ligand complex begins to significantly contribute to the spectrum.   Further changes in the spectrum ceased shortly after a 3:1 molar ratio of ligand to metal was reached indicating no further changes in speciation. The most notable differences seen between the spectra of the different ligands are both Et(m)TDPA and Et(p)TDPA (Figure 6.2 and Figure 6.3) show a higher absorbance for the final spectrum compared to that of Et(o)TDPA even when correcting for dilution of the sample during titration. As a result, the absorbance at 575 nm never decreases after formation of the final complex for Et(o)TDPA, while in both Et(m)TDPA and Et(p)TDPA the final complex has a larger extinction coefficient at this wavelength than the previous complex which can be seen from the rise in absorbance.
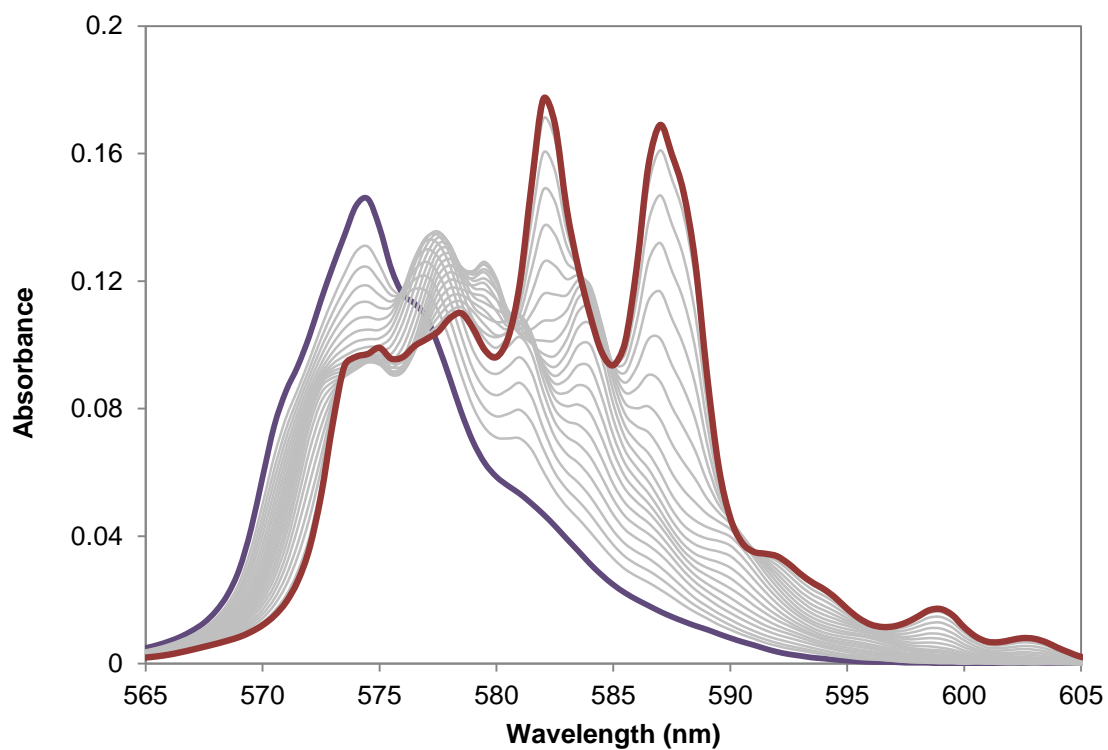
Figure 6.2: Titration of Nd^{3+} with Et(m)TDPA in acetonitrile
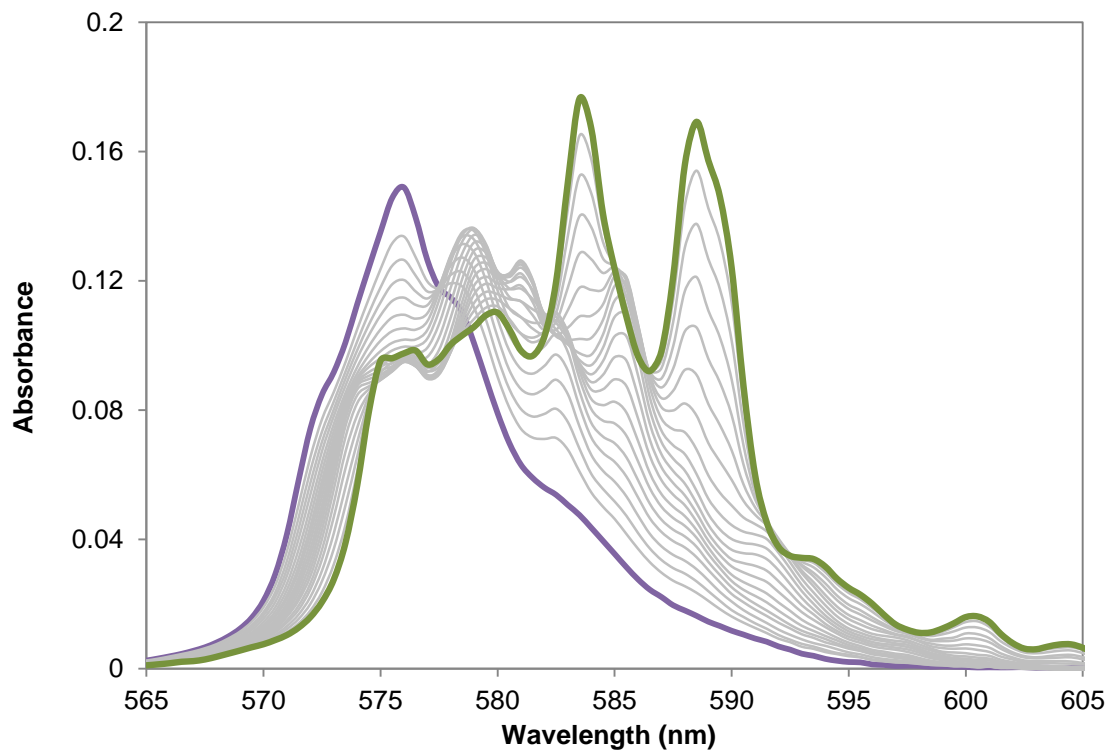
Figure 6.3: Titration of Nd^{3+} with Et(p)TDPA in acetonitrile

Table 6.1: Stability constants of Nd^{3+} EtTDPA complexes determined by UV-Vis spectroscopy ($I = 0.08$ M)

Stability Constant	Et(o)TDPA	Et(m)TDPA	**Et(p)TDPA**
log β_1	8.13 ± 0.22	9.44 ± 0.06	9.19 ± 0.10
log β_2	14.72 ± 0.43	16.81 ± 0.11	16.45 ± 0.19
log β_3	20.58 ± 0.64	22.36 ± 0.16	21.96 ± 0.28

In aqueous and acetonitrile solution Nd^{3+} has a coordination number of approximately nine, and thus it follows that a large tridentate ligand such as EtTDPA would not be capable of complexation beyond the M(EtTDPA)$_3$ species while still complexing in a tridentate fashion.[21,201] The obtained final spectra are also similar to those reported for the 3:1 dipicolinate:neodymium complex in water.[202] Refinement of three metal:ligand species by the HypSpec non-linear least squares data fitting program showed convergence when fitting the data to a model containing three species and the resulting stability constants are shown in Table 6.1. Et(o)TDPA shows the weakest complexation compared to the other two isomers which have much more similar stability constants. Though ortho does show the highest extraction affinity for trivalent lanthanides and actinides from high nitrate conditions (>2 M), at lower ionic strengths, such as in the current work, Et(o)TDPA is a weaker extract compared to either the meta or para isomer.[5] Plotting the expected speciation of neodymium as a function of the ligand to metal ratio shows maximum percentages of each species at the integer values corresponding to the number of complexed ligands as shown in for Et(p)TDPA in Figure

6.4. Complexation ends shortly after 3:1 ligand to metal ratio as was observed during actual titrations.
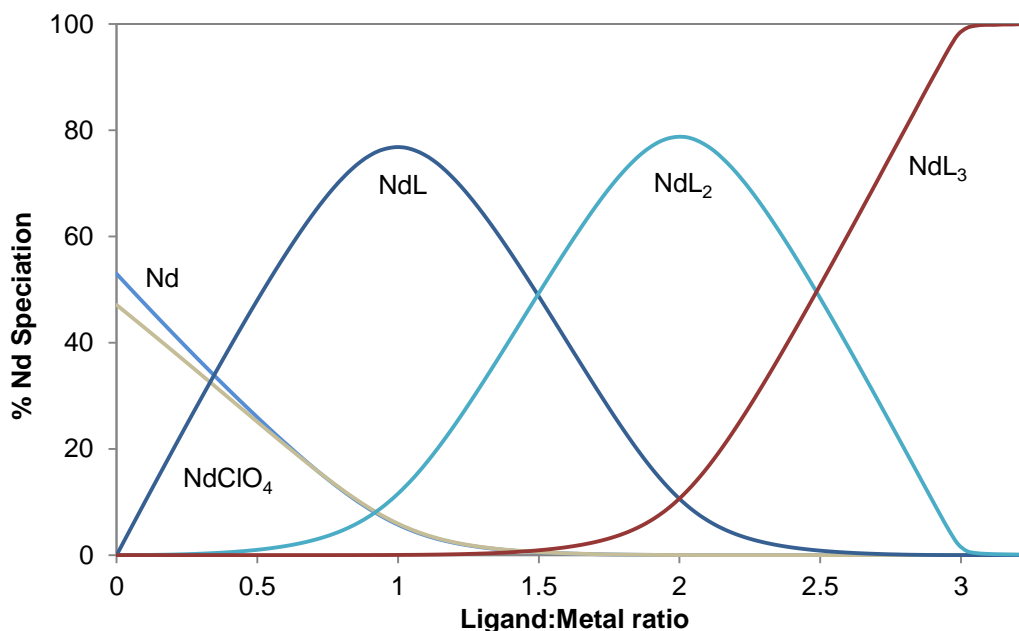
Figure 6.4: Neodymium speciation [%] with Et(p)TDPA in acetonitrile, [Nd] = 0.014 mol/L

The obtained stability constants are comparable but larger than those obtained previously for the ethyl-phenyl derivative of dipicolinic acid (N,N'-tetraethyldipicolinamidediamidic TEtDPA) in acetonitrile solution with values of 7.5, 13.8, and 21.5 for log β_1, β_2, and β_3 respectively.[10] This greater affinity for trivalent metals of EtTDPA compared to TEtDPA had been previously observed by solvent extraction of both americium and europium from nitric acid solutions.[107]
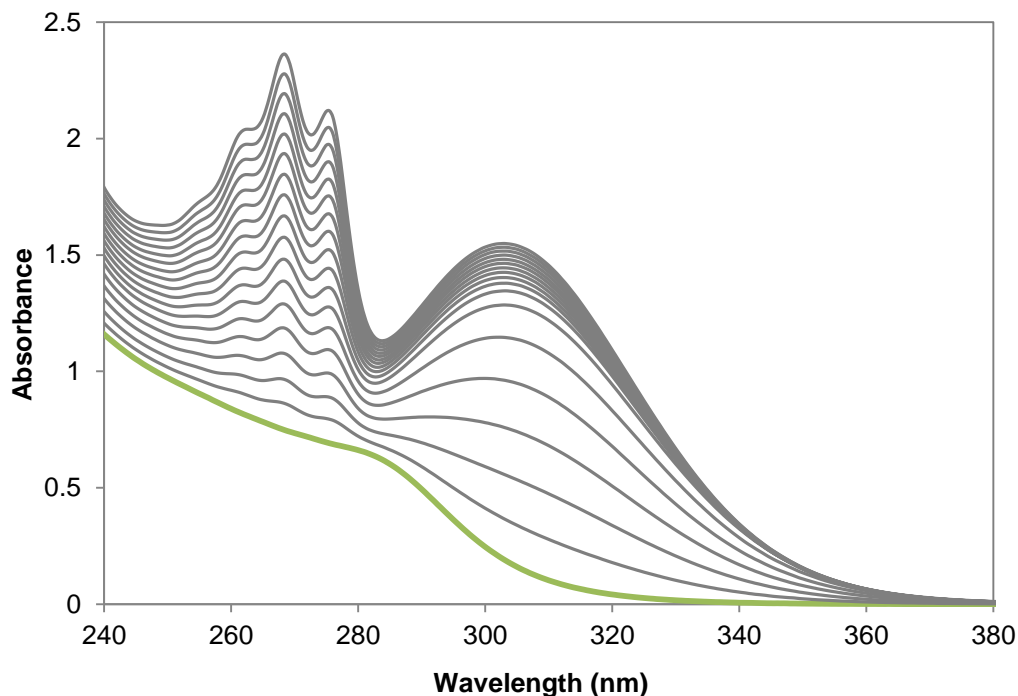
Figure 6.5: Titration of 10^{-4} M Et(p)TDPA with 10^{-5} M Nd^{3+} in acetonitrile

As stated previously instrument limitations prevent observing ligand spectral changes below 300 nm. Access to a new instrument with capability to scan well below 300 nm was eventually made available, allowing for validation of the stability constants obtained in the visible region. The titration of Et(p)TDPA (green) in acetonitrile with Nd^{3+} is shown in Figure 6.5. Addition of neodymium produces spectra consistent of back bonding into the carbonyl π^* orbitals with a peak at 305 nm, while the region from 260-280 nm is similar to spectra obtained for complexed pyridines as well as dipicolinic acid with the uranyl ion.[193,194] The lack of peak at 305 nm in the dipicolinate:uranyl literature indicating no covalent bonding is consistent with the more ionic character of the carboxylate oxygens compared to the amide oxygen of EtTDPA. Modeling the expected absorbance at 304 nm (Figure 6.6) using stability constant data obtained from the visible

region titations produced nearly an exact fit with experimental data, indicating that the calculated stability constants are accurate for this system.
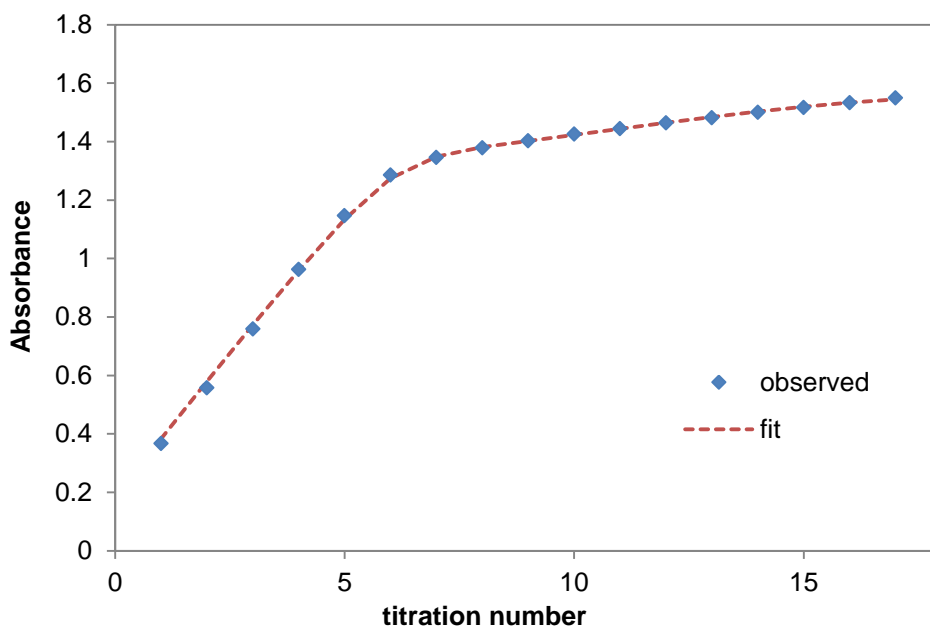
Figure 6.6: Fit at 304 nm by modeling data with obtained stability constants

6.2. Calorimetric Titrations

Titrations with the same solutions used in spectrophotometric experiments produced inconsistent data, most likely due to trace impurities of water and acid from the synthesis of $Nd(ClO_4)_3$ which did not have an effect on spectroscopic results, but contributed measureable heat during calorimetry. In order to negate this effect the neodymium triflate salt, which is less hygroscopic than the chloride or nitrate salts, was used. Contrary to aqueous media and initial reports on the behavior in acetonitrile, the lanthanide triflate does not dissociate to any appreciable degree in this solvent

144

system.[199,203,204] Though the triflate anion is significantly more complexing in acetonitrile than the perchlorate anion, this was compensated for when modelling the enthalpy output by using known stability constants of triflate complexes in acetonitrile.[199] Ionic strength was not controlled due to complications arising from the salt dissolution enthalpy, though the overall small change in metal concentration during titration did not have a great effect on the ionic strength of the system and thus was neglected during experiments.
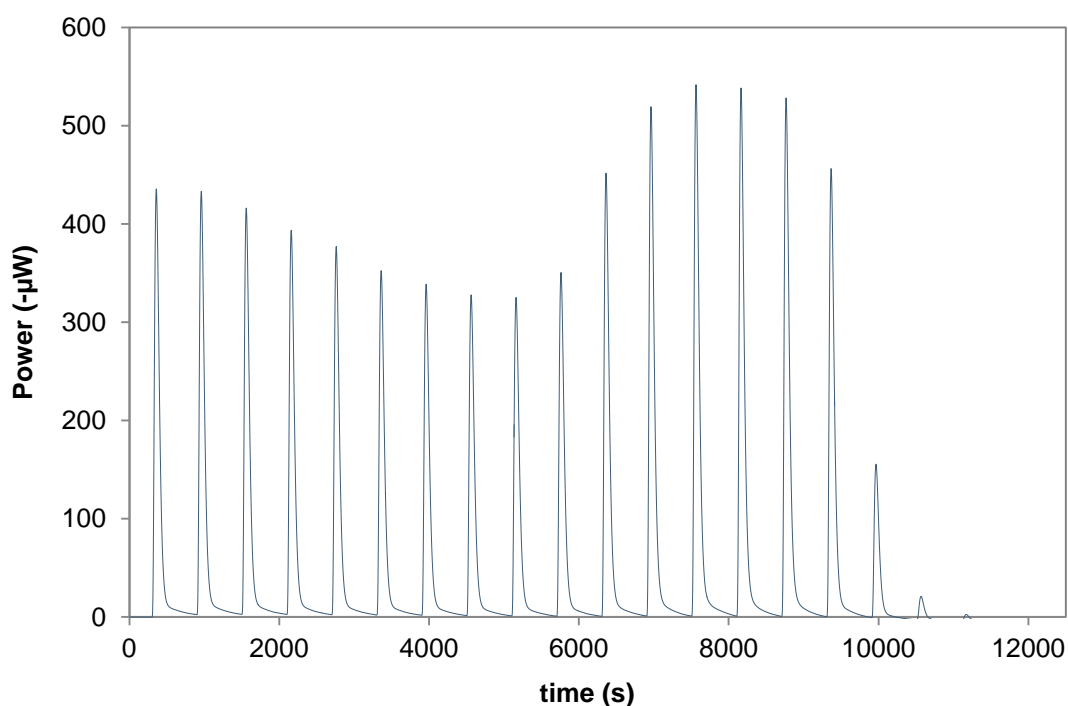
Figure 6.7: Power trace of Nd^{3+} titration with Et(o)TDPA in ACN

The heat evolution over time from the titration of Nd(III) with 8 μL of 0.247 M Et(o)TDPA is shown in Figure 6.7. Complexation of Nd(III) with EtTDPA ligands is an exothermic reaction, owing to the weak complexing ability of the acetonitrile solvent.

Unlike Et(m)TDPA and Et(p)TDPA, Et(o)TDPA initially has a smaller heat evolution with respect to the formation of the initial metal:ligand complexes. However, formation of the third metal ligand complex results in a visibly significant increase in the amount of heat measured. For all three ligands heat evolution drops to negligible amounts shortly after a ligand:metal ratio of three is reached, indicating no further complexation beyond the $M(EtTDPA)_3$ complex, as was also observed in spectroscopic measurements.
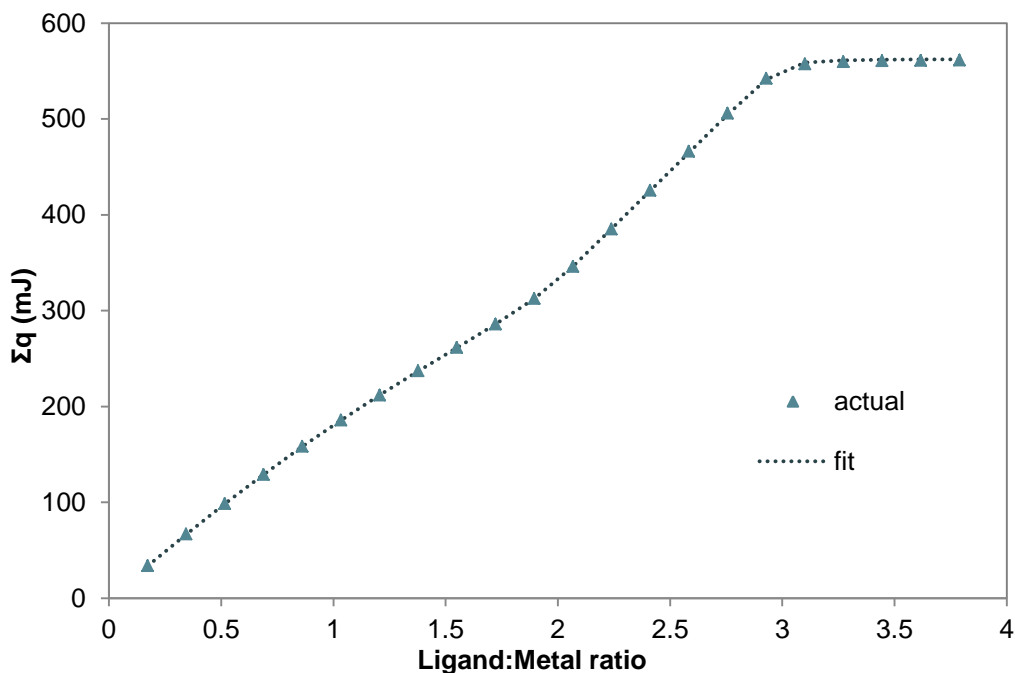
Figure 6.8: Cumulative heat experimental and model fit of Nd^{3+} titration with Et(o)TDPA

Modeling the system's enthalpy with HypDH produced a good fit to the actual data as shown in Figure 6.8. Often when model fits to heat data are reported the cumulative heat release rather than the stepwise heat release fit is presented. Through small corrections at each step the cumulative fit can agree well with experimental data, but the individual stepwise calculation does not. In this study the experimental data is also fit very well

when looking at stepwise heat release despite large swings in the data as shown in Figure 6.9. The stability constants obtained by calorimetric titration data are shown in Table 6.2. Within experimental error these values are mostly in agreement with those obtained from spectroscopic data, with the exception of the third complex of Et(m)TDPA and Et(p)TDPA. Though there are larger errors in the obtained values calorimetry is known to give less precision in stability constant determination, hence its use in combination with other investigative methods such as spectroscopy or potentiometry.[122,123]

Table 6.2: Stability constants of Nd^{3+} EtTDPA complexes determined by calorimetry

Stability Constant	Et(o)TDPA	Et(m)TDPA	**Et(p)TDPA**
log β_1	8.4 ± 0.3	9.7 ± 0.4	9.1 ± 0.1
log β_2	15.7 ± 0.4	16.9 ± 0.3	16.4 ± 0.3
log β_3	20.3 ± 0.2	20.7 ± 1.2	20.3 ± 1.1
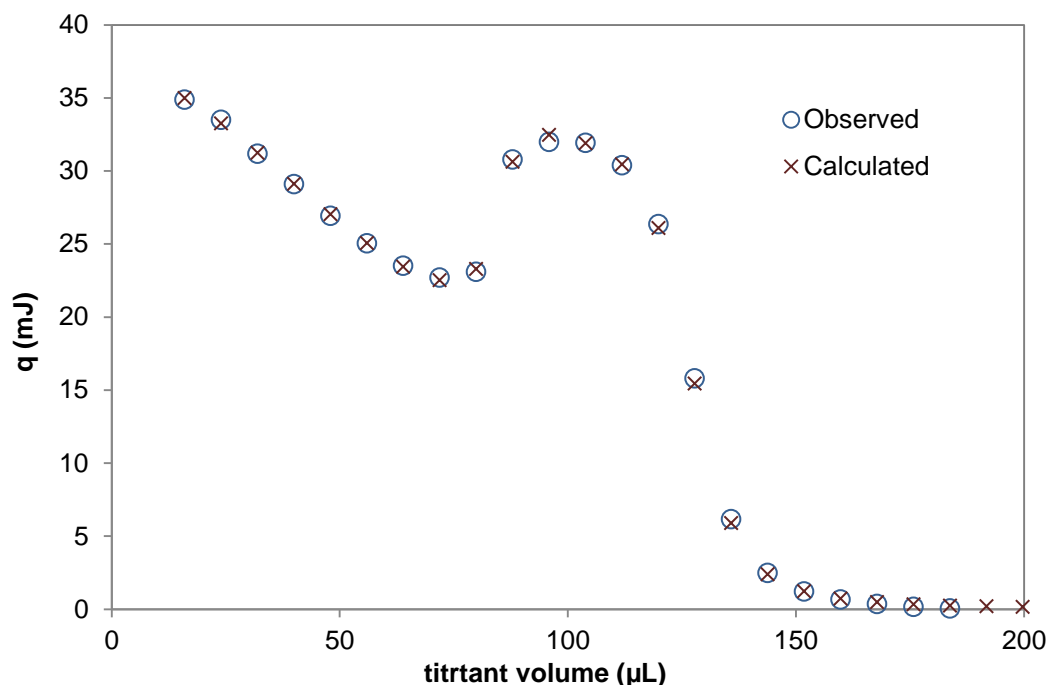
Figure 6.9: Stepwise heat of formation and model fit of Nd^{3+} titration with Et(p)TDPA

Using the calorimetric data it is also possible to obtain the other important thermodynamic parameters such as ΔG, ΔH, and ΔS. These values are presented in Table 6.3. It is immediately noticeable from the ln K values that after formation of the first metal:ligand complex there is essentially little to no effect of the tolyl-ring's methyl position in the further complexation ability for neodymium, as $K_1 = K_2 = K_3$ for ML_2 and are also quite similar for ML_3. The initially more negative enthalpies of Et(m)TDPA and Et(p)TDPA for the ML and ML_2 complexes stands out against the high negative enthalpy of -21.4 kJ/mol associated the ML_3 complex with Et(o)TDPA seen in Figure 6.8. The negative enthalpy is the result of the ion-dipole interaction between neodymium and acetonitrile.[205] Also of note is that the entropy term for the addition of a third ligand to the neodymium:EtTDPA complex results in very little entropy gain for any isomer and

148

the reaction is no longer entropy driven, possibly from the restriction of rotational movement in the confined space around the ion with three separate ligands attached.

Table 6.3: Thermodynamic parameters of Nd^{3+} complexation with EtTDPA at 298 K

Ligand	Species	ln K	ΔG (kJ/mol)	ΔH (kJ/mol)	ΔS (J/mol·K)
Et(o)TDPA	ML	3.7 ± 0.1	-47.9 ± 1.7	-13.2 ± 0.1	116.5 ± 1.1
	ML$_2$	3.2 ± 0.2	-41.6 ± 2.3	-17.1 ± 0.7	82.4 ± 1.4
	ML$_3$	2.0 ± 0.1	-26.2 ± 1.1	-21.4 ± 0.5	16.2 ± 0.7
Et(m)TDPA	ML	4.2 ± 0.2	-55.3 ± 2.3	-15.2 ± 0.1	134.7 ± 1.4
	ML$_2$	3.1 ± 0.1	-41.1 ± 1.7	-8.3 ± 0.7	110.0 ± 1.1
	ML$_3$	1.7 ± 0.5	-21.7 ± 6.8	-15.6 ± 0.5	20.4 ± 4.3
Et(p)TDPA	ML	4.0 ± 0.1	-51.9 ± 0.6	-20.1 ± 0.2	106.8 ± 0.4
	ML$_2$	3.2 ± 0.1	-41.6 ± 1.7	-10.4 ± 0.3	104.8 ± 1.1
	ML$_3$	1.7 ± 0.5	-22.2 ± 6.3	-15.7 ± 0.2	22.0 ± 4.0

6.3. Thermodynamics of Americium and Europium Extraction

Despite the importance of determining the previously mentioned thermodynamic parameters of neodymium complexation in acetonitrile, the speciation represented does not truly reflect that of known values from extraction of lanthanides and actinides by EtTDPA into FS-13. The ligand dependence on the extraction of trivalent actinides and lanthanides by EtTDPA in FS-13 from nitric acid has previously been shown to be 1.5,

149

rather than 3:1 as seen in the acetonitrile system with less complexing anions.[106,107] The

dependence of 1.5 was also seen for a CMPO-dipicolinamide hybrid during extractions of

americium(III).[206] A similar ligand in the same study was found to have a crystalline

structure of two praseodymium ions each complexed by a ligand molecule with a third

ligand bridging across the two ions, giving a $Pr_2L_3(NO_3)_6$ structure when ignoring inner

sphere coordinated waters. It is postulated that the EtTDPA:Am^{3+} complex coordinates

in this manner as well.
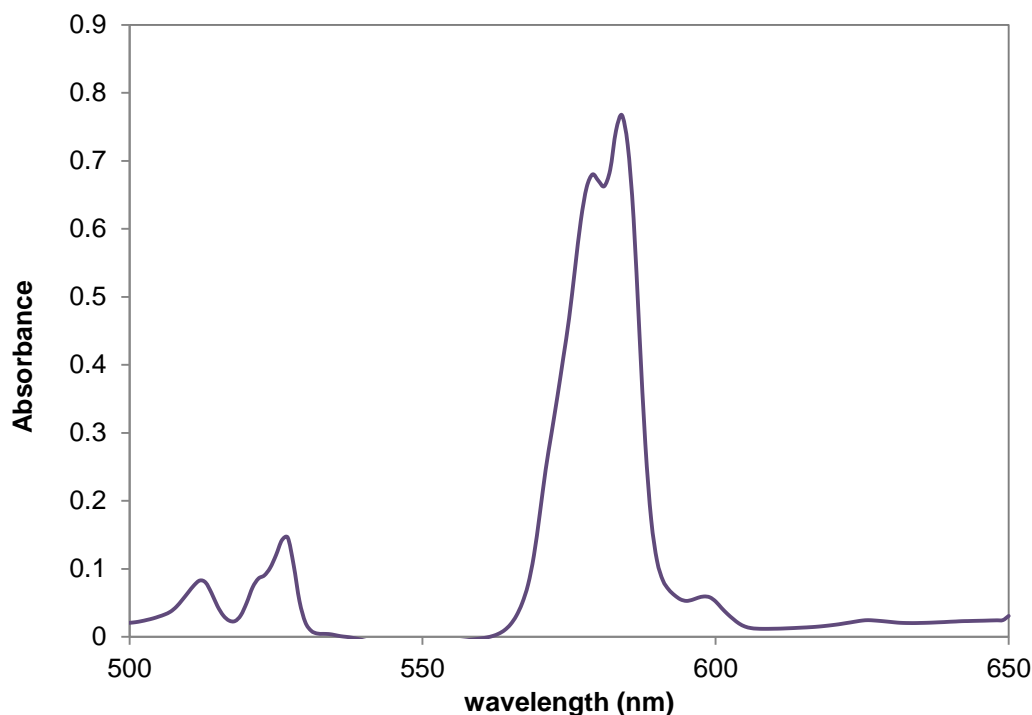
Figure 6.10: FS-13 phase after extraction of Nd^{3+} by Et(p)TDPA from 1.0 M HNO_3 and
5.0 M $LiNO_3$

From UV-Vis spectroscopy it can be inferred that the 3:1 ligand:metal complex does

not form when extracting from nitrate solutions. The extraction of neodymium into FS-

13 by Et(p)TDPA is shown in Figure 6.10. It is clear that the spectrum does not resemble

any of the species represented in the acetonitrile-perchlorate system. However, it does share similar qualities to when EtTDPA is titrated into solutions of the more complexing neodymium nitrate.[207] Conditional stability constants found there to be a maximum of two ligands complexed to a single neodymium ion in addition to complexed nitrate.

A more complete analysis of the thermodynamics of solvent extraction was done using the Van't Hoff method to determine the enthalpy and entropy of the extracted complexes of EtTDPA and europium or americium. By rearranging Equation (6.1) in terms of the equilibrium constant, one finds the equation of a line with respect to the inverse temperature:

$$\ln K = -\frac{\Delta H}{RT} + \frac{\Delta S}{R} \tag{6.4}$$

where the slope of the line is the negative of the enthalpy divided by the ideal gas constant R and the intercept is the entropy divided by R. These plots are shown in Figure 6.11 and Figure 6.12 for americium and europium respectively.

Table 6.4: Enthalpy and entropy data from extraction of Am and Eu by EtTDPA in FS-13

Ligand	Species	ΔH (kJ/mol)	ΔS (J/mol·K)
Et(o)TDPA	Am	-23 ± 1	-39 ± 3
	Eu	-17 ± 1	-33 ± 4
Et(m)TDPA	Am	-21 ± 2	-31 ± 7
	Eu	-15 ± 2	-26 ± 6
Et(p)TDPA	Am	-21 ± 6	-32 ± 18
	Eu	-14 ± 1	-25 ± 3
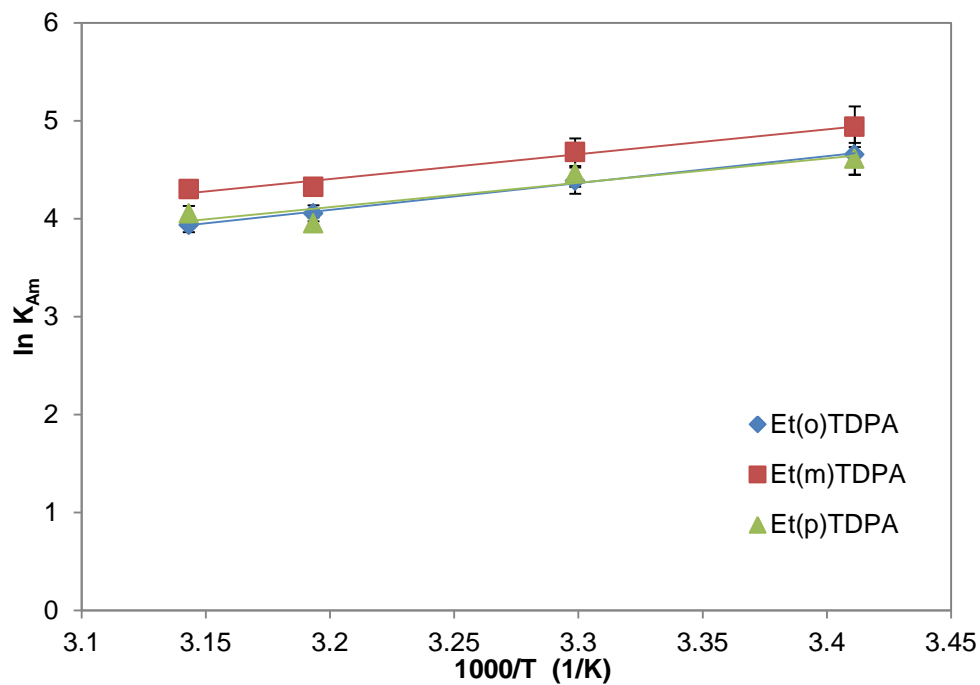
Figure 6.11: Van't Hoff plot of Am^{3+} extraction with 0.2 M EtTDPA from 0.5 M HNO_3 + 2.5 M $LiNO_3$
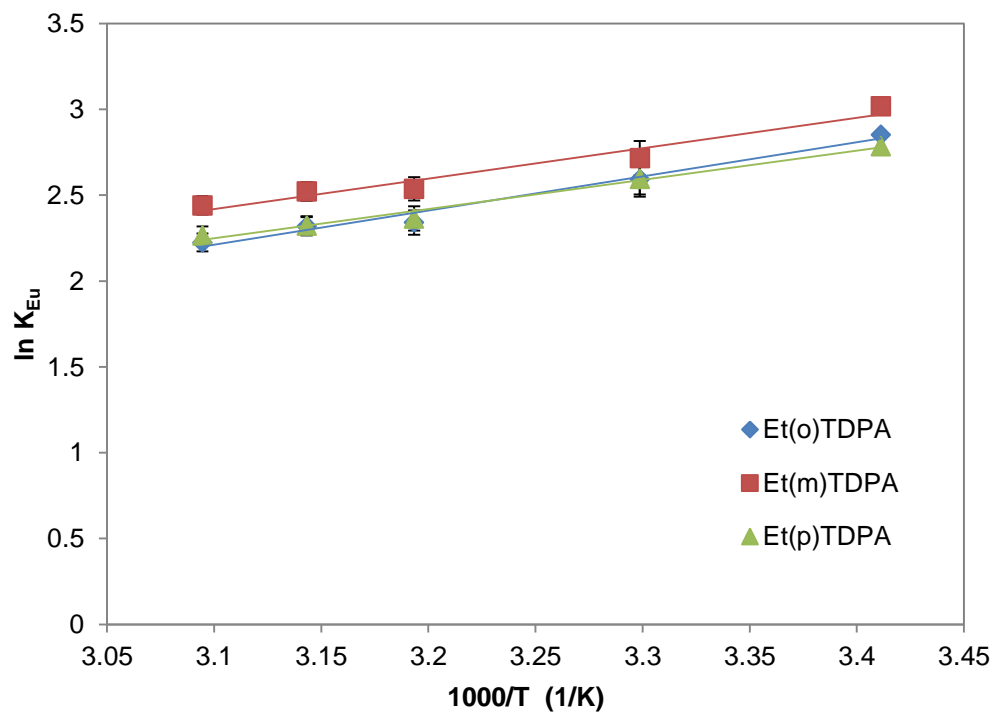
Figure 6.12: Van't Hoff plot of Eu^{3+} extraction with 0.2 M EtTDPA from 0.5 M HNO_3 + 2.5 M $LiNO_3$

Van't Hoff plots of americium and europium extraction were produced by using an aqueous phase of 0.5 M HNO_3 and 2.5 M $LiNO_3$ to facilitate extraction of the metal cations, but suppressing the amount of nitric acid extracted into the organic phase which could significantly alter the amount of free nitrate available for complexation. The equilibrium constants were calculated using Equation (4.21) and literature stability constants for nitrate complexation.[117] With increasing temperature the equilibrium constant decreases, meaning an exothermic reaction.

As seen in the acetonitrile-triflate system Et(m)TDPA and Et(p)TDPA have very similar thermodynamic behavior, while Et(o)TDPA has a more negative enthalpy and entropy during complexation with americium and europium. In all cases the enthalpies and entropies are more negative for americium than for europium. The negative entropies reflect the loss in rotational entropy of the free EtTDPA molecule from the extraction process as well as the forming the more ordered complex between the metal, nitrate, and EtTDPA in the organic phase. The errors in the entropy are quite large and are likely the result of the inherent assumption in the Van't Hoff method that the activities and stability constants remain constant over the temperature range of the entire experiment, which is a known disadvantage compared to direct heat analysis by calorimetry.[20,208]

7. CONCLUSIONS

In this work three novel ligands were synthesized for investigation into potential uses in nuclear fuel reprocessing. Isomers of N,N'-diethyl-N,N'-ditolyldipicolinamide were found to be effective extractants for all actinide ions from acidic solution with the exception of the neptunium(V). The order of extraction capability follows the effective ionic charge of the actinide elements: $An^{4+} > AnO_2^{2+} \sim An^{3+} > AnO_2^{+}$. EtTDPA was also found to not extract the molybdyl cation MoO_2^{2+} regardless of ligand concentration, while poorly extracting heptavalent technetium with a negative dependence on acid concentration. The non-extractability of molybdenum is not necessarily undesirable as aqueous phase complexants are often added to prevent extraction of elements such as molybdenum and zirconium during reprocessing due to the complex chemical behavior.

Good separation of the actinides is achieved from the trivalent lanthanides with some minor exceptions when performing extractions with 0.2 M EtTDPA and 3 M nitric acid. Pentavalent actinides are not well separated from the light lanthanides, while americium is not separated from the heavy lanthanides or uranium. The lack of separation from americium is less of concern as the heavy lanthanides are existent in negligible quantities in irradiated nuclear fuel as is uranium after separation by the PUREX process. In comparison to the previous UNEX ligand octyl-phenyl-CMPO, the distribution ratios of all elements are lower with isomers of EtTDPA. However, there is little separation between the trivalent f-elements when using CMPO as the extractant. EtTDPA provides an inherent separation factor between these elements from the N-donor pyridine group when extracting from nitric acid solutions and thus it is possible for the use of EtTDPA in

a UNEX-like group extraction recycling process, though a new stripping procedure would need to be investigated to selectively back extract elements from the organic phase.

Stability tests of the ligand showed it to be fairly resilient to damage caused by radiolysis and hydrolysis. The main products of these reactions were carboxylic acids, amines, and trifluoromethylated EtTDPA. These however did not cause any noticeable negative effects on extraction experiments with doses up to 125 kGy and hydrolysis times of 96 hours at 50 °C, while other ligands such as those used in the DIAMEX process show significant decrease in their extraction capability when subjected to similar criteria. Fuel raffinates that would undergo a group separation process by EtTDPA would typically have dose rates of 0.03-14 kGy/hr with nitric acid concentrations of up to 4 M. If short phase contact times are used, such as in centrifugal contactors, EtTDPA would be stable for several cycles with regards to the forward extraction of the trivalent metals. Back extraction with low acid was affected by the production of carboxylic acids, increasing the distribution of americium and europium when attempting to strip them from the organic phase by using dilute nitric acid. The difficulty in stripping was easily remedied by scrubbing the solution with a carbonate wash which then allowed the near complete stripping of metals into the aqueous phase and returned the distribution ratios to those seen with fresh EtTDPA.

The binding affinities of EtTDPA ligands with neodymium in acetonitrile solution were investigated as the FS-13 solvent was not suitable for this application. The use of UV-Vis spectrophotometry and calorimetry allowed for the determination of the

metal:ligand stability constants for trivalent neodymium and EtTDPA. Values obtained with both methods were in reasonable agreement with each other and with the results showing Et(o)TDPA as the weakest complexant for the trivalent metal under the conditions in the present study. The relative magnitudes of these complexes are consistent with known solvent extraction behavior, though the speciation in acetonitrile is not the same as that when extracted into FS-13. Formation of the third metal:ligand complex is inhibited by the low entropy associated with the formation of this complex.

Ideally these stability constants and other obtained thermodynamic parameters as well as the extraction and degradation data will aid in the future design and selection of ligands for reprocessing of used nuclear fuel. As of now, new research has been put forth using bipyridine based diamides for the purpose of selectively extracting trivalent actinides from trivalent lanthanides. Though results have been promising, their limited solubility in FS-13 and unknown degradation behavior may shift research efforts back towards dipicolinamidic ligands such as those presented in this dissertation.

8. REFERENCES

1.   Information Digest 2013-2014. *Nuclear Regulatory Comission* (2013).

2.   McMurray, R. L. *Understanding Radioactive Waste*. 75 (Batelle Press: Columbus, OH, 2003).

3.   Nilsson, M. & Nash, K. L. Review Article: A Review of the Development and Operational Characteristics of the TALSPEAK Process. *Solvent Extraction and Ion Exchange* **25**, 665–701 (2007).

4.   National Research Council *Disposition of High-Level Waste and Spent Nuclear Fuel*. 198 (Washington D.C., 2001).

5.   Benedict, M., Levi, H. & Pigford, T. *Nuclear Chemical Engineering*. *Nucl. Sci. Eng.;(United States)* (McGraw-Hill: 1982).

6.   Ahlstrom, P. E. *Partitioning and Transmutation Current Developments, 2004*. (Stockholm, 2004).

7.   Ansolabhere, S. *et al. The Future of Nuclear Power*. (2003) at <http://web.mit.edu/nuclearpower/>

8.   Macfarlane, A. & Ewing, R. *Uncertainty Underground*. (MIT Press: Cambridge, MA, 2006).

9.   Choppin, G. R., Liljenzin, J.O. & Rydberg, J. *Radiochemistry and Nuclear Chemistry*. (Butterworth-Heinemann: Woburn, MA, 2002).

10.   The Royal Society Science Policy Centre Report *Fuel Cycle Stewardship in a Nuclear Renaissance*. (2011).

11.   Pearson, R. G. Hard and Soft Acids and Bases, HSAB, Part II. *Journal of Chemical Education* **45**, 643–648 (1968).

12.   Pearson, R. G. Recent Advances in the Concept of Hard and Soft Acids and Bases. *Journal of Chemical Education* **64**, 561–567 (1987).

13.   Pearson, R. G. Hard and Soft Acids and Bases, HSAB, Part I. *Journal of Chemical Education* **45**, 581–587 (1968).

14.   Pearson, R. G. Hard and Soft Acids and Bases. *Journal of the American Chemical Society* **85**, 3533–3539 (1963).

15. Loveland, W. D., Morrissey, D. & Seaborg, G. *Modern Nuclear Chemistry*. (John Wiley & Sons Inc.: Hoboken, New Jersey, 2006).

16. Aspinall, H. C. *Chemistry of the f-Block Elements*. (Gordon and Breach Science Publishers: Amsterdam, Netherlands, 2001).

17. Nugent, L. Theory of the Tetrad Effect in the Lanthanide (III) and Actinide (III) Series. *Journal of Inorganic and Nuclear Chemistry* **32**, 3485–3491 (1970).

18. Clark, D. The Chemical Complexities of Plutonium. *Los Alamos Science* 364–381 (2000).

19. Cotton, S. *Lanthanide and Actinide Chemistry*. (John Wiley & Sons, Ltd.: 2007).

20. Zalupski, P. R. & Nash, K. L. Two-Phase Calorimetry. I. Studies on the Thermodynamics of Lanthanide Extraction by Bis(2-EthylHexyl) Phosphoric Acid. *Solvent Extraction and Ion Exchange* **26**, 514–533 (2008).

21. Bunzli, J. & Vuckovic, M. Solvation of Neodymium (III) Perchlorate and Nitrate in Organic Solvents as Determined by Spectroscopic Measurements. *Inorganica Chimica Acta* **95**, 105–112 (1984).

22. Morss, L. R., Edelstein, N. M. & Fuger, J. *The Chemistry of the Actinide and Transactinide Elements*. **3**, (Springer: Netherlands, 2006).

23. Eisberg, R., Resnick, R. & Brown, J. *Quantum Physics of Atoms, Molecules, Solids, Nuclei, and Particles*. *Physics Today* (John Wiley & Sons, Ltd.: Toronto, Canada, 1986).

24. Keller, O. L. The Chemistry of Protactinium, Neptunium, Americium, and Curium in the Nuclear Fuel Cycle. *Radiochimica Acta* **25**, 211–223 (1978).

25. Choppin, G. R. Actinide Speciation in Aquatic Systems. *Marine Chemistry* **99**, 83–92 (2006).

26. Guillaumont, R. & Mompean, F. *Chemical Thermodynamics 5: Update on the Chemical Thermodynamics of Uranium, Neptunium, Plutonium, Americium and Technetium*. **5**, (Elsevier B.V.: Amsterdam, Netherlands, 2003).

27. Nash, K. Aqueous Complexes in Separations of f-Elements: Options and Strategies for Future Development. *Separation Science and Technology* **34**, 911–929 (1999).

28. Choppin, G. R. & Unrein, P. J. Thermodynamics Study of Actinide Flourine Complexation. *Transplutonium Elements* 97–107 (1976).

29. Dam, H. H., Reinhoudt, D. N. & Verboom, W. Multicoordinate Ligands for Actinide/Lanthanide Separations. *Chemical Society Reviews* **36**, 367–77 (2007).

30. Moyer, B. A. *Ion Exchange and Solvent Extraction: A Series of Advances Volume 19*. (CRC Press: 2009).

31. Jensen, M. P. & Bond, A. H. Comparison of Covalency in the Complexes of Trivalent Actinide and Lanthanide Cations. *Journal of the American Chemical Society* **124**, 9870–7 (2002).

32. Kolarik, Z. Complexation and Separation of Lanthanides(III) and Actinides(III) by Heterocyclic N-donors in Solutions. *Chemical Reviews* **108**, 4208–52 (2008).

33. Zalupski, P. R., Nash, K. L. & Martin, L. R. Thermodynamic Features of the Complexation of Neodymium(III) and Americium(III) by Lactate in Trifluoromethanesulfonate Media. *Journal of Solution Chemistry* **39**, 1213–1229 (2010).

34. Harris, D. C. *Quantitative Chemical Analysis*. (W. H. Freeman and Company: New York, NY, 2003).

35. Chaumont, A. & Wipff, G. Solvation of Uranyl-CMPO Complexes in Dry vs. Humid Forms of the [BMI][PF6] Ionic Liquid. A Molecular Dynamics Study. *Physical Chemistry Chemical Physics : PCCP* **8**, 494–502 (2006).

36. Giridhar, P. & Venkatesan, K. Comparison of Diluent Characteristics of Imidazolium Hexafluorophosphate Ionic Liquid with n-Dodecane. *Journal of Radioanalytical and Nuclear Chemistry* **5**, 17–20 (2004).

37. Shimojo, K., Kurahashi, K. & Naganawa, H. Extraction Behavior of Lanthanides Using a Diglycolamide Derivative TODGA in Ionic Liquids. *Dalton Transactions* 5083–8 (2008).doi:10.1039/b810277p

38. Nakashima, K., Kubota, F., Maruyama, T. & Goto, M. Ionic Liquids as a Novel Solvent for Lanthanide Extraction. *Analytical Sciences: The International Journal of the Japan Society for Analytical Chemistry* **19**, 1097–8 (2003).

39. Stumpf, S., Billard, I., Panak, P. J. & Mekki, S. Differences of Eu(III) and Cm(III) Chemistry in Ionic Liquids: Investigations by TRLFS. *Dalton Transactions* **1**, 240–8 (2007).

40. Aguilar, M. & Cortina, J. L. *Solvent Extraction and Liquid Membranes: Fundamentals and Applications in New Materials*. (CRC Press: Boca Raton, FL, 2008).

41. Sasaki, Y. *et al.* An Additional Insight into the Correlation between the Distribution Ratios and the Aqueous Acidity of the TODGA System. *Solvent Extraction and Ion Exchange* **25**, 187–204 (2007).

42. Bond, A. *et al.* Plutonium Mobilization and Matrix Dissolution During Experimental Sludge Washing of Bismuth Phosphate, Redox, and PUREX Waste Simulants. *Separation Science and Technology* **36**, 1241–1256 (2001).

43. Hubscher-Bruder, V., Haddaoui, J., Bouhroum, S. & Arnaud-Neu, F. Recognition of Some Lanthanides, Actinides, and Transition- and Heavy-Metal Cations by N-donor Ligands: Thermodynamic and Kinetic Aspects. *Inorganic Chemistry* **49**, 1363–71 (2010).

44. Rawat, N., Bhattacharyya, A., Ghosh, S. K., Gadly, T. & Tomar, B. S. Thermodynamics of Complexation of Lanthanides with 2,6-bis(5,6-diethyl-1,2,4-triazin-3-yl) Pyridine. *Radiochimica Acta* **99**, 705–712 (2011).

45. Reinoso, García, M. M. *et al.* Solvent Extraction of Actinides and Lanthanides by CMP(O) and N-Acyl(thio)ureatetrafunctionalized Cavitands: Strong Synergistic Effect of Cobalt Bis(dicarbollide) Ions. *Solvent Extraction and Ion Exchange* **23**, 425–437 (2005).

46. Berg, J. M., Veirs, D. K., Vaughn, R. B., Cisneros, M. A. & Smith, C. A. Plutonium(IV) Complexation by Nitrate in Acid Solutions of Ionic Strengths From 2 to 19 Molal. *Los Alamos National Laboratory Report* 1–11 (2003).

47. Kumar, A. & Mohapatra, P. Extraction of Mo (VI) from Nitric Acid Medium by Di(octyl-phenyl) Phosphoric Acid. *Solvent Extraction and Ion Exchange* **19**, 491–505 (2001).

48. Schroeder, N. C., Attrep, M. & Marrero, T. *Los Alamos Technetium and Iodine Separations in the UREX Process*. **836**, 0–31 (2001).

49. Fuks, L. & Majdan, M. Features of Solvent Extraction of Lanthanides and Actinides. *Mineral Processing and Extractive Metallurgy Review* **21**, 25–48 (2000).

50. Miralles, N., Sastre, A., Martinez, M. & Aguilar, M. The Aggregation of Organophosphorus Acid Compounds in Toluene. *Analytical Sciences* **8**, 773–777 (1992).

51. Antonio, M. R. *et al.* Aggregation in Solvent Extraction Systems Containing a Malonamide, a Dialkylphosphoric Acid and their Mixtures. *Separation Science and Technology* **43**, 2572–2605 (2008).

160

52. Schulz, W. W. & Navratil, J. A. *Science and Technology of Tributylphosphate Volume I: Synthesis, Properties, Reactions and Analysis*. **I**, (CRC Press: Boca Raton, FL, 1984).

53. Coleman, C. F. & Leuze, R. E. Some Milestone Solvent Extraction Processes at the Oak Ridge National Laboratory. *Journal of the Tennessee Academy of Science* **53**, 102 (1978).

54. Warf, J. C. Extraction of Cerium(IV) Nitrate by Butyl Phosphate. *Journal of the American Chemical Society* **71**, 3257–3258 (1949).

55. Schulz, W. W., Burger, L. L. & Navratil, J. D. *Science and Technology of Tributyl Phosphate Volume III: Applications of Tributyl Phosphate in Nuclear Fuel Processing*. **III**, (CRC Press: Boca Raton, FL, 1990).

56. Navratil, J. A. & Schulz, W. W. *Science and Technology of Tributyl Phosphate Volume IIA and IIB: Selected Technical and Industrial Uses*. (CRC Press: Boca Raton, FL, 1984).

57. Navratil, J. D. Solvent Extraction In Nuclear Technology. *Pure & Appl. Chem* **58**, 885–888 (1986).

58. Best, G. F., Mckay, H. A. C. & Woodgate, P. R. Tri-n-butyl Phosphate as an Extracting Solvent for Inorganic Nitrates-III. *Journal of Inorganic and Nuclear Chemistry* **4**, 315–320 (1957).

59. Lee, T.-W. & Ting, G. Study on the Separation of Carrier-Free Yttrium-90 from Strontium-90. *Isotopenpraxis Isotopes in Environmental and Health Studies* **27**, 269–273 (1991).

60. Herbst, R. S. *et al.* Development and Testing of a Cobalt Dicarbollide Based Solvent Extraction Process for the Separation of Cesium and Strontium from Acidic Tank Waste. *Separation Science and Technology* **37**, 1807–1831 (2002).

61. Makrlík, E., Rais, J. & Baše, K. Individual Extraction Constants of Some Dicarbollylcobaltate Anions in the Water-Nitrobenzene System. *Journal of Radioanalytical and Nuclear Chemistry* **198**, 359–365 (1995).

62. Selucký, P., Plesek, J., Rais, J., Kyrs, M. & Kadlecova, L. Extraction of Fission Products into Nitrobenzene with Dicobalt Tris-dicarbollide and Ethyleneoxy-substituted Cobalt Bis-dicarbolide. *Journal of Radioanalytical and Nuclear Chemistry* **149**, 131–140 (1991).

63. Rzhekhina, E. K. *et al.* Reprocessing of Spent Solvent of the UNEX Process. *Radiochemistry* **49**, 493–498 (2007).

64. Mathur, J., Murali, M. & Nash, K. Actinide Partitioning—A Review. *Solvent Extraction and Ion Exchange* **19**, 357–390 (2001).

65. Horwitz, E. P. The Extraction of Selected Actinides In The (III)(IV) and (VI) Oxidation States From Hydrochloric Acid By Oϕ-D(iB)CMPO: The Truex-Chloride Process. *Solvent Extraction and Ion Exchange* **5**, 447–470 (1987).

66. Horwitz, E., Kalina, D., Kaplan, L. & Mason, G. Method for Extracting Lanthanides and Actinides from Acid Solutions. (1985).

67. Spencer, B., Counce, R. & Egan, B. Extraction of Nitric Acid from Aqueous Media with Oϕ-D(iB)CMPO-n-dodecane. *Environmental and Energy Engineering* **43**, 555–564 (1997).

68. Turanov, A. N., Karandashev, V. K. & Baulin, V. E. Effect of Ionic Liquids on the Extraction of Rare-Earth Elements by Bidentate Neutral Organophosphorus Compounds from Chloride Solutions. *Russian Journal of Inorganic Chemistry* **53**, 970–975 (2008).

69. Peppard, D. & Mason, G. Fractional Extraction of the Lanthanides as Their Di-alkyl Orthophosphates. *Journal of Inorganic and Nuclear Chemistry* **4**, 334–343 (1957).

70. Zalupski, P. R. *Non-Ideal Behavior in Solvent Extraction*. (2011).

71. Brown, M. A. Aqueous Complexation of Citric Acid and DTPA with Selected Trivalent and Tetravalent f-Elements. (2012).

72. Del Cul, G. D., Toth, L. M., Bond, W. D., Davis, G. D. & Dai, S. Citrate-Based "TALSPEAK" Actindide-Lanthandide Separation Process. *Separation Science and Technology* **32**, 431–446 (1997).

73. Stary, J. Separation of Transplutonium Elements. *Talanta* **13**, 421–437 (1966).

74. Weaver, B. & Kappelmann, F. Extraction of Lanthanides Over Trivalent Actinides by Monoacidic Organophosphates from Carboxylic Acids and from Mixtures of Carboxylic and Aminopolyacetic Acids. *Journal of Inorganic and Nuclear Chemistry* **30**, 263–272 (1968).

75. Tkac, P., Vandegrift, G. F., Lumetta, G. J. & Gelis, A. V. Study of the Interaction between HDEHP and CMPO and Its Effect on the Extraction of Selected

Lanthanides. *Industrial & Engineering Chemistry Research* **51**, 10433–10444 (2012).

76. Lumetta, G., Gelis, A. & Vandegrift, G. Review: Solvent Systems Combining Neutral and Acidic Extractants for Separating Trivalent Lanthanides from the Transuranic Elements. *Solvent Extraction and Ion Exchange* **28**, 287–312 (2010).

77. Matteson, B. The Chemistry of Acetohydroxamic Acid Related to Nuclear Fuel Reprocessing. (2010).

78. Vandegrift, G. F. *et al.* Designing and Demonstration of the UREX+ Process Using Spent Nuclear Fuel. *Atalante 2004* 1–9 (2004).

79. Todd, T. A., Brewer, K. N., Law, J. D., Wood, D. J. & Herbst, R. S. Development of a Universal Solvent for the Decontamination of Acidic Liquid Radioactive Wastes. *Czech Journal of Physics* **49**, 931–936 (1999).

80. Luther, T. A. *et al.* Some Aspects of Fundamental Chemistry of the Universal Extraction (UNEX) Process for the Simultaneous Separation of Major Radionuclides (Cesium, Strontium, Actinides, and Lanthanides) from Radioactive Wastes. *Journal of Radioanalytical and Nuclear Chemistry* **267**, 603–613 (2006).

81. Musikas, C. Solvent Extraction for the Chemical Separations of the 5f Elements. *Inorganica Chimica Acta* **140**, 197–206 (1987).

82. Musikas, C. Potentiality of Nonorganophosphorus Extractant in Chemical Separations of Actinides. *Separation Science and Technology* **23**, 1211–1225 (1988).

83. Sugo, B. Y., Sasaki, Y. & Tachimori, S. Studies on Hydrolysis and Radioylsis of N,N,N',N'-tetraoctyl-3-oxapentane-1,5-diamide. *Radiochimica Acta* **165**, 161–165 (2002).

84. Cuillerdier, C. & Musikas, C. Malonamides as New Extractants for Nuclear Waste Solutions. *Separation Science and Technology* **26**, 1229–1244 (1991).

85. Cuillerdier, C., Musikas, C. & Nigond, L. Diamides as actinide extractants for various waste treatments. *Separation Science and Technology* **28**, 155–175 (1993).

86. Serrano-Purroy, D. Recovery of Minor Actinides from HLLW Using the DIAMEX Process. *Radiochimica Acta* **93**, 351–355 (2005).

87. Serrano-Purroyl, B. D., Chrstiansenl, B., Glatzl, I., Malmbeckl, R. & Modol, G. Towards a DIAMEX Process Using High Active Concentrate . Production of Genuine Solutions. *Radiochimica Acta* **361**, 357–361 (2005).

88. Modolo, G., Vijgen, H., Baron, P. & Dinh, B. Demonstration of the TODGA Process for Partitioning of Actinides(III) from High Level Liquid Waste. *Proc. Intern. Conf. on P&T* 1–9 (2003).

89. Zhu, Z.-X., Sasaki, Y., Suzuki, H., Suzuki, S. & Kimura, T. Cumulative Study on Solvent Extraction of Elements by N,N,N′,N′-tetraoctyl-3-oxapentanediamide (TODGA) from Nitric Acid Into n-Dodecane. *Analytica Chimica Acta* **527**, 163–168 (2004).

90. Modolo, G. *et al.* Demonstration of a TODGA-Based Continuous Counter-Current Extraction Process for the Partitioning of Actinides from a Simulated PUREX Raffinate, Part II: Centrifugal Contactor Runs. *Solvent Extraction and Ion Exchange* **26**, 62–76 (2008).

91. Modolo, G., Asp, H., Schreinemachers, C. & Vijgen, H. Development of a TODGA based Process for Partitioning of Actinides from a PUREX Raffinate Part I: Batch Extraction Optimization Studies and Stability Tests. *Solvent Extraction and Ion Exchange* **25**, 703–721 (2007).

92. Suzuki, H., Sasaki, Y. & Apichaibukol, A. Extraction and Separation of Am(III) and Sr(II) by N,N,N',N'-tetraoctyl-3-oxapentanediamide (TODGA). *Radiochimica Acta* **92**, 463–466 (2004).

93. Guelis, A. Actinide and Lanthanide Separation Process (ALSEP). (2013).

94. Panak, P. J. & Geist, A. Complexation and Extraction of Trivalent Actinides and Lanthanides by Triazinylpyridine N-donor Ligands. *Chemical Reviews* **113**, 1199–236 (2013).

95. Hudson, M. J., Harwood, L. M., Laventine, D. M. & Lewis, F. W. Use of Soft Heterocyclic N-donor Ligands to Separate Actinides and Lanthanides. *Inorganic Chemistry* **52**, 3414–28 (2013).

96. Kolarik, Z., Mullich, U. & Gassner, F. Extraction of Am(lll) and Eu(lll) Nitrates by 2-6-di-(5, 6-dipropyl-1, 2, 4-triazin-3-yl) Pyridines. *Solvent Extraction and Ion Exchange* **17**, 1155–1170 (1999).

97. Madic, C., Lecomte, M., Baron, P. & Boullis, B. Separation of Long-Lived Radionuclides from High Active Nuclear Waste. *Comptes Rendus Physique* **3**, 797–811 (2002).

98. Weigl, M. & Geist, A. Kinetics of Americium(III) Extraction and Back Extraction with BTP. *Solvent Extraction and Ion Exchange* **24**, 845–860 (2006).

99. Ekberg, C. *et al.* An Overview and Historical Look Back at the Solvent Extraction Using Nitrogen Donor Ligands to Extract and Separate An(III) from Ln(III). *Radiochimica Acta* 225–233 (2008).

100. Mincher, B. J. *Degradation Issues in Aqueous Reprocessing Systems. Comprehensive Nuclear Materials* **5**, 367–388 (Elsevier Inc.: 2012).

101. Lewis, F. W. *et al.* Synthesis and Evaluation of Lipophilic BTBP Ligands for An/Ln Separation in Nuclear Waste Treatment: The Effect of Alkyl Substitution on Extraction Properties and Implications for Ligand Design. *European Journal of Organic Chemistry* **2012**, 1509–1519 (2012).

102. Magnusson, D., Christiansen, B., Malmbeck, R. & Glatz, J.-P. Investigation of the Radiolytic Stability of a CyMe$_4$-BTBP Based SANEX Solvent. *Radiochimica Acta* **97**, 497–502 (2009).

103. Geist, A. *et al.* 6,6′-Bis(5,5,8,8-tetramethyl-5,6,7,8-tetrahydro-benzo[1,2,4]triazin-3-yl) [2,2′]bipyridine, an Effective Extracting Agent for the Separation of Americium(III) and Curium(III) from the Lanthanides. *Solvent Extraction and Ion Exchange* **4**, 463–483 (2006).

104. Kwon, S. G., Lee, E. H., Yoo, J. & Park, Y. J. Extraction of Eu-152, Nd and Am-241 from the Simulated Liquid Wastes by Picolinamide (C8H17). *Journal of the Korean Nuclear Society* **31**, 498–505 (1999).

105. Kobayashi, T. *et al.* Effect of the Introduction of Amide Oxygen into 1,10-Phenanthroline on the Extraction and Complexation of Trivalent Lanthanide in Acidic Condition. *Separation Science and Technology* **45**, 2431–2436 (2010).

106. Paulenova, A., Alyapyshev, M. Y., Babain, V. A., Herbst, R. S. & Law, J. D. Extraction of Lanthanides with Diamides of Dipicolinic Acid from Nitric Acid Solutions. I. *Separation Science and Technology* **43**, 2606–2618 (2008).

107. Babain, V. A., Alyapyshev, M. Y. & Kiseleva, R. N. Metal Extraction by N, N′-dialkyl-N, N′-Diaryl-Dipicolinamides from Nitric Acid Solutions. *Radiochimica Acta* **95**, 217–223 (2007).

108. Alyapyshev, M. & Babain, V. Separation of Americium and Europium from Solutions of Nitric and Perchloric Acid Using Dipicolinic Acid Diamides. *Czechoslovak Journal of Physics* **56**, 469–475 (2006).

109. Romanovskiy, V. N. *et al.* Radionuclide Extraction by 2,6-Pyridinedicarboxylamide Derivatives and Chlorinated Cobalt Dicarbollide. *Separation Science and Technology* **41**, 2111–2127 (2006).

110. Alyapyshev, M. Y., Babain, V. A. & Tkachenko, L. I. Actinide-Lanthanide Separation with Solvents on the Base of Amides of Heterocyclic Diacids. *Global 2013* (2013).

111. Babain, V. A., Alyapyshev, M. Y., Smirnov, I. V. & Shadrin, a. Y. Extraction of Am and Eu with N,N′-Substituted Pyridine-2,6-dicarboxamides in Fluorinated Diluents. *Radiochemistry* **48**, 369–373 (2006).

112. Alyapyshev, M. Y., Babain, V. A. & Smirnov, I. V. Extractive Properties of Synergistic Mixtures of Dipicolinic Acid Diamides and Chlorinated Cobalt Dicarbollide. *Radiochemistry* **46**, 270–271 (2004).

113. Romanovskiy, V. N. *et al.* Radionuclide Extraction by 2,6-Pyridinedicarboxylamide Derivatives and Chlorinated Cobalt Dicarbollide. *Separation Science and Technology* **41**, 2111–2127 (2006).

114. Koma, Y., Koyama, T. & Tnaka, Y. Enhancement of the Mutual Separation of Lanthanide Elements in the Solvent Extraction Based on the CMPO-TBP Mixed Solvent. *Journal of Nuclear Science and Technology* **36**, 934–939 (1999).

115. Belair, S. *et al.* Modeling of the Extraction of Lanthanide Nitrates from Aqueous Solutions Over a Wide Range of Activities by CMPO. *Solvent Extraction and Ion Exchange* **22**, 791–811 (2004).

116. Mincher, B. A Slope Analysis Investigation of the Trivalent f-Series Metal CMPO Complex. *Solvent Extraction and Ion Exchange* **10**, 615–622 (1992).

117. Andersson, B. S., Ekberg, C., Liljenzin, J., Nilsson, M. & Skarnemark, G. Study of Nitrate Complex Formation with Trivalent Pm , Eu , Am. *Radiochimica Acta* **867**, 863–867 (2004).

118. Andersson, S. *et al.* Determination of Stability Constants of Lanthanide Nitrate Complex Formation Using a Solvent Extraction Technique. *Radiochimica Acta* **94**, 469–474 (2006).

119. Brown, M. A., Paulenova, A. & Gelis, A. V Aqueous Complexation of Thorium(IV), Uranium(IV), Neptunium(IV), Plutonium(III/IV), and Cerium(III/IV) with DTPA. *Inorganic Chemistry* **51**, 7741–8 (2012).

120. Rossotti, F. J. C. & Rossotti, H. *The Determination of Stability Constants*. (McGraw-Hill: 1962).

121. Meloun, M., Havel, J. & Hogfeldt, E. *Computation of Solution Equilibria: A Guide to Methods in Potentiometry, Extraction, and Spectrophotometry*. (Ellis Horwood Limited: Chichester, England, 1988).

122. Gans, P., Sabatini, A. & Vacca, A. Simultaneous Calculation of Equilibrium Constants and Standard Formation Enthalpies from Calorimetric Data for Systems with Multiple Equilibria in Solution. *Journal of Solution Chemistry* **37**, 467–476 (2008).

123. Gans, P., Sabatini, A. & Vacca, A. Investigation of Equilibria in Solution. Determination of Equilibrium Constants with the HYPERQUAD Suite of Programs. *Talanta* **43**, 1739–53 (1996).

124. Martell, A. & Motekaitis, R. *Determination and Use of Stability Constants*. (VCH Publishers Inc.: New York, NY, 1992).

125. Rubtsov, M. V. Tertiary Amines of Some Heterocycles as Possible Hypotensive Substances. *Russian Journal of General Chemistry* **28**, 161–166 (1958).

126. Savvin, S. B. *Arsenazo(III)*. 256 (Atomizdat: Moscow, 1966).

127. Rydberg, J., Cox, M., Musikas, C. & Choppin, G. R. *Solvent Extraction Principles and Practice, Revised and Expanded*. (Marcel Dekker Inc.: New York, NY, 2004).

128. VanPelt, C. E., Crooks, W. J. & Choppin, G. R. Thermodynamic Constant Determination for the Complexation of Trivalent Lanthanides with Polyoxometalates. *Inorganica Chimica Acta* **340**, 1–7 (2002).

129. Stiefel, E. I. Progress in Inorganic Chemistry, vol. 22. 1 (1977).

130. Tkac, P. & Paulenova, A. Speciation of Molybdenum (VI) In Aqueous and Organic Phases of Selected Extraction Systems. *Separation Science and Technology* **43**, 2641–2657 (2008).

131. Cruywagen, J., Heyns, J. & Westra, A. Protonation Equilibria of Mononuclear Vanadate: Thermodynamic Evidence for the Expansion of the Coordination Number in VO_2^+. *Inorganic Chemistry* **35**, 1556–1559 (1996).

132. Yokoi, K., Matsubayashi, N. & Miyanaga, T. Studies on the Structure of Molybdenum(VI) in Acidic Solution by XANES and EXAFS. *Polyhedron* **12**, 911–914 (1993).

133. Demet'ev, I. A., Kozin, A. O., Kondrat'ev, Y. V., Korol'kov, D. V. & Proyavkin, A. A. Mononuclear, Polynuclear, and Cluster Complexes of Molybdenum and Their Reactions as Models of Biochemical Systems and Processes. *Russian Journal of General Chemistry* **77**, 822–843 (2007).

134. Van Hecke, K. & Modolo, G. Separation of Actinides from Low Level Liquid Wastes (LLLW) by Extraction Chromatography Using Novel DMDOHEMA and TODGA Impregnated Resins. *Journal of Radioanalytical and Nuclear Chemistry* **261**, 269–275 (2004).

135. Watson, J. H. . & Ellwood, D. The Removal of the Pertechnetate Ion and Actinides from Radioactive Waste Streams at Hanford, Washington, USA and Sellafield, Cumbria, UK: The Role of Iron-Sulfide-Containing Adsorbent Materials. *Nuclear Engineering and Design* **226**, 375–385 (2003).

136. Schwochau, K. *Technetium: Chemistry and Radiopharmaceutical Applications*. (Wiley-VCH: Weinheim: 2000).

137. Friese, J. I., Nash, K. L., Jensen, M. P. & Sullivan, J. C. Interactions of Np(V) and U(VI) with Dipicolinic Acid. *Radiochimica Acta* **89**, 35–41 (2001).

138. Pathak, P. N., Kumbhare, L. B. & Manchanda, V. K. Effect of Structure of N,N Dialky Amides on the Extraction of U(VI) and Th(IV): A Thermodynamic Study. *Radiochimica Acta* **89**, 447–452 (2001).

139. Renaud, F. & Piguet, C. In Search for Mononuclear Helical Lanthanide Building Blocks with Predetermined Properties: Triple-stranded Helical Complexes with N, N, N',N'-•tetraethylpyridine-2,6-dicaboxamide. *Chem. Eur. J.* **3**, 1646–1659 (1997).

140. Lapka, J. L., Paulenova, A., Zacharov, L. N., Alyapyshev, M. Y. & Babain, V. A. The Coordination of Uranium(VI) with Diamides of Dipicolinic Acid. *IOP Conf. Ser. Mater. Sci. Eng* **9**, 1–7 (2010).

141. Lumetta, G. J., McNamara, B. K., Rapko, B. M. & Hutchison, J. E. Complexation of Uranyl ion by Tetrahexylmalonamides: An Equilibrium Modeling and Infrared Spectroscopic Study. *Inorganica Chimica Acta* **293**, 195–205 (1999).

142. Kim, K., Song, K., Lee, E., Choi, I. & Yoo, J. Oxidation State and Extraction of Neptunium with TBP. *Journal of Radioanalytical and Nuclear Chemistry* **246**, 215–219 (2000).

143. Sarsfield, B. M. J., Taylor, R. J. & Maher, C. J. Neptunium (V) Disproportionation and Cation–Cation Interactions in TBP/Kerosene Solvent. *Radiochimica Acta* **682**, 677–682 (2007).

144. Ananiev, A. & Shilov, V. Heterogeneous Catalytic Oxidation of Neptunium(IV) in Nitric Acid Solutions. *Radiochimica Acta* **91**, (2003).

145. Dinh, B. *et al.* Modified PUREX First-Cycle Extraction for Neptunium Recovery. *Proceedings of the International Solvent Extraction Conference (ISEC 2008)* 581–586 (2008).

146. Sinkov, S. I. *et al.* Bicyclic and Acyclic Diamides: Comparison of their Aqueous Phase Binding Constants with Nd(III), Am(III), Pu(IV), Np(V), Pu(VI), and U(VI). *Inorganic Chemistry* **43**, 8404–13 (2004).

147. Choppin, G. & Rao, L. Reduction of Neptunium (VI) by Organic Compounds. *Transuranic Elements* 262–275 (1992).

148. Friedman, H. & Toth, L. Absorption Spectra of Np (III),(IV),(V) and (VI) in Nitric Acid Solution. *Journal of Inorganic and Nuclear Chemistry* **42**, 1347–1349 (1980).

149. Wisnubroto, D. S., Nagasaki, S., Enokida, Y. & Suzuki, A. Effect of TBP on Solvent Extraction of Np (V) with M-Octyl (phenyl)-, N-N Diisobutylcarbamoylmethylphosphine Oxide Effect of TBP on Solvent Extraction of Np (V) with n-Octyl (phenyl) -N , N- Diisobutylcarbamoylmethylphosphine Oxide. *Journal of Nuclear Science and Technology* **29**, 263–283 (1992).

150. Geipel, G. Speciation of Actinides. *Handbook of Elemental Speciation II - Species in the Environment, Food, Medicine and Occupational Health* 509–563 (2005).

151. Brown, D. & Maddock, A. G. Protactinium. *Quarterly Reviews, Chemical Society* **17**, 289–341 (1963).

152. Myasoedov, B. F., Kirby, H. W. & Tananaev, I. G. Protactinium. (1978).

153. Baes, C. & Mesmer, R. *The Hydrolysis of Cations*. (Wiley: 1976).

154. Hyde, E. *The Radiochemistry of Thorium*. (1959).

155. Sasaki, Y. & Choppin, G. Extraction and Mutual Separation of Actinide (III),(IV),(V) and (VI) Ions by N, N'-dimethyl-N, N'-dihexyl-3-oxapentanediamide and Thenoyltrifluoroacetone. *Journal of Radioanalytical and Nuclear Chemistry* **246**, 267–273 (2000).

156. Hobart, D., Morris, D., Palmer, P. & Newton, T. *Formation, Characterization, and Stability of Plutonium(IV) Colloid; A Progress Report*. (1989).

157. Choppin, G. R., Bond, A. H. & Hromadka, P. M. Redox Speciation of Plutonium. *Journal of Radioanalytical and Nuclear Chemistry* **219**, 203–210 (1997).

158. Coleman, G. *The Radiochemistry of Plutonium*. (1965).

159. Bard, A., Parsons, R. & Jordan, J. *Standard Potentials in Aqueous Solutions*. (Marcel Dekker Inc.: New York, NY, 1985).

160. Vladimirova, M. & Kulikov, I. Formation of H_2 and O_2 in Radiolysis of Water Sorbed on PuO_2. *Radiochemistry* **44**, 86–90 (2002).

161. Anan, A. V & Shilov, V. P. Catalytic Reduction of Pu (IV) with Formic Acid in Nitric Acid Solutions. *Radiochemistry* **46**, 242–245 (2004).

162. Seaborg, G. & Loveland, W. *The Elements Beyond Uranium*. (Wiley: New York, NY, 1990).

163. Allen, P. G., Veirs, D. K., Conradson, S. D., Smith, C. a. & Marsh, S. F. Characterization of Aqueous Plutonium(IV) Nitrate Complexes by Extended X-ray Absorption Fine Structure Spectroscopy. *Inorganic Chemistry* **35**, 2841–2845 (1996).

164. Brown, M. A., Tkac, P., Paulenova, A. & Vandegrift, G. F. Influence of Temperature on the Extraction of Pu(IV) by Tri-n-butyl Phosphate from Acidic Nitrate Solutions. *Separation Science and Technology* **45**, 50–57 (2009).

165. Mincher, B. J., Elias, G., Martin, L. R. & Mezyk, S. P. Radiation Chemistry and the Nuclear Fuel Cycle. *Journal of Radioanalytical and Nuclear Chemistry* **282**, 645–649 (2009).

166. Buxton, G., Greenstock, C., Helman, W. & Ross, A. Critical Review of Rate Constants for Reactions of Hydrated Electrons, Hydrogen Atoms and Hydroxyl Radicals. *J. of Phys. Chem. Ref. Data* **17**, 513–586 (1988).

167. Løgager, T. & Sehested, K. Formation and Decay of Peroxynitrous Acid: A Pulse Radiolysis Study. *The Journal of Physical Chemistry* **97**, 6664–6669 (1993).

168. Elias, G., Mincher, B. J., Mezyk, S. P., Muller, J. & Martin, L. R. Toluene Nitration in Irradiated Nitric Acid and Nitrite Solutions. *Radiation Physics and Chemistry* **80**, 554–560 (2011).

169. Olah, G. A., Lin, H. C., Olah, J. A. & Narang, S. C. Electrophilic and Free Radical Nitration of Benzene and Toluene with Various Nitrating Agents. *Proceedings of the National Academy of Sciences of the United States of America* **75**, 1045–9 (1978).

170. Halfpenny, E. & Robinson, P. The Nitration and Hydroxylation of Aromatic Compounds by Pernitrous Acid. *J. Chem. Soc.* **2**, 939–947 (1952).

171. Elias, G., Mincher, B. J., Mezyk, S. P., Cullen, T. D. & Martin, L. R. Anisole Nitration During Gamma-Irradiation of Aqueous Nitrite and Nitrate Solutions: Free Radical Versus Ionic Mechanisms. *Environmental Chemistry* **7**, 183 (2010).

172. McMurry, J. *Organic Chemistry*. 796 (Brooks/Cole – Thomson: Belmont, CA, 2003).

173. Mincher, B. J., Herbst, R. S., Tillotson, R. D. & Mezyk, S. P. γ-Radiation Effects on the Performance of HCCD:PEG for Cs and Sr Extraction. *Solvent Extraction and Ion Exchange* **25**, 747–755 (2007).

174. Khlopin Radium Institute *Applicability of the Russian Separation Technology to Processing of US Radioactive Wastes. Final Report*. (1999).

175. Chambers, R. D. & Hutchinson, J. Synthesis: Carbon with Three Or Four Attached Heteroatoms. *Comprehensive Organic Functional Group Transformations* 1–34 (1995).

176. Ma, J.A. & Cahard, D. Strategies for Nucleophilic, Electrophilic, and Radical Trifluoromethylations. *Journal of Fluorine Chemistry* **128**, 975–996 (2007).

177. Prakash, G. K. S., Hu, J. & Olah, G. A. Nucleophilic Trifluoromethylation Using Trifluoromethyl Sulfone or Sulfoxide. *Organic Letters* **5**, 3253–3256 (2003).

178. Mowafy, E. A. Evaluation of Selectivity and Radiolysis Behavior of Some Promising Isonicotinamids and Dipicolinamides as Extractants. *Radiochimica Acta* **95**, 539–545 (2007).

179. Mowafy, E. A. The effect of Previous Gamma-Irradiation on the Extraction of U(VI), Th(IV), Zr(IV), Eu(III) and Am(III) by Various Amides. *Journal of Radioanalytical and Nuclear Chemistry* **260**, 179–187 (2004).

180. Logunov, M. V. *et al.* Radiation Resistance of a Series of Organophosphorus Extractants. *Radiochemistry* **48**, 55–61 (2006).

181. O`Connor, C. Acidic and Basic Amide Hydrolysis. *Q. Rev. Chem. Soc.* **24**, 553–564 (1970).

182. Birchall, T. & Gillespie, R. Nuclear Magnetic Resonance Studies of The Protonation Of Weak Bases In Fluorosulphuric Acid: II. Amides, Thioamides, And Sulphonamides. *Canadian Journal of Chemistry* **41**, 2642–2650 (1963).

183. Cox, R. & Druet, L. Protonation Acidity Constants for Some Benzamides, Acetamides, and Lactams. *Canadian Journal of Chemistry* **59**, 1568–1573 (1981).

184. Pretsch, E., Bhülmann, P. & Affolter, C. *Structure Determination of Organic Compounds*. 255–282 (Springer-Verlag: Berlin, Germany, 2000).

185. J N. Sharma , R. Ruhela, K. K. Singh, M. Kumar, C. Janardhanan, P. V. Achutan, S. Manohar, P. K. Wattal, and A. K. S. Studies on Hydrolysis and Radiolysis of Tetra(2-ethylhexyl)diglycolamide (TEHDGA)/Isodecyl Alcohol/n-Dodecane Solvent System. *Radiochimica Acta* **98**, 485–491 (2010).

186. Rapko, B. M., McNamara, B. K., Rogers, R. D., Lumetta, G. J. & Hay, B. P. Coordination of Lanthanide Nitrates with N,N,N',N'-Tetramethylsuccinamide. *Inorganic Chemistry* **38**, 4585–4592 (1999).

187. Mowafy, E. A. Evaluation of Selectivity and Radiolysis Behavior of Some Promising Isonicotinamids and Dipicolinamides as Extractants. *Radiochimica Acta* **95**, 539–545 (2007).

188. Berthon, L., Morel, J. & Zorz, N. DIAMEX Process for Minor Actinide Partitioning: Hydrolytic and Radiolytic Degradations of Malonamide Extractants. *Separation Science and Technology* **36**, 709–728 (2001).

189. Hoffman, R. V. *Organic Chemistry: An Intermediate Text*. 67 (John Wiley & Sons: Hoboken, New Jersey, 2004).

190. Lumetta, G. J. *et al.* Deliberate Design of Ligand Architecture Yields Dramatic Enhancement of Metal Ion Affinity. *Journal of the American Chemical Society* **124**, 5644–5 (2002).

191. Ismail, S. A Spectrophotometric Study on Neodymium Nitrate Complexation in Aqueous Methanol. (1989).

192. Pathak, P. N., Ansari, S. a, Godbole, S. V, Dhobale, a R. & Manchanda, V. K. Interaction of Eu^{3+} with N,N,N',N'-tetraoctyl Diglycolamide: A Time Resolved Luminescence Spectroscopy Study. *Spectrochimica Acta. Part A, Molecular and Biomolecular Spectroscopy* **73**, 348–52 (2009).

193. Marie, C. *et al.* Complexation of Lanthanides(III), Americium(III), and Uranium(VI) with Bitopic N,O ligands: An Experimental and Theoretical Study. *Inorganic Chemistry* **50**, 6557–66 (2011).

194. Xu, C., Tian, G., Teat, S. J. & Rao, L. Complexation of U(VI) with Dipicolinic Acid: Thermodynamics and Coordination Modes. *Inorganic Chemistry* **52**, 2750–6 (2013).

195. Rao, L. & Tian, G. Thermodynamic Study of the Complexation of Uranium (VI) with Nitrate at Variable Temperatures. *The Journal of Chemical Thermodynamics* **40**, 1001–1006 (2008).

196. Tian, G., Martin, L. R., Zhang, Z. & Rao, L. Thermodynamic, Spectroscopic, and Computational Studies of Lanthanide Complexation with Diethylenetriaminepentaacetic Acid: Temperature Effect and Coordination Modes. *Inorganic Chemistry* **50**, 3087–96 (2011).

197. Tian, G., Martin, L. R. & Rao, L. Complexation of Lactate with Neodymium(III) and Europium(III) at Variable Temperatures: Studies by Potentiometry, Microcalorimetry, Optical Absorption, and Luminescence Spectroscopy. *Inorganic Chemistry* **49**, 598–605 (2010).

198. Harris, D. C. & Bertolucci, M. D. *Symmetry and Spectroscopy*. (Oxford University Press Inc.: New York, NY, 1978).

199. Bernardo, P. Di & Choppin, G. Lanthanide (III) Trifluoromethanesulfonate Complexes in Anhydrous Acetonitrile. *Inorganica Chimica Acta* **207**, 85–91 (1993).

200. Saez, R. & Caro, P. A. *Rare Earths*. (Pujol & Amado S L L: Madrid, Spain, 2003).

201. Bünzli, J. & Milicic-Tang, A. FT-IR and Fluorometric Investigation of Rare-Earth and Metal Ion Solvation Part 16. Solid State and Solution Study of Acetonitrile-Coordinated Lanthanide Solvates [Ln(CH3CN)9](AlCl4)3. *Inorganica Chimica Acta* **252**, 221–228 (1996).

202. Stephens, E., Schoene, K. & Richardson, F. Hypersensitivity in the 4f-4f Absorption Spectra of Neodymium (III) Complexes in Aqueous Solution. *Inorganic Chemistry* **23**, 1641–1648 (1984).

203. Seminara, A. & Rizzarelli, E. Trifluoromethane and a Non-Coordinating Anion in Lanthanide Complexes. *Inorganica Chimica Acta* **40**, 249–256 (1980).

204. Cassol, A., Di Bernardo, P., Portanova, R., Tolazzi, M. & Zanonato, P. L. Complexing Ability of the Trifluoromethanesulfonate Complexes of the Heavier Lanthanides(III) Towards n-Butylamine in Anhydrous Acetonitrile. *Inorganica Chimica Acta* **262**, 1–8 (1997).

205. Di Bernardo, P., Melchior, A., Tolazzi, M. & Zanonato, P. L. Thermodynamics of Lanthanide(III) Complexation in Non-Aqueous Solvents. *Coordination Chemistry Reviews* **256**, 328–351 (2012).

206. Rosario-Amorin, D. *et al.* Synthesis, Lanthanide Coordination Chemistry, and Liquid-Liquid Extraction Performance of CMPO-Decorated Pyridine and Pyridine N-oxide Platforms. *Inorganic Chemistry* **52**, 3063–83 (2013).

207. Lapka, J. L. Determination of Neodymium:Dipicolinamide Stability Constants in Alcoholic Solution. *ISEC 2011* (2011).

208. Zalupski, P. R. *et al.* Two-Phase Calorimetry. II. Studies on the Thermodynamics of Cesium and Strontium Extraction by Mixtures of HCCD and PEG-400 in FS-13. *Solvent Extraction and Ion Exchange* **28**, 161–183 (2010).